$\mathcal{K}$-Modification and A Novel Approach to Output Feedback Adaptive Control

A Dissertation
Presented to
The Academic Faculty

by

Kilsoo Kim

In Partial Fulfillment
of the Requirements for the Degree
Doctor of Philosophy in the
School of Aerospace Engineering

Georgia Institute of Technology
May 2011

$\mathcal{K}$-Modification and A Novel Approach to Output Feedback Adaptive Control

Approved by:

Professor James Craig, Committee Chair
School of Aerospace Engineering
Georgia Institute of Technology

Professor Anthony Calise, Advisor
School of Aerospace Engineering
Georgia Institute of Technology

Professor Eric Johnson
School of Aerospace Engineering
Georgia Institute of Technology

Professor Eric Feron
School of Aerospace Engineering
Georgia Institute of Technology

Dr. Bong-Jun Yang
Research Scientist
Optimal Synthesis Inc.

Date Approved: April 1 2011

DEDICATION

To my brothers

Eokmann Kim and Kilseop Kim

ACKNOWLEDGEMENTS

It is a great pleasure to have an opportunity to show my thanks to all the people I have known and that were a help to me in completing this dissertation.

First I would like to thank my advisor, Dr. Anthony J. Calise for his support, advice, and guidance over the years that I have been working with him. Without him, I could not have come to the completion of this thesis. I have been greatly influenced by his passion for research and have learned from his insight and wisdom. I would also like to thank my committee members, Dr. James I. Craig, Dr. Eric N. Johnson, Dr. Eric M. J. Feron, and Dr. Bong-Jun Yang for their valuable suggestions and insights that greatly improved the quality of the thesis. Dr. Yang has helped me since I started doing my research in the area of adaptive control. He tried to deal with all the questions I asked. I am deeply appreciative for his efforts. I would also like to thank Dr. Jechiel Jagoda, the associate chair for graduate studies and research, for the moral and financial support he has provided to me over the many years I spent in the School of Aerospace Engineering. Without this support I could not have completed my thesis.

I would like to thank all of my past and present fellow co-works in the Aerospace Engineering department: Ali Kutay, Ramachandra Sattigeri, Dongwon Jung, Suresh Kannan, Allen Wu, Nimrod Rooz, Girish Chowdhary, Jonathan Muse, and Rajeev Chandramohan. My special gratitude goes to Tansel Yucelen with whom I have worked and coauthored several papers.

I also thank Dr. Kyungsoo Kook who has been friend since childhood, and who has supported me. Finally, I really appreciate my family for their patient support and encouragement. They have shaped what and who I am.

Contents

List of Tables

List of Figures

SUMMARY

This dissertation presents novel adaptive control laws in both state feedback and output feedback forms. In the setting of state feedback adaptive control $\mathcal{K}$-modification provides a tunable stiffness term that results in a frequency dependent filtering effect, smoother transient responses, and time delay robustness in an adaptive system. $\mathcal{K}$-modification is combined with the recently developed Kalman filter (KF) based adaptive control and derivative-free (DF) adaptive control. $\mathcal{K}$-modification and its combinations with KF adaptive control and DF adaptive control preserve the advantages of each of these methods and can also be combined with other modification methods such as σ- and e-modification. An adaptive output feedback control law based on a state observer is also developed. The main idea behind this approach is to apply a parameter dependent Riccati equation to output feedback adaptive control. The adaptive output feedback approach assumes that a state observer is employed in the nominal controller design. The observer design is modified and employed in the adaptive part of the design in place of a reference model. This is combined with a novel adaptive weight update law. The weight update law ensures that estimated states follow both the reference model states and the true states so that both state estimation errors and state tracking errors are bounded. Although the formulation is in the setting of model following adaptive control, the realization of the adaptive controller uses the observer of the nominal controller in place of the reference model to generate an error signal. Thus the only components that are added by the adaptive controller are the realizations of the basis functions and the weight adaptation law. The realization is even less complex than that of implementing a model reference adaptive controller in the case of state feedback. The design procedure of output feedback adaptive control is illustrated with two examples: a simple wingrock dynamics model and a more complex aeroelastic aircraft transport model.

Chapter I

INTRODUCTION

1.1 Background and Motivation

Adaptive control is a natural way to control a system with uncertainties and to enhance robustness of uncertain systems with minimal sacrifice in performance. The goal of adaptive control is to achieve improved system performance with minimal reliance on accurate modeling. Adaptive control approaches directly or indirectly adjust feedback control gains and improve system performance in the face of system uncertainty. Direct adaptive control adjusts the control gains directly in response to system variations, whereas indirect adaptive control uses parameter update laws to identify system parameters and adjust feedback gains to account for system variation. Adaptive control can be used to satisfy performance requirements in the presence of large scale parameter uncertainty, and can provide improved safety in the event of actuator failure.

Applying an adaptive controller implies replacement of an existing control system in some instances. However, it is highly desirable to consider an adaptive approach that can be implemented in a form that augments an existing controller, rather than replace it with an entirely new control system. This rationale has been a main driving force for applying adaptive control in Ref's. [1, 2, 4, 14, 66] and in this thesis.

The use of a neural network (NN) in adaptive control broadens the class of uncertainties that can be treated by adaptive control. It is well established that a NN can approximate any continuous function to any desired accuracy on a compact set [21, 26]. This universal approximator property of NNs has been applied as a tool for designing adaptive controllers for uncertain nonlinear systems [13]. In the early to mid 1990's, the feasibility of using NNs was illustrated in identification and control for uncertain nonlinear systems through various simulation studies [44–46, 49]. The potential of employing NNs to compensate for structural flexibility treated as an uncertainty in systems was demonstrated in [15,30,31,37,56]. These

approaches were essentially experimental evaluations of the simulation studies in [45, 49] and lacked a stability proof. Since the mid 1990's, several control methods together with stability proofs based on Lyapunov's direct method have been proposed to employ NNs in a state feedback setting [10, 40, 53, 57]. The NN-based control method in [40] was tested on a single-link flexible beam and shown to outperform conventional PD and PID controllers in [24]. Extensions to NN-based adaptive output feedback have been developed either by employing a high-gain observer [22,59,61], or by incorporating a second NN in the estimation process [28, 36].

1.2 Modifications in MRAC

Model Reference Adaptive Control (MRAC) is derived from the model following problem or model reference control problem. The general idea behind MRAC is to create a closed loop controller with parameters that can be updated to change the response of the system. The output of the system is compared to a desired response from a reference model and the control parameters are updated based on this error. The objective is for the parameters to converge to a set of values that cause the plant response to match the response of the reference model.

There have also been numerous efforts focused on improving MRAC laws. Modification terms related to adding damping are commonly introduced in the weight update law. So-called σ-modification [33] adds a pure damping term, while e-modification [47] adds a variable damping term that depends on the magnitude of the error signal. In general, these modification terms are added to ensure that the adapted weights remain bounded. A projection operator [54] has also been used to bound the weights. Background learning [34] uses current and past data concurrently in the adaptation process to improve adaptive system performance. Q-modification [64] was intended to improve adaptation performance by using a moving window of the integrated system uncertainty. An optimal control theory based modification term [51] was also developed in order to improve adaptation in the presence of large adaptive gain. Recently, an adaptive loop recovery (ALR) approach [7] has been introduced as a modification term with the goal of recovering the loop transfer properties

of a reference model. A Kalman filter (KF) based approach [67, 71] has been suggested as a modification method that achieves better conditioning in terms of the magnitude of the adaptation gain required for a given level of tracking performance and the associated level of control activity.

In this thesis we develop a novel modification term called $\mathcal{K}$-modification [35] which can be used to introduce a stiffness term to the aforementioned methods of modification. When combined with well known σ- or e-modification it provides a means for influencing both the natural frequency and damping ratio in the error transients.

The KF optimization approach is extended to a KF-based adaptation law in [72]. This generalization allows one to replace a fixed gain adaptation law with a time varying gain adaptation law that is optimization based. A model reference adaptive control law, referred to as KF-σ-$\mathcal{K}$, is developed in this thesis by combining KF-based adaptation with σ- and $\mathcal{K}$-modification methods to maintain the benefits provided by each of these individual methods. It is shown that the KF-σ-$\mathcal{K}$ combination is preferable to the combination of KF-, $\mathcal{K}$-, and e-modification in view of prescribed damping and stiffness.

There have been numerous approaches focused on MRAC dealing with nonlinear uncertain dynamical system [6, 9, 32, 33, 41, 47, 48, 54, 58, 63]. These approaches are based on Lyapunov theory and derive a weight update law in the form of an ordinary differential equation for the weight estimates by assuming that there exists an unknown constant ideal set of weights. This assumption seems to be reasonable and MRAC architecture works well on most systems. But the assumption of constant ideal weights may require a higher adaptation gain than is needed to achieve a prescribed level of performance. High adaptation gain can excite unmodelled dynamics, produce an excessive amount of control activity [67, 71], and amplify the effect of sensor noise.

Recently a derivative-free model reference adaptive control (DF-MRAC) [68, 70] was introduced as an extension of the iterative learning approach adopted in [11]. DF-MRAC uses the information of delayed weight estimates and the information of current system states and errors. In DF-MRAC, the assumption of constant unknown ideal weights is relaxed to the existence of time-varying weights such that fast variation in weights is allowed

without assuming the existence of their derivatives. The error dynamics are shown to be uniformly ultimately bounded (UUB) using a Lyapunov-Krasovskii functional without employing any modification terms in the adaptive law.

In this thesis $\mathcal{K}$-modification is applied to DF-MRAC to combine the benefits provided by each of these individual methods. Instead of using the pure integral form of stiffness in $\mathcal{K}$-modification [35], its numerical integral form is used. This results in a derivative-free version of $\mathcal{K}$-modification model reference adaptive control (DF-$\mathcal{K}$-MRAC). The error dynamics are shown to be UUB without the need for additional modification terms to bound the weight estimates. In addition, it is shown DF-$\mathcal{K}$-MRAC allows greater flexibility in selecting the parameters in the DF-MRAC adaptive law.

1.3 Adaptive Output Feedback Control

Research in adaptive output feedback control of uncertain nonlinear systems is motivated by the many emerging applications that employ novel actuation devices for active control of flexible structures and fluid flows. These applications include actuators such as piezo-electric films and synthetic jets, which are typically nonlinearly coupled to the plant dynamics they are intended to control. Models for these applications vary from accurate low frequency models to models that only crudely approximate the true dynamics even at low frequencies. Examples of applications include active damping of flexible structures, control of aeroservoelastic aircraft, and active control of flows.

There have been primarily two approaches to dealing with adaptive output feedback control. One approach is based on a state estimation, whereas the other avoids the use of a state observer. Esfandiari and Khalil [20] introduced a high gain observer for the reconstruction of the unavailable states. Kristic, Kanellakopoulos, Kokotovic [38] and Marino, Tomei [43] have presented backstepping-based approaches to adaptive output feedback control of uncertain systems, which are affine with respect to unknown parameters. They use derivatives of inputs and outputs directly, which is not desirable if there is noise in the system.

Kim and Lewis [36] suggested a NN in the observer structure. Adaptive output feedback

control using a high gain observer and radial basis function NNs has also been proposed by Seshagiri and Khalil [59] for nonlinear systems represented by input-output models. Another method involving design of an adaptive observer using function approximators and backstepping control was given by Choi and Farrel [12] for a limited system that can be transformed to output feedback form in which nonlinearities depend on measurements only. In Calise, Hovakimyan, and Idan [8], a direct adaptive output feedback control design procedure was developed for uncertain nonlinear systems without state estimation but with a stable low pass filter to satisfy a strictly positive real (SPR) condition. Their approach requires that the input vector to the NN be composed of current and past input/output data. However, their approach is limited to single input systems. Hovakimyan, Nardi, Calise, and Kim [27] considered adaptive output feedback control of uncertain nonlinear systems with an error observer instead of a state observer. Volyanskyy, Haddad, and Calise [64] introduced Q-modification to the adaptive output feedback control problem. Yucelen, Haddad, and Calise [73] used a nonminimal state space realization, which constructs a higher input-output equivalent system from the original system. Lavretsky [39] introduced an adaptive output feedback design using asymptotic properties of LQG/LTR controllers, that asymptotically satisfies the SPR condition.

All of the above approaches, with the exception of that in Ref. [39], significantly increase the level of complexity in adaptive control control design. Our approach is similar in spirit to that of Ref. [39], with the exception that it is less restrictive in that we do not attempt to satisfy an SPR condition, which naturally leads to a formation that relies on the existence of a positive definite solution of a parameter dependent Riccati equation. Therefore, our approach is applicable to non-minimum phase systems.

In this thesis we develop an adaptive output feedback approach assuming that a state observer is employed in the nominal controller design. The observer design is modified and employed in the adaptive part of the design in place of a reference model. This is combined with a novel adaptive weight update law. The weight update law ensures that estimated states follow both the reference model states and the true states so that both state estimation errors and state tracking errors are bounded. Although the formulation is

in the setting of model following adaptive control, the realization of the adaptive controller uses the observer of the nominal controller in place of the reference model to generate an error signal. Thus the only components that are added by the adaptive controller are the realizations of the basis functions and the weight adaptation law. The realization is even less complex than that of implementing a model reference adaptive controller in the case of state feedback.

The stability analysis employs a Lyapunov candidate function that entails the solution of a parameter dependent Riccati equation (rather than a Lyapunov equation) to show that all error signals are uniformly ultimately bounded (UUB). It is shown how the upper limit for the Riccati equation parameter is employed in the design of the adaptive law, and also influences the ultimate bounds for the state estimate error and the adapted weight error.

1.4 Applications

Three dynamics models are used to illustrate the design procedure of the developed theories in this thesis: a wing-rock dynamics model, a rigid spacecraft, and an aeroelastic generic transport model. The same wing-rock dynamics model is used in $\mathcal{K}$-modification and KF based σ- and $\mathcal{K}$-modification. The rigid spacecraft dynamics model is used to illustrate DF-MRAC with $\mathcal{K}$-modification. The output feedback form of the wing-rock dynamics model is used for a parameter-dependent Riccati equation approach to output feedback adaptive control in Chapter III. Finally, an aeroelastic generic transport model is used for the output feedback adaptive control approach in Chapter IV.

1.4.1 Wing Rock Dynamics

Wing rock is an phenomenon of lateral-directional instability for airplanes flying at high angles of attack, which occurs not only to low-aspect-ratio-configurations but also high-aspect-ratio configurations. Wing rock is triggered by flow asymmetries, developed by negative roll damping, and sustained by nonlinear aerodynamic roll damping. This wing rock phenomenon and its control have been studied in Ref's. [19, 29, 42, 50, 60, 62]. The

differential equation describing the wing rock motion is given by [42, 50, 60]

$$\ddot{\phi} = \frac{\rho U_\infty^2 Sb}{2I_{xx}} C_l + d_0 u \tag{1}$$

where ϕ is the roll angle, ρ is density of air, U_∞ is free-stream velocity, b is wing span, I_{xx} is wing mass moment of inertia, and d_0 is the control effectiveness element relating the input signal u and the angular acceleration. From Ref's. [19, 29, 42, 60], the roll-moment coefficient is expressed as

$$C_l = a_0 + a_1\phi + a_2\dot{\phi} + a_3|\phi|\dot{\phi} + a_4|\dot{\phi}|\dot{\phi} + a_5\phi^3 \tag{2}$$

where the aerodynamic parameters a_i are nonlinear functions of the angle of attack. The state space representation is

$$\begin{aligned} \dot{x}_1 &= x_2 \\ \dot{x}_2 &= f(x) + d_0 u \end{aligned} \tag{3}$$

where $x = (x_1, x_2)^{\mathrm{T}} = (\phi, \dot{\phi})^{\mathrm{T}} \in \mathbb{R}^2$ and

$$f(x) = b_0 + b_1\phi + b_2\dot{\phi} + b_3|\phi|\dot{\phi} + b_4|\dot{\phi}|\dot{\phi} + b_5\phi^3 \tag{4}$$

with the parameters $b_i = \Big(\rho U_\infty^2 Sb/2I_{xx}\Big) a_i$ for $i = 0, 1, \ldots, 5$.

1.4.2 Rigid Spacecraft

For the rotational equations of motion for a rigid spacecraft, Euler's second law is used

$$\underline{\dot{H}}_c = \underline{M}_c \tag{5}$$

where $\underline{H}_c$ is the angular momentum vector evaluated with respect to the center of mass of the rigid body and $\underline{M}_c$ is the net applied moment about the mass center. Since $\underline{H}_c = I_b\underline{\omega}$, $\underline{\omega} = [\omega_1, \omega_2, \omega_3]^{\mathrm{T}}$ is the angular velocity and $\dot{I}_b = 0$ in a body attached frame, the time derivative of $\underline{H}_c$ in the body attached frame is

$$\begin{aligned} &\underline{\dot{H}}_c + \underline{\omega}\times\underline{H}_c = \underline{M}_c \\ &I_b\underline{\dot{\omega}} + \underline{\omega}\times I_b\underline{\omega} = \underline{M}_c \\ &\underline{\dot{\omega}} = -I_b^{-1}\underline{\omega}\times I_b\underline{\omega} + I_b^{-1}\underline{M}_c \end{aligned} \tag{6}$$

where $\times$ denotes vector product. Using the following property of vector product

$$\underline{\omega}\times I_b = \begin{bmatrix} 0 & -\omega_3 & \omega_2 \\ \omega_3 & 0 & -\omega_1 \\ -\omega_2 & \omega_1 & 0 \end{bmatrix} I_b \tag{7}$$

the equation of motion for rigid spacecraft in (6) can be written as

$$\begin{aligned} \dot{\underline{\omega}} &= -I_b^{-1} X I_b \underline{\omega} + I_b^{-1} \underline{M}_c \\ \dot{\underline{\omega}} &= A\underline{\omega} + B\big[u + \Delta(\underline{\omega})\big] \end{aligned} \tag{8}$$

where

$$\begin{aligned} X &\equiv \begin{bmatrix} 0 & -\omega_3 & \omega_2 \\ \omega_3 & 0 & -\omega_1 \\ -\omega_2 & \omega_1 & 0 \end{bmatrix}, \\ A &\equiv 0_{3\times 3}, \quad \Delta(\underline{\omega}) \equiv -X I_b \underline{\omega}, \quad u \equiv \underline{M}_c \end{aligned} \tag{9}$$

1.4.3 Aeroelastic Generic Transport Model

An aeroelastic model of the longitudinal dynamics of a generalized transport model (GTM) was developed in Ref. [52]. This model, illustrated in Figure 1, accounts for interactions between wing bending and torsion and rigid body longitudinal aircraft dynamics with an assumption that the aeroelastic effect of GTM is contributed only by the wing structures. The blue dashed line indicates the location of six slats and six flaps. This model is used to illustrate the application of the adaptive output feedback approach in Chapter IV.

The structural dynamics are modeled using Galerkin's method [25]. In the wing aeroelasticity, the bending and torsional deflections ($\mathcal{W}(x,t)$, $\Theta(x,t)$) were approximated by the method of separation of variables as

$$\begin{aligned} \mathcal{W}(x,t) &= w(t)\Phi(x) \\ \Theta(x,t) &= \theta(t)\Psi(x) \end{aligned} \tag{10}$$

where $w(t)$ and $\theta(t)$ are the generalized coordinates, and $\Phi(x)$ and $\Psi(x)$ are the assumed normalized mode shapes subject to fixed-end symmetric boundary conditions at the wing

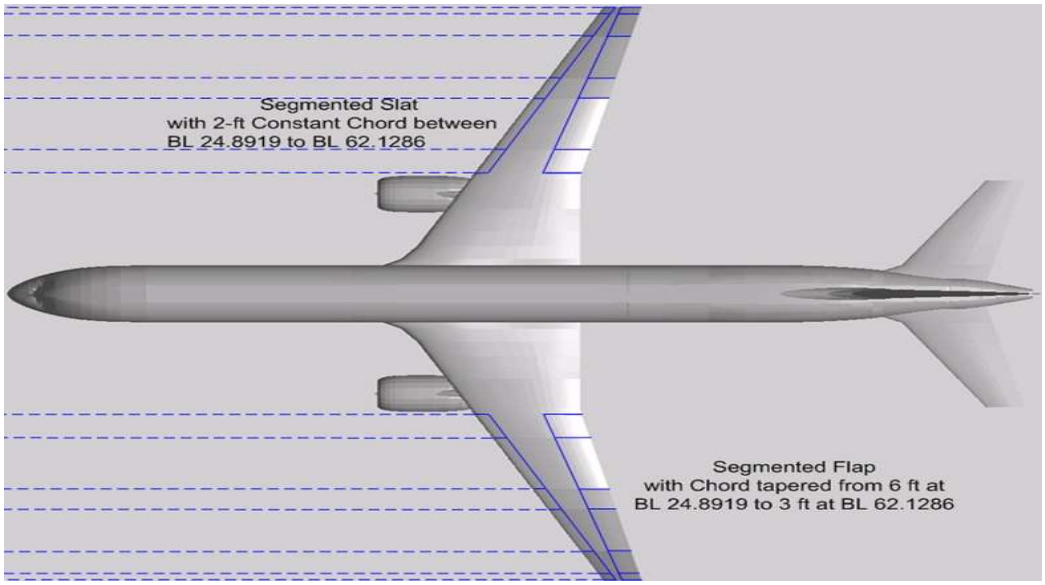

Figure 1: Aeroelastic Generic Transport Model.

root $x = 0$ and the wing tip section $x = L$, and it is shown in Figure 2

$$\begin{aligned} \Phi(x) &= \cosh(cx) - \cos(cx) - \frac{\cosh(cL) + \cos(cL)}{\sinh(cL) + \sin(cL)}\big[\sinh(cx) - \sin(cx)\big] \\ \Psi(x) &= \sqrt{2}\sin\frac{\pi x}{2L} \end{aligned} \tag{11}$$

where $cL = 1.8751$ is the eigenvalue of the first bending mode of a uniform cantilever beam, and the mode shapes $\Psi(x)$ and $\Psi(x)$ satisfy the normalization condition

$$\int_0^L \Phi^2(x)dx = \int_0^L \Psi^2(x)dx = L \tag{12}$$

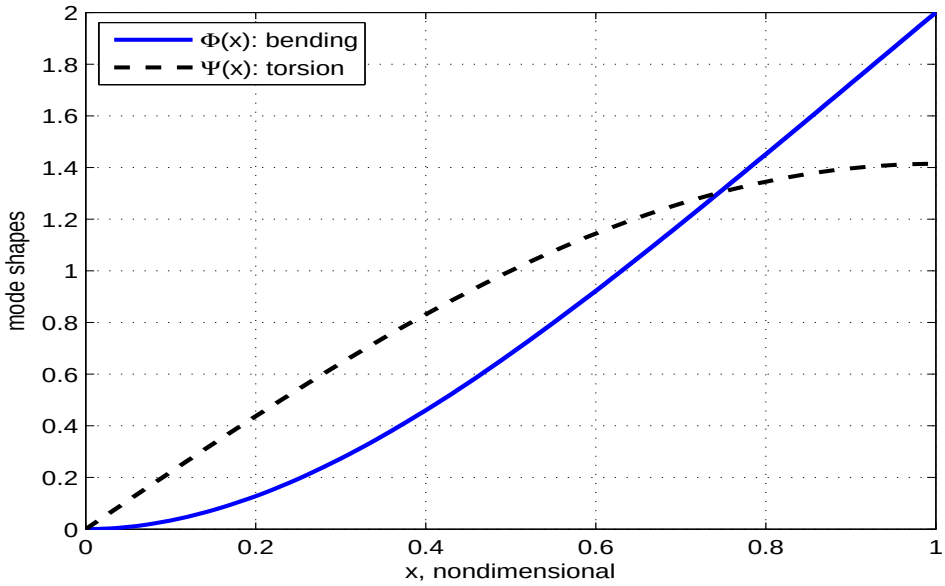

Figure 2: Mode shapes of bending and torsion.

1.5 Thesis Organization

Chapter II develops the theory of a stiffness modification in adaptive control. It also illustrates how to combine $\mathcal{K}$-modification with σ-modification and KF-based adaptive control while preserving the benefits provided by each of these individual methods. Chapter III presents a parameter dependent Riccati equation approach for analyzing the stability properties of a novel output feedback adaptive control law. The methods developed in Chapter III are applied to the aeroelastic GTM in Chapter IV. Conclusions and future research directions are summarized in Chapter V.

1.6 Notation

The following notations are used in this thesis: $\mathbb{R}^n$ denotes the set of $n \times 1$ real column vectors, $\mathbb{R}^{n\times m}$ denotes the set of $n \times m$ real matrices, $(\cdot)^{\mathrm{T}}$ denotes transpose, and $(\cdot)^{-1}$ denotes inverse, $\mathrm{vec}(A)$ is the vector form of a matrix A in which the columns of A are stacked into a vector, $\mathrm{diag}[A, B]$ is a block diagonal matrix formed with matrices A and B on the diagonal, and I_n is an $n \times n$ identity matrix. $\mathrm{tr}[A]$ is the trace of matrix A, $|\cdot|$ denotes vector norm, $\|\cdot\|$ denotes matrix maximum singular value, $\|\cdot\|_F$ denotes Frobenius norm, $\lambda_{\min}(A)$ and $\lambda_{\max}(A)$ denote the minimum and maximum eigenvalues of matrix A, respectively. $\hat{(\cdot)}$ denotes the estimate of $(\cdot)$ and $\tilde{(\cdot)}$ denotes the difference between $(\cdot)$ and $\hat{(\cdot)}$.

Chapter II

STATE FEEDBACK ADAPTIVE CONTROL WITH $\mathcal{K}$-MODIFICATION

2.1 State Feedback Adaptive Control

Consider the stabilizable uncertain nonlinear system

$$\dot{x}(t) = Ax(t) + B[u(t) + \Delta(x(t))] \tag{13}$$

where $A \in \mathbb{R}^{n\times n}, B \in \mathbb{R}^{n\times m}$ are known matrices, $x(t) \in \mathbb{R}^n$ is the state vector, $u(t) \in \mathbb{R}^m$ is the control input vector, $\Delta(\cdot) : \mathbb{R}^n \to \mathbb{R}^m$ is the matched uncertainty, and $y(t) \in \mathbb{R}^p$ is the output vector. The nominal control for the system (13) is given by

$$u_{\mathrm{n}}(t) = -K_x x(t) + K_r r(t) \tag{14}$$

where $r(t) \in \mathbb{R}^r$ is the bounded reference command and $K_x \in \mathbb{R}^{m\times n}$ and $K_r \in \mathbb{R}^{m\times r}$ are given state and input gain matrices. With the system and nominal controller matrices given, a reference model can be constructed in the form

$$\dot{x}_{\mathrm{m}}(t) = A_{\mathrm{m}} x_{\mathrm{m}}(t) + B_{\mathrm{m}} r(t) \tag{15}$$

where $x_{\mathrm{m}}(t) \in \mathbb{R}^n$ is the model state vector.

Assumption 2.1.1 *A_{m} and B_{m} are chosen such that*

$$\begin{aligned} A_{\mathrm{m}} &= A - BK_x \\ B_{\mathrm{m}} &= BK_r \end{aligned} \tag{16}$$

where A_{m} is Hurwitz by design.

Assumption 2.1.2 *The uncertainty in (13) can be linearly parameterized in the form*

$$\Delta(x) = W^{\mathrm{T}}\beta(x) + \varepsilon(x), \quad |\varepsilon(x)| < \epsilon, \quad \forall x \in D_x \subset \mathbb{R}^n \tag{17}$$

where D_x is a sufficiently large compact set, $W \in \mathbb{R}^{q\times m}$ is an unknown constant weight matrix with known bound $\overline{W}$, $\beta(\cdot) : \mathbb{R}^n \to \mathbb{R}^q$ is a bounded basis, and $\varepsilon(\cdot) : \mathbb{R}^n \to \mathbb{R}^m$ is the residual error.

The objective is to augment the nominal control law in (14) so that $x(t)$ asymptotically tracks $x_{\mathrm{m}}(t)$. The augmented control has the form

$$u(t) = u_{\mathrm{n}}(t) - u_{\mathrm{ad}}(t) \tag{18}$$

where

$$u_{\mathrm{ad}}(t) = \hat{W}^{\mathrm{T}}(t)\beta(x(t)) \tag{19}$$

satisfies the adaptive law [33, 47]

$$\dot{\hat{W}}(t) = \gamma\beta(x(t))e^{\mathrm{T}}(t)PB - \dot{\hat{W}}_m(t) \tag{20}$$

where γ is the positive adaptive learning rate, $e(t) = x(t) - x_{\mathrm{m}}(t)$, $\dot{\hat{W}}_m(t)$ is a modification term, i.e. $\dot{\hat{W}}_m(t) = \sigma\hat{W}(t)$ for σ-modification [33] and $\dot{\hat{W}}_m(t) = \lambda|e(t)|\hat{W}(t)$ for e-modification [47] with the positive damping learning rates of σ and λ, and P is a positive-definite solution of the Lyapunov equation for any $Q > 0$

$$0 = A_{\mathrm{m}}^{\mathrm{T}}P + PA_{\mathrm{m}} + Q \tag{21}$$

Figure 3 summarizes the conventional MRAC structure as described above.

This chapter is organized as follows: Section 2.2 introduces $\mathcal{K}$-modification adaptive control, Section 2.3 explains KF-σ-$\mathcal{K}$ adaptive control, and Section 2.4 explains DF-$\mathcal{K}$-MRAC.

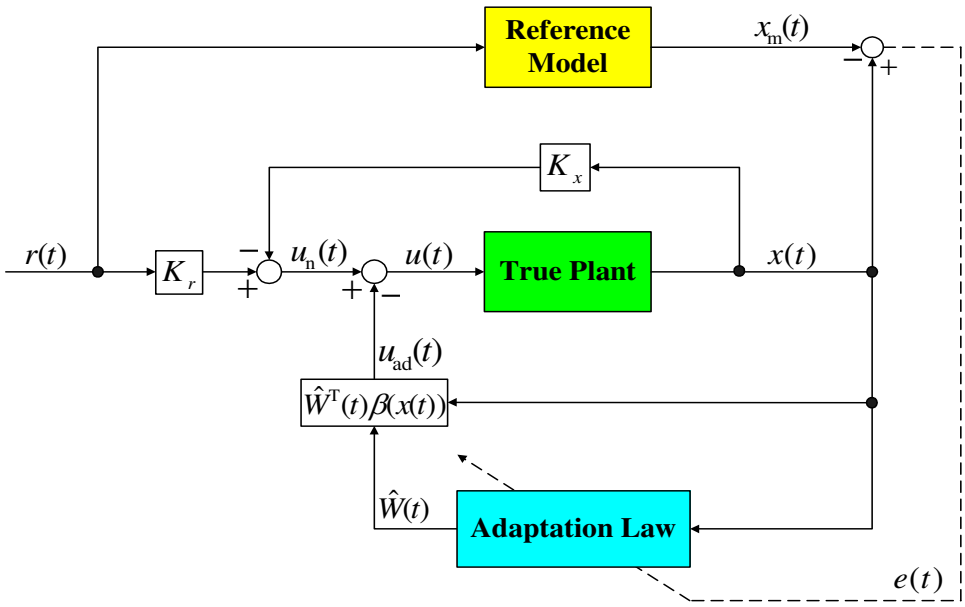

Figure 3: Overall Control System Architecture.

2.2 $\mathcal{K}$-modification

The motivation behind $\mathcal{K}$-modification is the desire to achieve a prescribed natural frequency and damping ratio for the error transients. In this section, $\mathcal{K}$-modification is defined by introducing a stiffness term in the weight update law. The second order characteristics of the update law are studied with respect to damping ratio and natural frequency with a combination of σ- and e-modification terms. The effect of $\mathcal{K}$-modification is interpreted in terms of a state space representation.

2.2.1 Adaptive Control Design with $\mathcal{K}$-modification

The weight adaptation law with $\mathcal{K}$-modification and σ-modification takes the form

$$\dot{\hat{W}}(t) = \gamma\beta(x(t))e^{\mathrm{T}}(t)PB - \sigma\hat{W}(t) - k\int_{t-T}^{t}\hat{W}(s)ds, \quad T > 0 \tag{22}$$

where k is the positive stiffness learning rate.

To understand the effect of $\mathcal{K}$-modification, differentiate the update law in (22) with respect to time and apply the following error dynamics

$$\dot{e}(t) = A_{\mathrm{m}}e(t) - B\tilde{W}^{\mathrm{T}}(t)\beta(x(t)) + B\varepsilon(x(t)) \tag{23}$$

where $\tilde{W}(t) = \hat{W}(t) - W$, and additionaly its dynamics can be written as

$$\dot{\tilde{W}}(t) = \gamma\beta(x(t))e^{\mathrm{T}}(t)PB - \sigma\hat{W}(t) - k\int_{t-T}^{t}\hat{W}(s)ds \tag{24}$$

Then the update law in (22) can be written in the following second order form

$$\ddot{\hat{W}}(t) + C_w\dot{\hat{W}}(t) + K_w\hat{W}(t) = F_w \tag{25}$$

where the damping C_w, stiffness K_w, and forcing F_w terms are:

$$\begin{aligned}
C_w &= \sigma \\
K_w &= \gamma\Big[\beta_x(x(t))Be^{\mathrm{T}}(t) + \beta(x(t))B^{\mathrm{T}}\Big]PB\beta^{\mathrm{T}}(x(t)) + k \\
F_w &= \gamma\Big[\beta_x(x(t))\Big(A_{\mathrm{m}}x(t) + B_{\mathrm{m}}r(t) + B\Delta(x(t))\Big)e^{\mathrm{T}}(t) + \beta(x(t))\Big(A_{\mathrm{m}}e(t) + B\Delta(x(t))\Big)^{T}\Big]PB \\
&\quad + k\hat{W}(t-T)
\end{aligned} \tag{26}$$

When e-modification instead of σ-modification is used with $\mathcal{K}$-modification, we have:

$$
\begin{aligned}
C_w &= \lambda|e(t)| \\
K_w &= \gamma\Big[\beta_x(x(t))Be^{\mathrm{T}}(t) + \beta(x(t))B^{\mathrm{T}}\Big]PB\beta^{\mathrm{T}}(x(t)) + \lambda\frac{e^{\mathrm{T}}(t)\dot{e}(t)}{|e(t)|} + k \\
F_w &= \gamma\Bigg[\beta_x(x(t))\Big(A_{\mathrm{m}}x(t) + B_{\mathrm{m}}r(t) + B\Delta(x(t))\Big)e^{\mathrm{T}}(t) + \beta(x(t))\Big(A_{\mathrm{m}}e(t) + B\Delta(x(t))\Big)^{T}\Bigg]PB \\
&\quad + k\hat{W}(t-T)
\end{aligned}
\tag{27}
$$

where $\hat{W}(t-T)$ is the T time delayed value of $\hat{W}(t)$.

Remark 2.2.1 *The characteristics of the second order form of the weight update law in (25) is analogous to that of a mechanical system. The effects of $\mathcal{K}$-modification on the update law appear only in the stiffness term, K_w, and the forcing term, F_w. The stiffness term is affine in k and forcing term can be viewed as an input that is filtered by the adaptive law. The uncertainty enters the $\hat{W}$ dynamics in (25) only through F_w. The effects of σ- and e- modification on the update law appear in the damping term C_w in both cases. Note that C_w only depends on σ and that K_w is independent of σ in the case of σ-modification, whereas e-modification affects both C_w, in a manner that depends on $|e(t)|$, and K_w in a more complicated manner.*

In the scalar control case ($m = 1$), the filtering effect of the second order weight update law in (25) can be characterized in terms of an equivalent damping ratio and natural frequency:

For the case of σ- and $\mathcal{K}$-modification,

$$
\zeta(t) = \frac{C_w(t)}{2\sqrt{K_w(t)}} = \frac{\sigma}{2\sqrt{\gamma\Big[\beta_x(x(t))Be^{\mathrm{T}}(t) + \beta(x(t))B^{\mathrm{T}}\Big]PB\beta^{\mathrm{T}}(x(t)) + k}} \tag{28}
$$

$$
\omega_{\mathrm{n}}(t) = \sqrt{K_w(t)} = \sqrt{\gamma\Big[\beta_x(x(t))Be^{\mathrm{T}}(t) + \beta(x(t))B^{\mathrm{T}}\Big]PB\beta^{\mathrm{T}}(x(t)) + k} \tag{29}
$$

For the case of e- and $\mathcal{K}$-modification,

$$
\zeta(t) = \frac{C_w(t)}{2\sqrt{K_w(t)}} = \frac{\lambda|e(t)|}{2\sqrt{\gamma\Big[\beta_x(x(t))Be^{\mathrm{T}}(t) + \beta(x(t))B^{\mathrm{T}}\Big]PB\beta^{\mathrm{T}}(x(t)) + \lambda\frac{e^{\mathrm{T}}(t)\dot{e}(t)}{|e(t)|} + k}} \tag{30}
$$

$$\omega_{\mathrm{n}}(t) = \sqrt{K_w(t)} = \sqrt{\gamma\Big[\beta_x(x(t))Be^{\mathrm{T}}(t) + \beta(x(t))B^{\mathrm{T}}\Big]PB\beta^{\mathrm{T}}(x(t)) + \lambda\frac{e^{\mathrm{T}}(t)\dot{e}(t)}{|e(t)|} + k} \quad (31)$$

Remark 2.2.2 *It is clear from (28)-(31) that the product, $\zeta(t)\omega_{\mathrm{n}}(t)$ is proportional only to σ in the case of σ-modification and to $\lambda|e(t)|$ in the case of e-modification. In an under-damped second order system, this product determines the settling time. The above suggests that for a given σ, one should select k so that the resulting damping ratio is reasonable. It is interesting to note that e- modification has the effect of causing the damping ratio to approach zero as $|e(t)|$ approaches zero.*

Remark 2.2.3 *The term $\hat{W}(t-T)$ in (26) and (27) can alternatively be written using Pade's approximation. Using Laplace transform and Pade's first order approximation*

$$\mathcal{L}\big[\hat{W}(t-T)\big] = \mathbf{e}^{-sT}\hat{W}(s) \approx \frac{-s+2T}{s+2T}\hat{W}(s) \quad (32)$$

where $\mathcal{L}$ denotes the Laplacian operator. The Laplace transform of (25) with σ-modification is

$$\begin{aligned} &\mathcal{L}\Big[\ddot{\hat{W}}(t) + C_w\dot{\hat{W}}(t) + K_w(t)\hat{W}(t)\Big] = \mathcal{L}\Big[F_w\Big] \\ &\mathcal{L}\Big[\ddot{\hat{W}}(t)\Big] + \sigma\mathcal{L}\Big[\dot{\hat{W}}(t)\Big] + \mathcal{L}\Big[K_w(t)\hat{W}(t)\Big] = \mathcal{L}\Big[F_w\Big] \end{aligned} \quad (33)$$

The left hand side of (33) can be written as

$$\begin{aligned} &\Big[s^2\hat{W}(s) - s\hat{W}(0) - \dot{\hat{W}}(0)\Big] + \Big[s\hat{W}(0) - \hat{W}(0)\Big] \\ &+ \mathcal{L}\Big[\underbrace{\Big(\gamma\big[\beta_x(x(t))Be^{\mathrm{T}}(t) + \beta(x(t))B^{\mathrm{T}}\big]PB\beta^{\mathrm{T}}(x(t))\Big)}_{K_{ww}(t)}\hat{W}(t)\Big] + k\hat{W}(s) \end{aligned} \quad (34)$$

With (32) the right hand side of (33) can be written as

$$\mathcal{L}\Big[\underbrace{\Big(\gamma\Big[\beta_x(x(t))\Big(A_{\mathrm{m}}x(t) + B_{\mathrm{m}}r(t) + B\Delta(x(t))\Big)e^{\mathrm{T}}(t) + \beta(x(t))\Big(A_{\mathrm{m}}e(t) + B\Delta(x(t))\Big)^T\Big]PB\Big)}_{F_{ww}(t)}\Big]$$

$$+ k\frac{-s+2T}{s+2T}\hat{W}(s) \quad (35)$$

With (34), (35), and zero initial conditions, (33) can be written as

$$\Big(s^2 + (\sigma+2T)s + 2(\sigma T + k)\Big)\hat{W}(s) = (1 + \frac{2T}{s})\mathcal{L}\big[-K_{ww}(t)\hat{W}(t) + F_{ww}(t)\big] \quad (36)$$

The inverse Laplace transform of (36) is

$$\begin{aligned}&\ddot{\hat{W}}(t) + \big(\sigma + 2T\big)\dot{\hat{W}}(t) + \big(2\sigma T + 2k + K_{ww}(t)\big)\hat{W}(t)\\ &= F_{ww}(t) + 2T\int_0^t \Big(F_{ww}(t) - K_{ww}(t)\hat{W}(t)\Big)dt\end{aligned} \tag{37}$$

Differentiating (37) with respect to t results in the following 3^{rd} *order system*

$$\begin{aligned}&\dddot{\hat{W}}(t) + \big(\sigma + 2T\big)\ddot{\hat{W}}(t) + \big(2\sigma T + 2k + K_{ww}(t)\big)\dot{\hat{W}}(t) + \Big(\dot{K}_{ww}(t) + 2TK_{ww}(t)\Big)\hat{W}(t)\\ &= \dot{F}_{ww}(t) + 2TF_{ww}(t)\end{aligned} \tag{38}$$

This form has the disadvantage that it now is 3^{rd} *order, but may be advantageous in that* $\hat{W}(t)$ *now appears only on the left hand side of the differential equation.*

Remark 2.2.4 *For the case of scalar control, the second order weight update law (25) can be also expressed in state-space form*

$$\begin{aligned}\dot{\Sigma}(t) &= A_\Sigma(t)\Sigma(t) + B_\Sigma F_w(t)\\ \Sigma_y(t) &= C_\Sigma\Sigma(t)\end{aligned} \tag{39}$$

where $\Sigma(t) = [\hat{W}^{\mathrm{T}}(t), \dot{\hat{W}}^{\mathrm{T}}(t)]^{\mathrm{T}} \in \mathbb{R}^{2q}$ *is the state,* $\Sigma_y(t) = \hat{W}(t) \in \mathbb{R}^q$ *is the output,* $F_w(t) \in \mathbb{R}^q$ *is the input, and* $A_\Sigma(t) \in \mathbb{R}^{2q\times 2q}, B_\Sigma \in \mathbb{R}^{2q\times q}, C_\Sigma \in \mathbb{R}^{q\times 2q}$ *are:*

$$A_\Sigma(t) = \begin{bmatrix} 0_{q\times q} & I_{q\times q}\\ -K_w(t) & -C_w\end{bmatrix}, \qquad B_\Sigma = [0_{q\times q}, I_{q\times q}]^{\mathrm{T}}, \qquad C_\Sigma = [I_{q\times q}, 0_{q\times q}] \tag{40}$$

In comparison to e- and σ*-modification,* $\mathcal{K}$*-modification can be viewed as containing a feedback of the delayed weight estimates, which is a consequence of introducing the stiffness term in the update law. This is illustrated in Figure 4, where* $F_o(t)$ *is the value of* $F_w(t)$ *for* $k = 0$*.* $F_o(t)$ *may have oscillations, which can be reduced by the feedback of the* T *time delayed estimated weight* $\hat{W}(t-T)$*. This effect is illustrated in the wing-rock example to be presented later.*

The following theorem summarizes the stability properties associated with the use of σ-modification. Projection is used to ensure that the weights remain bounded. The notation $\mathrm{Proj}(\cdot,\cdot)$ is used to denote the projection operator [54].

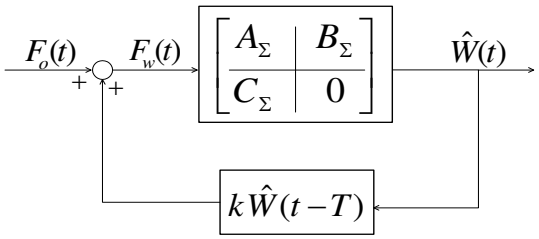

Figure 4: State-space representation of 2nd order weight update law.

Define $\zeta(t) = \left[e(t)^{\mathrm{T}} \mathrm{vec}(\tilde{W}(t)^{\mathrm{T}})\right]^{\mathrm{T}}$ and $B_r = \{\zeta(t) : |\zeta(t)| \leq r\}$ such that $B_r \subset D_\zeta$ for a sufficiently large domain D_ζ. Denote $\tilde{P} \equiv \mathrm{diag}\left[P, \gamma^{-1}I\right]$ and $\alpha \equiv \min_{|\zeta(t)|=r}\left(\zeta(t)^{\mathrm{T}}\tilde{P}\zeta(t)\right) = r^2\lambda_{\min}\left(\tilde{P}\right)$. Define $\Omega_\alpha = \{\zeta(t) \in B_r : \zeta(t)^{\mathrm{T}}\tilde{P}\zeta(t) \leq \alpha\}$. Further define

$$\begin{aligned} c_3 \equiv & \frac{1}{\gamma}\left|\left|\mathrm{tr}\left[\tilde{W}^{\mathrm{T}}(t)\left(\sigma\hat{W}(t) + k\int_{t-T}^{t}\hat{W}(s)ds\right)\right]\right|\right| \\ \Theta_e \equiv & \frac{\|PB\|\epsilon}{\lambda_{\min}(Q)} + \sqrt{\frac{\|PB\|^2\epsilon^2}{\lambda_{\min}(Q)^2} + \frac{2c_3}{\lambda_{\min}(Q)}} \end{aligned} \tag{41}$$

and the projection operator bound, $\Theta_{\tilde{W}}$.

Theorem 2.2.1 *Consider the uncertain nonlinear system given by (13) with $u(t)$ given by (18) and reference model given by (15), subject to Assumptions 2.1.1 and 2.1.2. If $\zeta(0) \in \Omega_\alpha$ and $r^2 > \frac{\lambda_{\max}(P)\Theta_e^2 + \Theta_{\tilde{W}}^2/\gamma}{\lambda_{\min}\left(\tilde{P}\right)}$, then the closed loop system errors defined by (23) and (24) with weight update law*

$$\dot{\hat{W}}(t) = \mathrm{Proj}\left(\hat{W}(t),\ \gamma\beta(x(t))e^{\mathrm{T}}(t)PB - \sigma\hat{W}(t) - k\int_{t-T}^{t}\hat{W}(s)ds\right) \tag{42}$$

where $\gamma > 0$ and $\sigma > 0$, are uniformly ultimately bounded (UUB).

Proof: Consider the Lyapunov function candidate

$$\mathcal{V}(e(t), \tilde{W}(t)) = \frac{1}{2}e^{\mathrm{T}}(t)Pe(t) + \frac{1}{2\gamma}\mathrm{tr}\left[\tilde{W}^{\mathrm{T}}(t)\tilde{W}(t)\right] = \frac{1}{2}\zeta(t)^{\mathrm{T}}\tilde{P}\zeta(t) \tag{43}$$

The derivative of (43) with respect to time can be written as

$$\begin{aligned} \dot{\mathcal{V}} = & \ e^{\mathrm{T}}(t)P\left[A_{\mathrm{m}}e(t) - B\tilde{W}^{\mathrm{T}}(t)\beta(x(t)) + B\varepsilon(x(t))\right] + \frac{1}{\gamma}\mathrm{tr}\left[\tilde{W}^{\mathrm{T}}(t)\dot{\hat{W}}(t)\right] \\ = & -\frac{1}{2}e^{\mathrm{T}}(t)Qe(t) + e^{\mathrm{T}}(t)PB\varepsilon(x(t)) - e^{\mathrm{T}}(t)PB\tilde{W}^{\mathrm{T}}(t)\beta(x(t)) \\ & + \frac{1}{\gamma}\mathrm{tr}\left[\tilde{W}^{\mathrm{T}}(t)\mathrm{Proj}\left(\hat{W}(t),\ \gamma\beta(x(t))e^{\mathrm{T}}(t)PB - \sigma\hat{W}(t) - k\int_{t-T}^{t}\hat{W}(s)ds\right)\right] \end{aligned} \tag{44}$$

Using

$$e^{\mathrm{T}}(t)PB\tilde{W}^{\mathrm{T}}(t)\beta(x(t)) = \mathrm{tr}\Big[\tilde{W}^{\mathrm{T}}(t)\beta(x(t))e^{\mathrm{T}}(t)PB\Big] \tag{45}$$

(44) can be written as

$$\begin{aligned}\dot{\mathcal{V}} =& -\frac{1}{2}e^{\mathrm{T}}(t)Qe(t) + e^{\mathrm{T}}(t)PB\varepsilon(x(t)) - \mathrm{tr}\Big[\tilde{W}^{\mathrm{T}}(t)\beta(x(t))e^{\mathrm{T}}(t)PB\Big] \\ &+ \frac{1}{\gamma}\mathrm{tr}\Big[\tilde{W}^{\mathrm{T}}(t)\mathrm{Proj}\Big(\hat{W}(t),\ \gamma\beta(x(t))e^{\mathrm{T}}(t)PB - \sigma\hat{W}(t) - k\int_{t-T}^{t}\hat{W}(s)ds\Big)\Big]\end{aligned} \tag{46}$$

Letting $Y(t) \equiv \gamma\beta(x(t))e^{\mathrm{T}}(t)PB - \sigma\hat{W}(t) - k\int_{t-T}^{t}\hat{W}(s)ds$, then (46) can be expressed as

$$\begin{aligned}\dot{\mathcal{V}} =& -\frac{1}{2}e^{\mathrm{T}}(t)Qe(t) + e^{\mathrm{T}}(t)PB\varepsilon(x(t)) - \mathrm{tr}\Big[\tilde{W}^{\mathrm{T}}(t)\beta(x(t))e^{\mathrm{T}}(t)PB\Big] \\ &+ \frac{1}{\gamma}\mathrm{tr}\Big[\tilde{W}^{\mathrm{T}}(t)\mathrm{Proj}\Big(\hat{W}(t), Y(t)\Big) - \tilde{W}^{\mathrm{T}}(t)Y(t)\Big] + \frac{1}{\gamma}\mathrm{tr}\Big[\tilde{W}^{\mathrm{T}}(t)Y(t)\Big]\end{aligned} \tag{47}$$

Furthermore, (47) can be written as

$$\begin{aligned}\dot{\mathcal{V}} =& -\frac{1}{2}e^{\mathrm{T}}(t)Qe(t) + e^{\mathrm{T}}(t)PB\varepsilon(x(t)) - \mathrm{tr}\Big[\tilde{W}^{\mathrm{T}}(t)\beta(x(t))e^{\mathrm{T}}(t)PB\Big] \\ &+ \frac{1}{\gamma}\mathrm{tr}\Big[\tilde{W}^{\mathrm{T}}(t)\Big\{\mathrm{Proj}\big(\hat{W}(t), Y(t)\big) - Y(t)\Big\}\Big] + \mathrm{tr}\Big[\tilde{W}^{\mathrm{T}}(t)\beta(x(t))e^{\mathrm{T}}(t)PB\Big] \\ &- \frac{1}{\gamma}\mathrm{tr}\Big[\tilde{W}^{\mathrm{T}}(t)\Big(\sigma\hat{W}(t) + k\int_{t-T}^{t}\hat{W}(s)ds\Big)\Big]\end{aligned} \tag{48}$$

A property of the trace operator is that

$$\mathrm{tr}\Big[\tilde{W}^{\mathrm{T}}(t)\Big\{\mathrm{Proj}\big(\hat{W}(t), Y(t)\big) - Y(t)\Big\}\Big] \leq 0 \tag{49}$$

It also ensures that $\tilde{W}(t)$ satisfies a pre-specified bound, $\Theta_{\tilde{W}}$. Therefore, (48) becomes

$$\begin{aligned}\dot{\mathcal{V}} \leq& -\frac{1}{2}e^{\mathrm{T}}(t)Qe(t) + e^{\mathrm{T}}(t)PB\varepsilon(x(t)) - \frac{1}{\gamma}\mathrm{tr}\Big[\tilde{W}^{\mathrm{T}}(t)\Big(\sigma\hat{W}(t) + k\int_{t-T}^{t}\hat{W}(s)ds\Big)\Big] \\ \leq& -\frac{1}{2}\lambda_{\min}(Q)|e(t)|^2 + \|PB\|\epsilon|e(t)| - \frac{\sigma}{\gamma}\mathrm{tr}\Big[\tilde{W}^{\mathrm{T}}(t)\hat{W}(t)\Big] - \frac{k}{\gamma}\mathrm{tr}\Big[\tilde{W}^{\mathrm{T}}(t)\int_{t-T}^{t}\hat{W}(s)ds\Big]\end{aligned} \tag{50}$$

Due to the projection operator in (42), the third and fourth terms in the second row of (50) are bounded. Let

$$\begin{aligned}c_1 \equiv& \frac{1}{2}\lambda_{\min}(Q) \\ c_2 \equiv& \|PB\|\epsilon \\ c_3 \equiv& \frac{1}{\gamma}\Big|\Big|\mathrm{tr}\Big[\tilde{W}^{\mathrm{T}}(t)\big(\sigma\hat{W}(t) + k\int_{t-T}^{t}\hat{W}(s)ds\big)\Big]\Big|\Big|\end{aligned} \tag{51}$$

Finally, (50) becomes

$$\dot{\mathcal{V}} \leq -c_1|e(t)|^2 + c_2|e(t)| + c_3 = -c_1\Big(|e(t)| - \frac{c_2}{2c_1}\Big)^2 + \frac{c_2^2}{4c_1} + c_3 \tag{52}$$

Consequently, we can conclude that

$$|e(t)| > \Theta_e, \quad \|\tilde{W}(t)\| > \Theta_{\tilde{W}} \tag{53}$$

renders $\dot{\mathcal{V}} < 0$. With reference to the sets depicted in Figure 5, define $\Omega_\beta \equiv \{\zeta(t) \in B_r : \zeta(t)^{\mathrm{T}}\tilde{P}\zeta(t) \leq \lambda_{\max}(P)\Theta_e^2 + \Theta_{\tilde{W}}^2/\gamma\}$. Then Ω_α is a positively invariant set if $\Omega_\beta \subset \Omega_\alpha$. This requires that $\lambda_{\max}(P)\Theta_e^2 + \Theta_{\tilde{W}}^2/\gamma < \alpha$. The minimum size of B_r that ensures this condition is

$$r^2 > \frac{\lambda_{\max}(P)\Theta_e^2 + \Theta_{\tilde{W}}^2/\gamma}{\lambda_{\min}(\tilde{P})} \tag{54}$$

Therefore, if $\zeta(0) \in \Omega_\alpha$, then the error dynamics are UUB. ■

Remark 2.2.5 *Invariancy in the error dynamics together with the fact that $x_{\mathrm{m}}(t)$ is bounded ensures that $x(t)$ remains in D_x, if D_x is sufficiently large. It is apparent from (54) that this implies a lower bound on γ that is related to the bound on $x_{\mathrm{m}}(t)$ and the size of D_x, and the lower bound in (54). However it also implies an upper bound on γ. When γ is sufficiently large, then $\lambda_{\min}(\tilde{P}) = 1/\gamma$ and the limiting from this condition in (54) is $r^2 > \gamma\lambda_{\max}(P)\Theta_e^2$.*

Figure 5 illustrates the sets employed in the proof of Theorem 2.2.1.

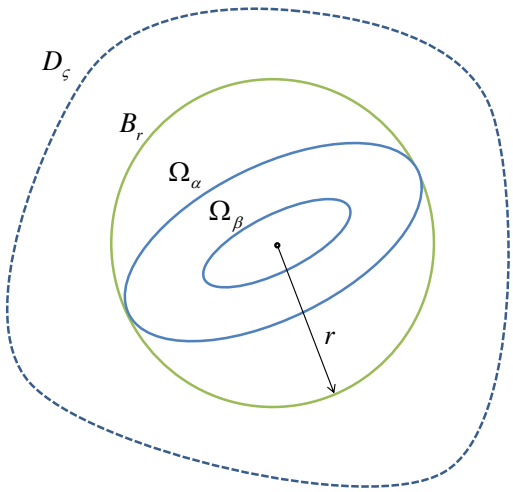

Figure 5: Geometric representation of the sets in Theorem 2.2.1.

The following theorem summarizes the stability properties associated with the use of e-modification. Again, projection is used to ensure that the weights remain bounded. Define

$$\begin{aligned} c_3 \equiv & \frac{k}{\gamma}\Big|\Big|\mathrm{tr}\Big[\tilde{W}^{\mathrm{T}}(t)\int_{t-T}^{t}\hat{W}(s)ds\Big]\Big|\Big| \\ \Theta_e \equiv & \frac{\|PB\|\epsilon+\frac{\lambda}{\gamma}\Big|\Big|\mathrm{tr}\big[\tilde{W}^{\mathrm{T}}(t)\hat{W}(t)\big]\Big|\Big|}{\lambda_{\min}(Q)}+\sqrt{\frac{\Big(\|PB\|\epsilon+\frac{\lambda}{\gamma}\Big|\Big|\mathrm{tr}\big[\tilde{W}^{\mathrm{T}}(t)\hat{W}(t)\big]\Big|\Big|\Big)^2}{\lambda_{\min}(Q)^2}+\frac{2c_3}{\lambda_{\min}(Q)}} \end{aligned} \tag{55}$$

and the projection operator bound, $\Theta_{\tilde{W}}$, as before.

Theorem 2.2.2 *Consider the uncertain nonlinear system given by (13) with $u(t)$ given by (18) and reference model given by (15), subject to Assumptions 2.1.1 and 2.1.2. If $\zeta(0)\in\Omega_\alpha$ and $r^2>\frac{\lambda_{\max}(P)\Theta_e^2+\Theta_{\tilde{W}}^2/\gamma}{\lambda_{\min}(\bar{P})}$, then the closed loop system errors defined by (23) and (24) with weight update law*

$$\dot{\hat{W}}(t)=\mathrm{Proj}\Big(\hat{W}(t),\ \gamma\beta(x(t))e^{\mathrm{T}}(t)PB-\lambda|e(t)|\hat{W}(t)-k\int_{t-T}^{t}\hat{W}(s)ds\Big) \tag{56}$$

where $\gamma>0$ and $\lambda>0$, are UUB.

Proof: Consider the Lyapunov function candidate in (43). In this case (46) becomes

$$\begin{aligned} \dot{\mathcal{V}}=&-\frac{1}{2}e^{\mathrm{T}}(t)Qe(t)+e^{\mathrm{T}}(t)PB\varepsilon(x(t))-\mathrm{tr}\Big[\tilde{W}^{\mathrm{T}}(t)\beta(x(t))e^{\mathrm{T}}(t)PB\Big] \\ &+\frac{1}{\gamma}\mathrm{tr}\Big[\tilde{W}^{\mathrm{T}}(t)\mathrm{Proj}\Big(\hat{W}(t),\ \gamma\beta(x(t))e^{\mathrm{T}}(t)PB-\lambda|e(t)|\hat{W}(t)-k\int_{t-T}^{t}\hat{W}(s)ds\Big)\Big] \end{aligned} \tag{57}$$

Letting $Y_e(t)\equiv\gamma\beta(x(t))e^{\mathrm{T}}(t)PB-\lambda|e(t)|\hat{W}(t)-k\int_{t-T}^{t}\hat{W}(s)ds$, then (47) becomes

$$\begin{aligned} \dot{\mathcal{V}}=&-\frac{1}{2}e^{\mathrm{T}}(t)Qe(t)+e^{\mathrm{T}}(t)PB\varepsilon(x(t))-\mathrm{tr}\Big[\tilde{W}^{\mathrm{T}}(t)\beta(x(t))e^{\mathrm{T}}(t)PB\Big] \\ &+\frac{1}{\gamma}\mathrm{tr}\Big[\tilde{W}^{\mathrm{T}}(t)\mathrm{Proj}\Big(\hat{W}(t),Y_e(t)\Big)-\tilde{W}^{\mathrm{T}}(t)Y_e(t)\Big]+\frac{1}{\gamma}\mathrm{tr}\Big[\tilde{W}^{\mathrm{T}}(t)Y_e(t)\Big] \end{aligned} \tag{58}$$

Following the remaining steps in the proof of Theorem 2.2.1, and defining

$$\begin{aligned} c_1 \equiv & \frac{1}{2}\lambda_{\min}(Q) \\ c_2 \equiv & \|PB\|\epsilon+\frac{\lambda}{\gamma}\Big|\Big|\,\mathrm{tr}\Big[\tilde{W}^{\mathrm{T}}(t)\hat{W}(t)\Big]\Big|\Big| \\ c_3 \equiv & \frac{k}{\gamma}\Big|\Big|\mathrm{tr}\Big[\tilde{W}^{\mathrm{T}}(t)\int_{t-T}^{t}\hat{W}(s)ds\Big]\Big|\Big| \end{aligned} \tag{59}$$

we arrive at

$$\dot{\mathcal{V}} \leq -c_1|e(t)|^2 + c_2|e(t)| + c_3 = -c_1\Big(|e(t)| - \frac{c_2}{2c_1}\Big)^2 + \frac{c_2^2}{4c_1} + c_3 \tag{60}$$

The remaining arguments are the same as in the proof of Theorem 2.2.1, so the only things that changes are the expressions for c_2 and c_3 in (59). ■

2.2.2 Illustrative Example with Wing Rock Dynamics

This section presents two sets of simulation results involving wing-rock dynamics [60]. First, $\mathcal{K}$- combined with e-modification (e-$\mathcal{K}$-modification) results are shown for different values of the adaptation parameters. Second, time delay effects on $\mathcal{K}$ combined with e-modification (e-$\mathcal{K}$-modification) and $\mathcal{K}$ combined with σ-modification (σ-$\mathcal{K}$-modification) are given.

Consider the following wing-rock dynamics

$$\begin{aligned} \dot{x}_1(t) &= x_2(t) \\ \dot{x}_2(t) &= u(t) + \Delta(x(t)) \end{aligned} \tag{61}$$

where $x_1(t)$ and $x_2(t)$ represent roll angle ($\phi(t)$) and roll rate ($\dot{\phi}(t)$),

$$\Delta(x(t)) = b_0 + b_1 x_1(t) + b_2 x_2(t) + b_3|x_1(t)|x_2(t) + b_4|x_2(t)|x_2(t) + b_5 x_1^3(t) \tag{62}$$

with $b_{0,1,2,3,4,5} = [0, 0.2314, 0.6918, -0.6245, 0.0095, 0.0214]$. The control objective here is to eliminate the oscillations caused by the wing rock phenomenon by stabilizing the roll dynamics about the equilibrium condition $(x_1(t), x_2(t)) = (0, 0)$. The initial conditions are selected to be $x_1(0) = \phi(0) = 6^\circ$ and $x_2(0) = \dot{\phi}(0) = 3^\circ$/sec. The reference model is selected to be second order with a natural frequency of 0.5 rad/sec and a damping ratio of 0.707. A combination of bias and sigmoidal basis functions are used, so that $\beta(x) = \big[1, \beta_1(x_1), \beta_2(x_2)\big]^{\mathrm{T}}$, where $\beta_i(x_i) = \frac{1}{1+e^{-x_i}}$. The responses of the nominal closed loop system and the reference model are shown in Figure 6.

Figures 7 through 10 show results with e-$\mathcal{K}$-modification with the adaptation parameter settings summarized in Table 1. In Case 1, the adaptation gain is applied with zero stiffness gain. Figure 7 shows that as the adaptation gain increases the roll angle oscillation and its frequency increase as well as the control effort. Case 2 introduces $\mathcal{K}$-modification with

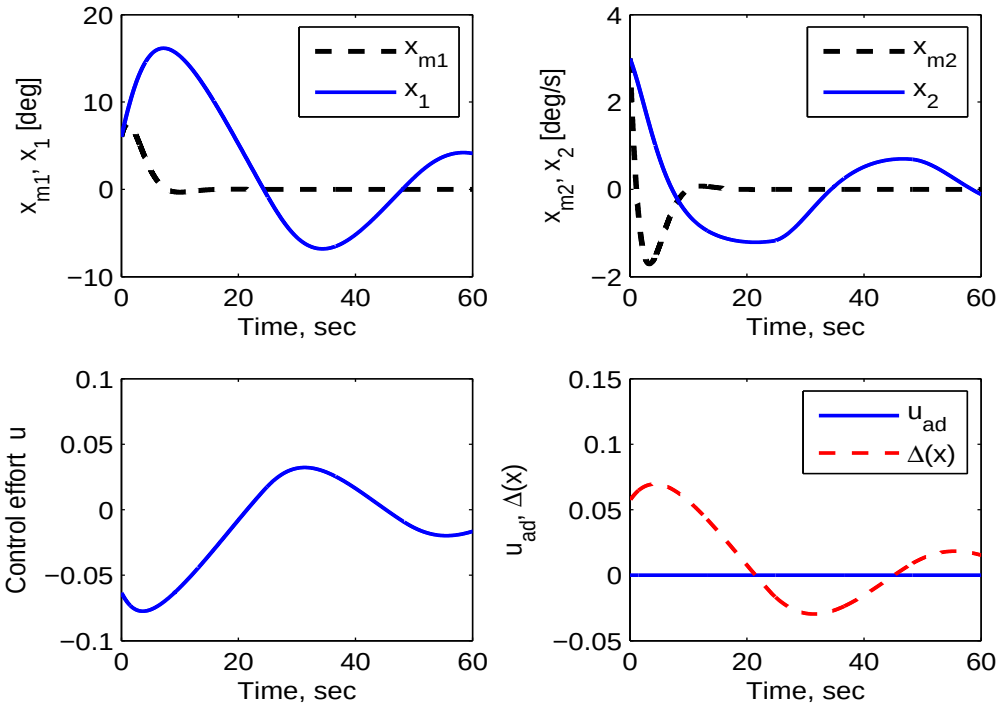

Figure 6: Reference model, aircraft, and nominal control responses with uncertainty.

$k = 100$ and $T = 0.01$ second. Figure 8 shows that the roll angle oscillation and the control effort dramatically decrease. In Case 3, the stiffness gain is increased with fixed adaptation gain. Figure 9 shows that as the stiffness gain increases the roll angle oscillation and its frequency decrease as well as the control effort decreases. Case 4 presents the effect that the value of T used in the weight update law in (22) has on performance with fixed adaptation and stiffness gain. Figure 10 shows that the roll angle oscillation and its frequency as well as the control effort are significantly decreased for values of T in the range 0.01 - 0.1 seconds.

Table 1: Adaptation parameter settings.

	Adaptation gain γ	e-modification λ fixed	Stiffness gain k	T [second]
Case 1	10, 25, 100	100	0	0
Case 2	10, 25, 100	100	250	0.01
Case 3	25	100	100, 250, 500	0.01
Case 4	25	100	250	0.01, 0.05, 0.1

Figures 11 and 12 show responses of e-$\mathcal{K}$-modification with time delay in the control input channel. Oscillations appear in Figure 11, where e-modification alone is used with

time a delay of 0.1 second. Figure 12 shows that these oscillations are significantly reduced by employing $\mathcal{K}$-modification.

Figures 13 and 14 show responses of σ-$\mathcal{K}$-modification with time delay in the control input channel. Oscillations appear in Figure 13, where σ-modification alone is used with time a delay of 0.5 second. Figure 14 shows that these oscillations are significantly reduced by employing $\mathcal{K}$-modification.

2.2.3 Conclusion

This section suggests a way to introduce a tunable stiffness term in the weight update law of an adaptive control system such that smooth transient characteristics can be obtained. The proposed $\mathcal{K}$-modification can be interpreted as a feedback of time delayed values of the weights and filters inputs of the uncertainty according to the tuned damping ratio and natural frequency. The examples also illustrate that robustness to time delay is also improved, however there is no proof of this fact. The example of wing rock dynamics illustrates that oscillations in adaptive systems can be significantly reduced through the appropriate choice of the stiffness parameter in combination with other adaptation gains. $\mathcal{K}$-modification can be also used in combination with other modification methods.

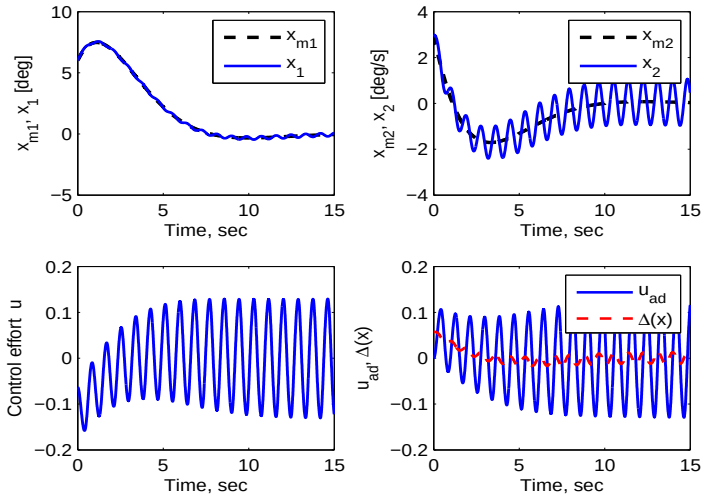

(a) Adaptive control using $\gamma = 10, \lambda = 100, k = 0$

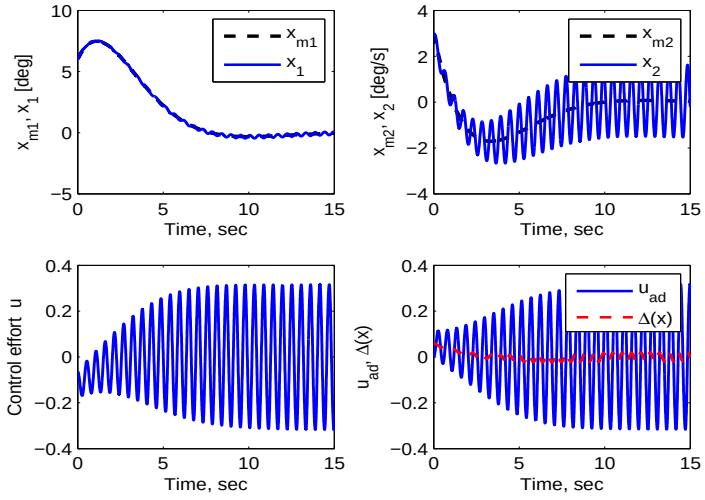

(b) Adaptive control using $\gamma = 25, \lambda = 100, k = 0$

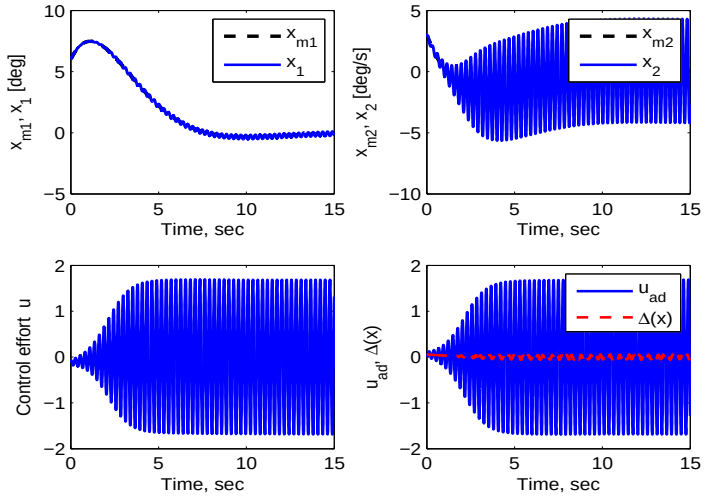

(c) Adaptive control using $\gamma = 100, \lambda = 100, k = 0$

Figure 7: Case 1 - Increasing adaptation gain without stiffness gain.

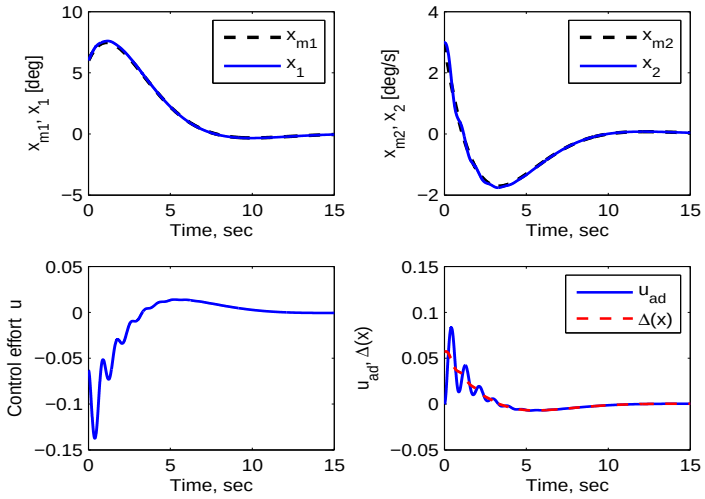

(a) Adaptive control using $\gamma = 10, \lambda = 100, k = 250, T = 0.01$

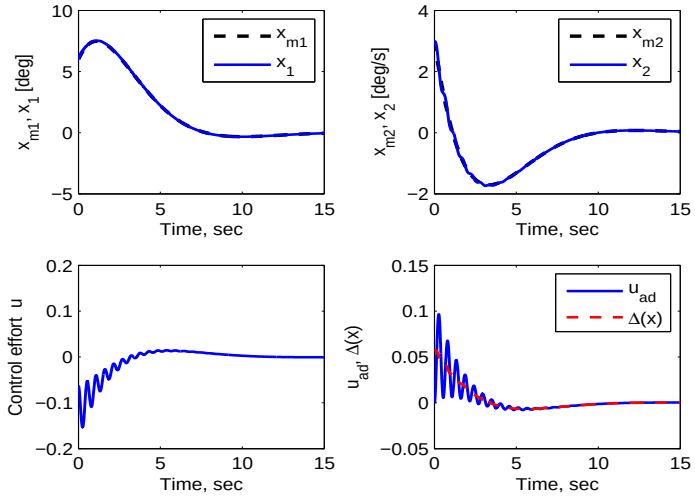

(b) Adaptive control using $\gamma = 25, \lambda = 100, k = 250, T = 0.01$

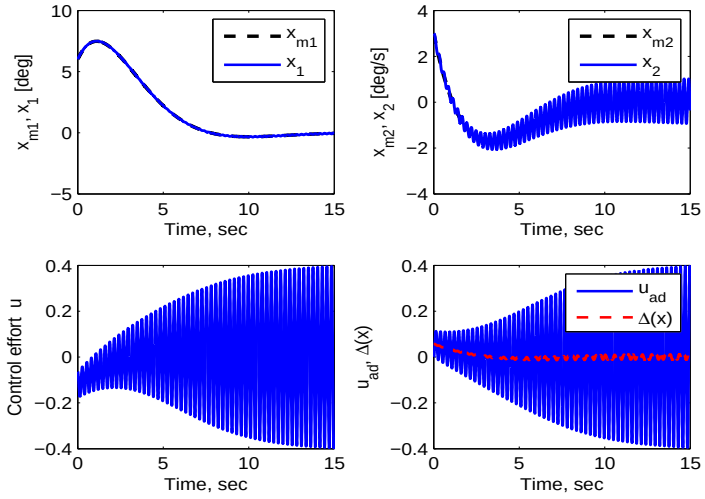

(c) Adaptive control using $\gamma = 100, \lambda = 100, k = 250, T = 0.01$

Figure 8: Case 2 - Increasing adaptation gain with an stiffness gain.

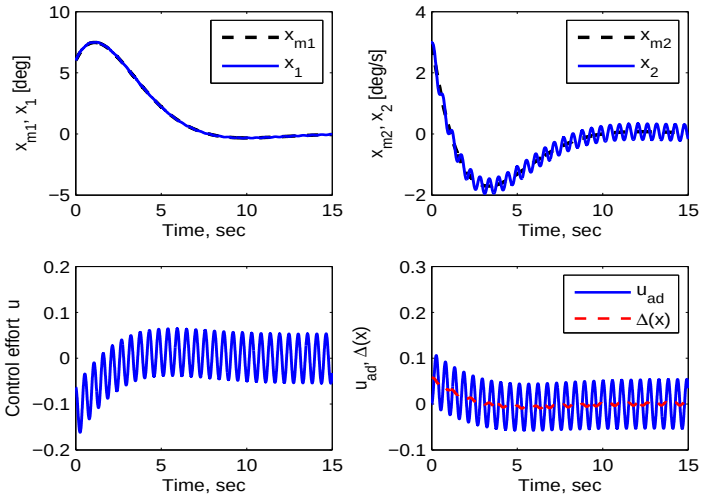

(a) Adaptive control using $\gamma = 25, \lambda = 100, k = 100, T = 0.01$

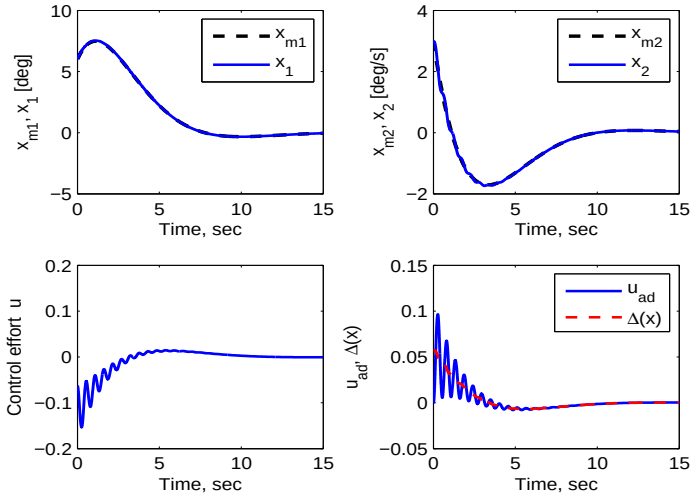

(b) Adaptive control using $\gamma = 25, \lambda = 100, k = 250, T = 0.01$

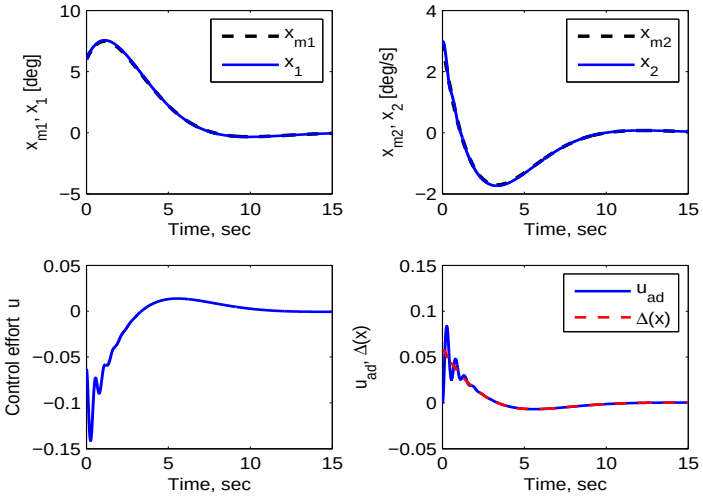

(c) Adaptive control using $\gamma = 25, \lambda = 100, k = 500, T = 0.01$

Figure 9: Case 3 - Increasing stiffness gain.

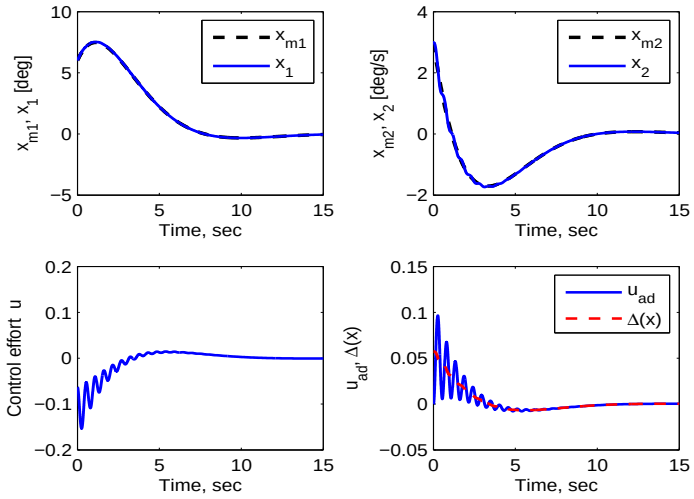

(a) Adaptive control using $\gamma = 25, \lambda = 100, k = 250, T = 0.01$

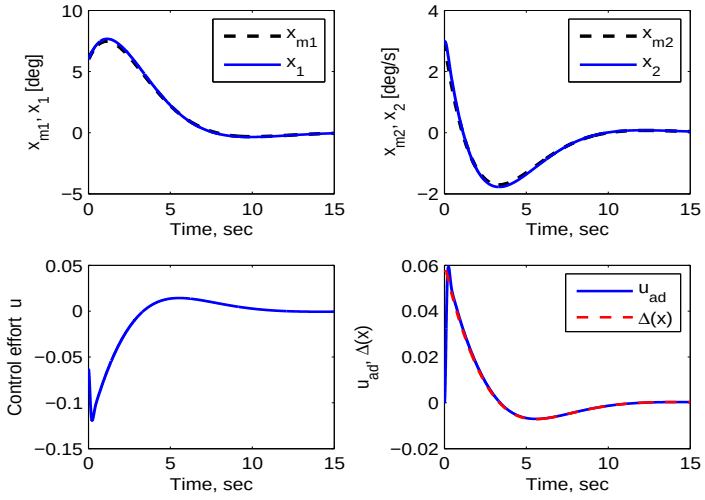

(b) Adaptive control using $\gamma = 25, \lambda = 100, k = 250, T = 0.05$

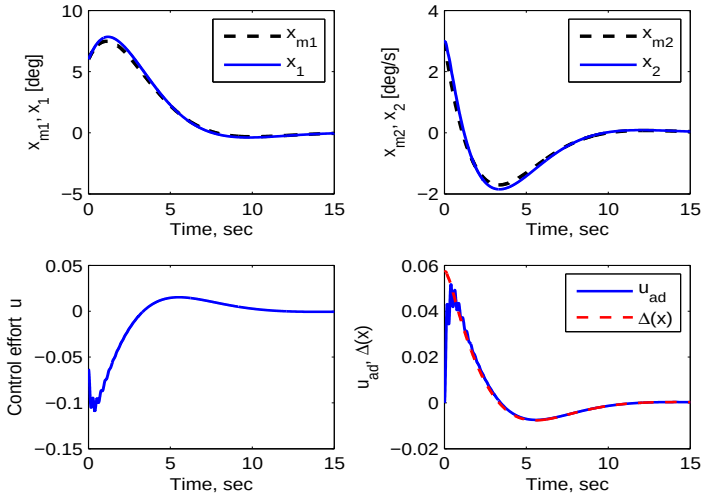

(c) Adaptive control using $\gamma = 25, \lambda = 100, k = 250, T = 0.1$

Figure 10: Case 4 - Increasing updating time interval.

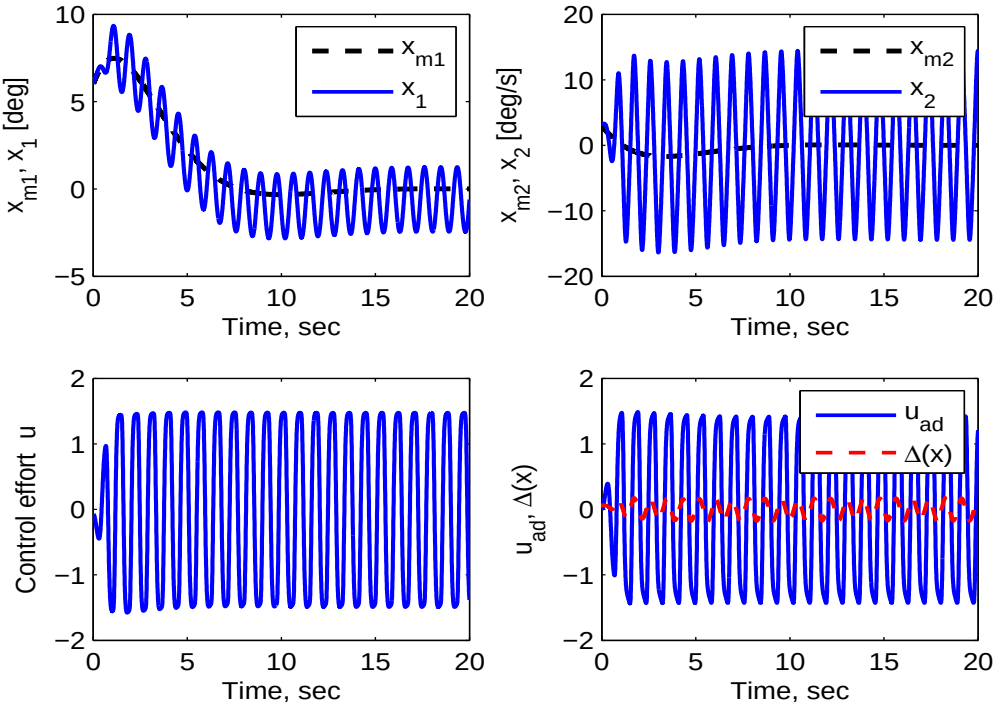

Figure 11: Adaptive control with e-modification and a time delay of 0.1 sec.

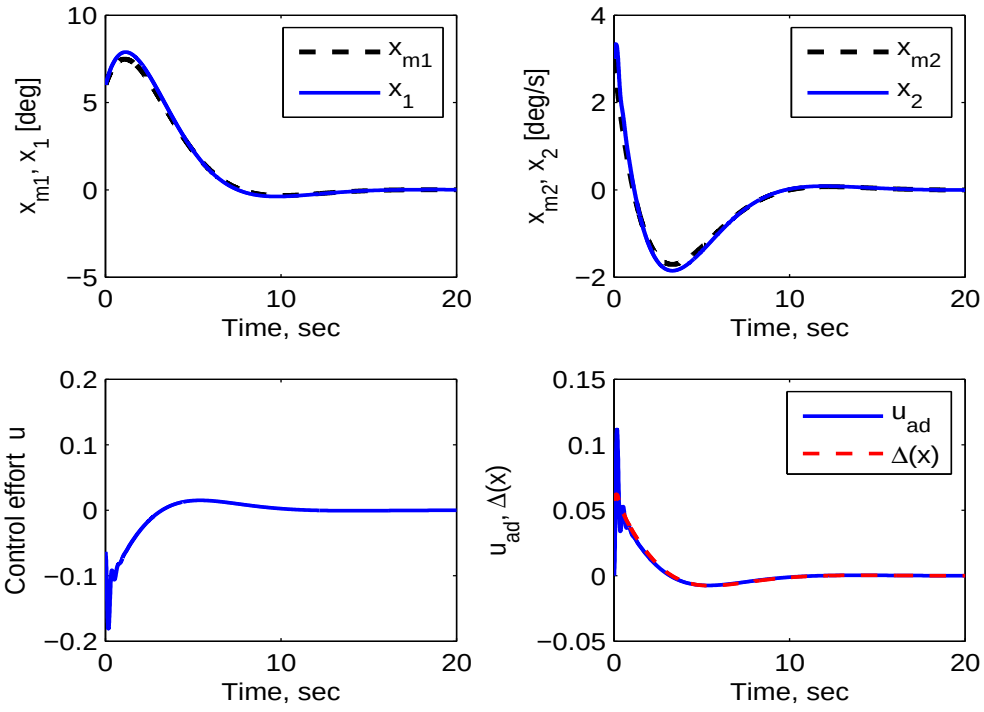

Figure 12: Adaptive control with e-$\mathcal{K}$-modification and a time delay of 0.1 sec.

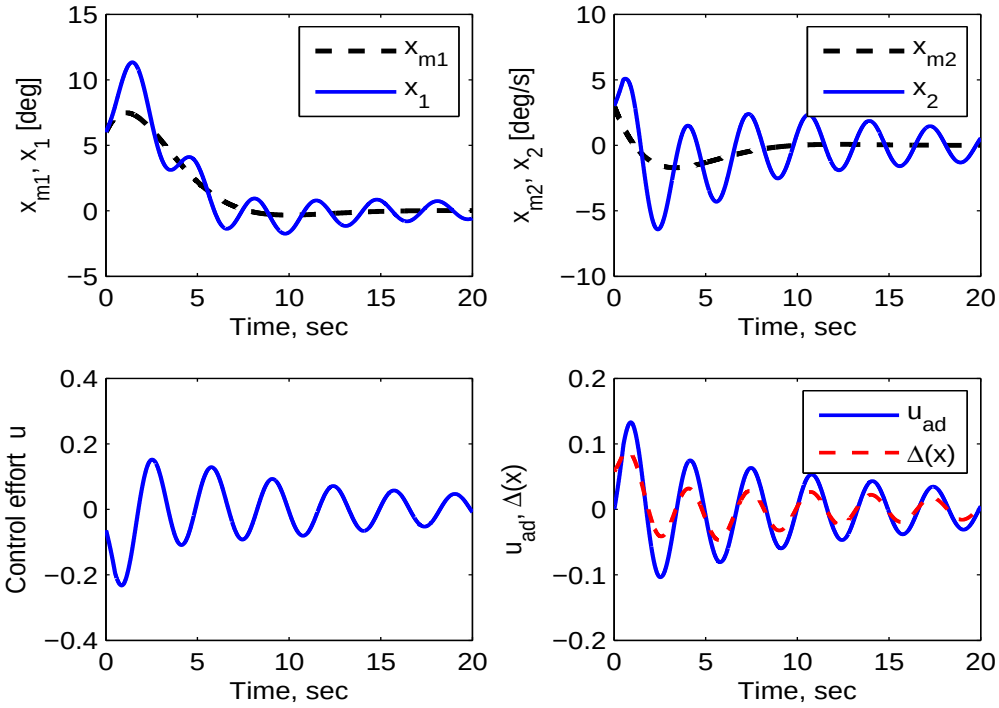

Figure 13: Adaptive control with σ-modification and a time delay of 0.5 sec.

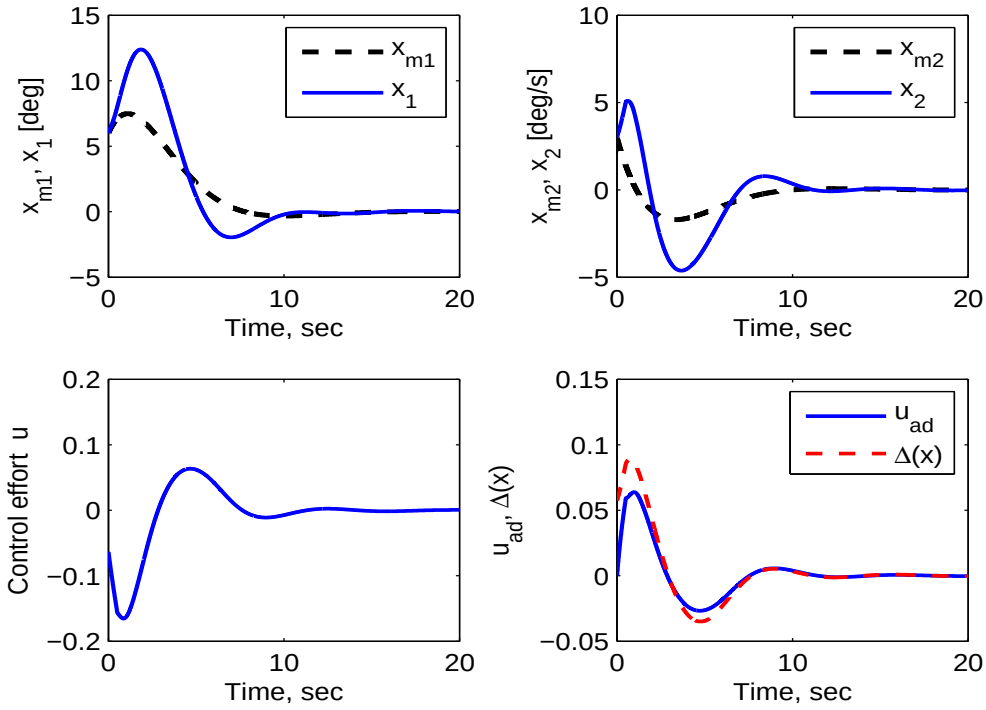

Figure 14: Adaptive control with σ-$\mathcal{K}$-modification and a time delay of 0.5 sec.

2.3 A Kalman Filter Approach to $\mathcal{K}$-modification

Recently a Kalman filter (KF) based adaptive control was developed in Ref. 71. It provides an optimal time varying adaptation gain and achieves better performance than with fixed gain. In this section, KF based adaptive control is combined with $\mathcal{K}$-modification which was introduced in Section 2.2. This section is organized as follows: subsection 2.3.1 provides a brief introduction to KF based adaptive control and its combination with σ- and $\mathcal{K}$-modification. In subsection 2.3.2, a numerical example illustrates the properties of $\mathcal{K}$-modification and KF-σ-$\mathcal{K}$ through the same wing-rock simulation from Section 2.2. Conclusions are given in subsection 2.3.3.

2.3.1 KF based σ- and $\mathcal{K}$-modification

The KF based approach to adaptive control is developed by imposing a constraint on the adapted weights, subject to the following assumption.

Assumption 2.3.1 *The constraint on the ideal weight matrix in an adaptive control design has the linear form*

$$W^{\mathrm{T}}(t)\phi_1(t,x(t),u(t)) = \phi_2(t,x(t),u(t)) \tag{63}$$

where $W(t) \in \mathbb{R}^{s\times m}$ is an unknown weight matrix, $\phi_1(\cdot) : [0,\infty) \times \mathbb{R}^n \times \mathbb{R}^m \to \mathbb{R}^{s\times 1}$ is a given regressor, and $\phi_2(\cdot) : [0,\infty) \times \mathbb{R}^n \times \mathbb{R}^m \to \mathbb{R}^{m\times 1}$ is also a given regressor.

The problem of estimating $W(t)$ while enforcing the linear constraint in (63) can be viewed as a standard problem in estimation theory by defining the stochastic process in a vector form

$$\begin{aligned} \dot{w}(t) &= q(t) \\ z(t) &= \tilde{\phi}_1^{\mathrm{T}}\big(t,x(t),u(t)\big)w(t) + r(t) \end{aligned} \tag{64}$$

where $z(t)$ is a measurement, $w(t) \equiv \mathrm{vec}(\hat{W}(t)) \in \mathbb{R}^{ms}$, $\tilde{\phi}_1(x(t)) \in \mathbb{R}^{ms\times ml}$, and both $q(t)$ and $r(t)$ are zero-mean, Gaussian, white noise processes with known covariances. The estimate of $z(t)$ is expressed as

$$\hat{z}(t) = \tilde{\phi}_1^{\mathrm{T}}\big(t,x(t),u(t)\big)\hat{w}(t) \tag{65}$$

The Kalman filter associated with this problem formulation can be given as:

$$\dot{\hat{W}}(t) = -S(t)\phi_1\big(t, x(t), u(t)\big)R^{-1}\Big[\phi_1(t, x(t), u(t))^{\mathrm{T}}\hat{W}(t) - \phi_2(t, x(t), u(t))^{\mathrm{T}}\Big] \tag{66}$$

where $R \in \mathbb{R}^{l\times l} > 0$ and $S(t)$ satisfies the differential Riccati equation given by

$$\dot{S}(t) = -S(t)\phi_1\big(t, x(t), u(t)\big)R(t)^{-1}\phi_1\big(t, x(t), u(t)\big)^{\mathrm{T}}S(t) + Q_R \tag{67}$$

where $S(t) \in \mathbb{R}^{s\times s}$ and $Q_R \in \mathbb{R}^{s\times s} > 0$. The details are given in [72].

The KF-σ-$\mathcal{K}$ adaptive law is obtained by letting $\phi_1\big(t, x(t), u(t)\big)$ and $\phi_2\big(t, x(t), u(t)\big)$ be the following:

$$\begin{aligned}\phi_1\big(t, x(t), u(t)\big) &= \sqrt{\sigma}I\\ \phi_2\big(t, x(t), u(t)\big) &= \frac{1}{\sqrt{\sigma}}\beta(x(t))e^{\mathrm{T}}(t)PB - \frac{k}{\sqrt{\sigma}}\int_{t-T}^{t}\hat{W}(s)ds\end{aligned} \tag{68}$$

Then, from the constraint in (63) and the equations in (66)-(67), the KF-σ-$\mathcal{K}$ adaptive control law takes on the following form:

$$\begin{aligned}\dot{\hat{W}}(t) &= \Gamma(t)\Big[\beta(x(t))e^{\mathrm{T}}(t)PB - \sigma\hat{W}(t) - k\int_{t-T}^{t}\hat{W}(s)ds\Big]\\ \Gamma(t) &= S(t)R^{-1}\\ \dot{S} &= -S(t)R^{-1}S(t)\sigma + Q_R\end{aligned} \tag{69}$$

where $S(0) \geq 0$, $R = rI > 0$, and $Q_R > 0$.

Remark 2.3.1 *The solution of the differential Riccati equation in (69), $S(t)$, exists, and is symmetric, positive definite, and uniformly bounded for all $t \geq 0$.*

The following theorem summarizes the stability properties associated with KF based σ- and $\mathcal{K}$-modification. Projection is used to ensure that the weights remain bounded. Define $\zeta(t) = \big[e(t)^{\mathrm{T}}\mathrm{vec}(\tilde{W}(t)^{\mathrm{T}})\big]^{\mathrm{T}}$ and $B_r = \{\zeta(t) : |\zeta(t)| \leq r\}$ such that $B_r \subset D_\zeta$ for a sufficiently large domain D_ζ. Denote $\tilde{P} \equiv \mathrm{diag}\big[P, \Gamma^{-1}(t)\big]$ and $\alpha \equiv \min_{|\zeta(t)|=r}\Big(\zeta(t)^{\mathrm{T}}\tilde{P}\zeta(t)\Big) = r^2\lambda_{\min}\big(\tilde{P}\big)$. Define $\Omega_\alpha = \{\zeta(t) \in B_r : \zeta(t)^{\mathrm{T}}\tilde{P}\zeta(t) \leq \alpha\}$. Further define

$$\begin{aligned}c_3 &\equiv \Big|\Big|-\mathrm{tr}\Big[\tilde{W}^{\mathrm{T}}(t)\sigma\hat{W}(t) - k\int_{t-T}^{t}\hat{W}(s)ds\Big] + \frac{1}{2}\mathrm{tr}\Big[\tilde{W}^{\mathrm{T}}(t)\big(\sigma I - M\big)\tilde{W}(t)\Big]\Big|\Big|\\ \Theta_e &\equiv \frac{\|PB\|\epsilon}{\lambda_{\min}(Q)} + \sqrt{\frac{\|PB\|^2\epsilon^2}{\lambda_{\min}(Q)^2} + \frac{2c_3}{\lambda_{\min}(Q)}}\end{aligned} \tag{70}$$

where $M \equiv rS^{-1}(t)Q_RS^{-1}(t)$, and the projection operator bound, $\Theta_{\tilde{W}}$.

Theorem 2.3.1 *Consider the nonlinear uncertain dynamical system given by (13) with the control law given by (18) and reference model given by (15), subject to Assumptions 2.1.1 and 2.1.2. If* $\zeta(0) \in \Omega_\alpha$ *and* $r^2 > \frac{\lambda_{\max}(P)\Theta_e^2 + \|\Gamma^{-1}(t)\|\Theta_{\tilde{W}}^2}{\lambda_{\min}\left(\tilde{P}\right)}$*, then the closed loop system errors given by (23) and (24) with weight update law*

$$\begin{aligned}
\dot{\hat{W}}(t) &= \Gamma(t)\Big\{\mathrm{Proj}\Big(\hat{W}(t),\ \ \beta(x(t))e^{\mathrm{T}}(t)PB - \sigma\hat{W}(t) - k\int_{t-T}^{t}\hat{W}(s)ds\Big)\Big\} \\
\Gamma(t) &= S(t)R^{-1} \\
\dot{S} &= -S(t)R^{-1}S(t)\sigma + Q_R
\end{aligned} \tag{71}$$

where $S(0) > 0$*,* $R = rI > 0$*, and* $Q_R > 0$*, are UUB.*

Proof: Consider the Lyapunov function candidate

$$\mathcal{V}(e(t), \tilde{W}(t)) = \frac{1}{2}e^{\mathrm{T}}(t)Pe(t) + \frac{1}{2}\mathrm{tr}\big[\tilde{W}^{\mathrm{T}}(t)\Gamma^{-1}(t)\tilde{W}(t)\big] \tag{72}$$

where $\Gamma(t) = S(t)R^{-1}$ is positive definite and uniformly bounded KF adaptation gain. To show ultimate boundedness, the proposed weight update law in (71) is used to update the NN weights to force the adaptive parameters to evolve in a prescribed compact region. The time derivative of (72) is written as

$$\begin{aligned}
\dot{\mathcal{V}} = \ & e^{\mathrm{T}}(t)P\Big[A_{\mathrm{m}}e(t) - B\tilde{W}^{\mathrm{T}}(t)\beta(x(t)) + B\varepsilon(x(t))\Big] \\
& + \mathrm{tr}\Big[\tilde{W}^{\mathrm{T}}(t)\Gamma(t)\dot{\hat{W}}(t)\Big] + \frac{1}{2}\mathrm{tr}\Big[\tilde{W}^{\mathrm{T}}(t)\frac{d}{dt}(\Gamma^{-1}(t))\tilde{W}(t)\Big]
\end{aligned} \tag{73}$$

Using the Lyapunov equation in (21) and the weight update law in (71), (73) can be written as

$$\begin{aligned}
\dot{\mathcal{V}} = & -\frac{1}{2}e^{\mathrm{T}}(t)Qe(t) + e^{\mathrm{T}}(t)PB\varepsilon(x(t)) - e^{\mathrm{T}}(t)PB\tilde{W}^{\mathrm{T}}(t)\beta(x(t)) \\
& + \mathrm{tr}\Big[\tilde{W}^{\mathrm{T}}(t)\mathrm{Proj}\Big(\hat{W}(t), \beta(x(t))e^{\mathrm{T}}(t)PB - \sigma\hat{W}(t) - k\int_{t-T}^{t}\hat{W}(s)ds\Big)\Big] \\
& + \frac{1}{2}\mathrm{tr}\Big[\tilde{W}^{\mathrm{T}}(t)\frac{d}{dt}(\Gamma^{-1}(t))\tilde{W}(t)\Big]
\end{aligned} \tag{74}$$

Using the property of trace operator in (45), (74) can be expressed as

$$\begin{aligned}
\dot{\mathcal{V}} = & -\frac{1}{2}e^{\mathrm{T}}(t)Qe(t) + e^{\mathrm{T}}(t)PB\varepsilon(x(t)) \\
& + \mathrm{tr}\Big[\tilde{W}^{\mathrm{T}}(t)\mathrm{Proj}\Big(\hat{W}(t), \beta(x(t))e^{\mathrm{T}}PB - \sigma\hat{W}(t) - k\int_{t-T}^{t}\hat{W}(s)ds\Big) - \tilde{W}^{\mathrm{T}}(t)\Big(\beta(x(t))e^{\mathrm{T}}PB\Big)\Big] \\
& + \frac{1}{2}\mathrm{tr}\Big[\tilde{W}^{\mathrm{T}}(t)\frac{d}{dt}(\Gamma^{-1}(t))\tilde{W}(t)\Big]
\end{aligned} \tag{75}$$

Letting $Y_h = \beta(x(t))e^{\mathrm{T}}PB - \sigma\hat{W}(t) - k\int_{t-T}^{t}\hat{W}(s)ds$, (75) becomes

$$\begin{aligned}\dot{\mathcal{V}} =& -\frac{1}{2}e^{\mathrm{T}}(t)Qe(t) + e^{\mathrm{T}}(t)PB\varepsilon(x(t)) \\ &+ \mathrm{tr}\Big[\tilde{W}^{\mathrm{T}}(t)\big\{\mathrm{Proj}\big(\hat{W}(t), Y(t)\big) - Y(t)\big\}\Big] - \mathrm{tr}\Big[\tilde{W}^{\mathrm{T}}(t)\sigma\hat{W}(t) + k\int_{t-T}^{t}\hat{W}(s)ds\Big] \\ &+ \frac{1}{2}\mathrm{tr}\Big[\tilde{W}^{\mathrm{T}}(t)\frac{d}{dt}(\Gamma^{-1}(t))\tilde{W}(t)\Big]\end{aligned} \tag{76}$$

Also using the inequality property of the projection operator in (49), which ensures that $\tilde{W}(t)$ satisfies a pre-specified bound, $\Theta_{\tilde{W}}$, and

$$\frac{d}{dt}\big(\Gamma^{-1}(t)\big) = -\Gamma^{-1}(t)\dot{\Gamma}(t)\Gamma^{-1}(t) = \sigma I - rS^{-1}(t)Q_R S^{-1}(t) \tag{77}$$

we have

$$\begin{aligned}\dot{\mathcal{V}} \leq& -\frac{1}{2}e^{\mathrm{T}}(t)Qe(t) + e^{\mathrm{T}}(t)PB\varepsilon(x(t)) - \mathrm{tr}\Big[\tilde{W}^{\mathrm{T}}(t)\sigma\hat{W}(t) + k\int_{t-T}^{t}\hat{W}(s)ds\Big] \\ &+ \frac{1}{2}\mathrm{tr}\Big[\tilde{W}^{\mathrm{T}}(t)\big(\sigma I - M\big)\tilde{W}(t)\Big]\end{aligned} \tag{78}$$

where $M \equiv rS^{-1}(t)Q_R S^{-1}(t)$ is bounded. Due to the projection operator in (71) and boundedness of M, the third and fourth terms are bounded. From (78) we have that

$$\dot{\mathcal{V}} \leq -c_1|e(t)|^2 + c_2|e(t)| + c_3 = -c_1\big(|e(t)| - \frac{c_2}{2c_1}\big)^2 + \frac{c_2^2}{4c_1} + c_3 \tag{79}$$

where

$$\begin{aligned}c_1 \equiv& \frac{1}{2}\lambda_{\min}(Q) \\ c_2 \equiv& \|PB\|\epsilon \\ c_3 \equiv& \Big|\Big|-\mathrm{tr}\Big[\tilde{W}^{\mathrm{T}}(t)\sigma\hat{W}(t) - k\int_{t-T}^{t}\hat{W}(s)ds\Big] + \frac{1}{2}\mathrm{tr}\Big[\tilde{W}^{\mathrm{T}}(t)\big(\sigma I - M\big)\tilde{W}(t)\Big]\Big|\Big|\end{aligned} \tag{80}$$

Consequently,

$$|e(t)| > \Theta_e, \quad \|\tilde{W}(t)\| > \Theta_{\tilde{W}} \tag{81}$$

renders $\dot{\mathcal{V}} < 0$. The remaining arguments in the proof of Theorem 2.2.1 still apply. ■

Remark 2.3.2 *Similar to Remark 2.2.5, invariancy in the error dynamics together with the fact that $x_{\mathrm{m}}(t)$ is bounded ensures that $x(t)$ remains in D_x, if D_x is sufficiently large. It is apparent from (54) that this implies a lower bound on $\Gamma(t)$ that is related to the bound on $x_{\mathrm{m}}(t)$ and the size of D_x, and the lower bound in (54). However it also implies an upper bound on $\Gamma(t)$. When $\|\Gamma(t)\|$ is sufficiently large, then $\lambda_{\min}\big(\tilde{P}\big) = \|\Gamma^{-1}(t)\|$ and the limiting from this condition in (54) is $r^2 > \|\Gamma(t)\|\lambda_{\max}(P)\Theta_e^2$.*

2.3.2 Illustrative Example with Wing Rock Dynamics

KF-σ-$\mathcal{K}$ results are illustrated by comparing them to σ-$\mathcal{K}$-modification with and without time delay using the wing rock example introduced in Section 2.2. Figures 15 and 16 show comparisons of σ-$\mathcal{K}$-modification and KF-σ-$\mathcal{K}$ with all adaptation parameters set to 1.0. in both cases. Figure 15 shows the response without time delay, while Figure 16 shows result with a time delay of 0.1 sec. These results indicate that it is not as important to tune the adaptation parameters with KF-σ-$\mathcal{K}$ as it is with σ-$\mathcal{K}$-modification.

2.3.3 Conclusion

The proposed KF based σ- and $\mathcal{K}$ adaptive control law combines the benefits provided by each of individual methods. The system error signals are proven to be uniformly ultimately bounded using the projection based weight update law. It also requires less effort with regard to having to tune the parameters in the adaptive law even though it provides more freedom of tuning parameters of damping and stiffness. KF based σ- and $\mathcal{K}$ adaptive control law reduces significantly oscillations shown in the wing rock simulation with an unit values of damping and stiffness terms when a time delay is applied to the control channel.

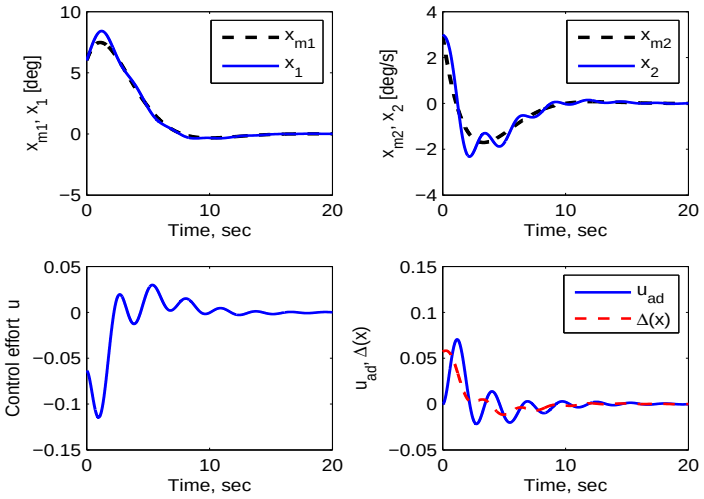

(a) σ-$\mathcal{K}$-mod. with $\gamma = 1$, $\sigma = 1$, $k = 1$, $T = 0.1$

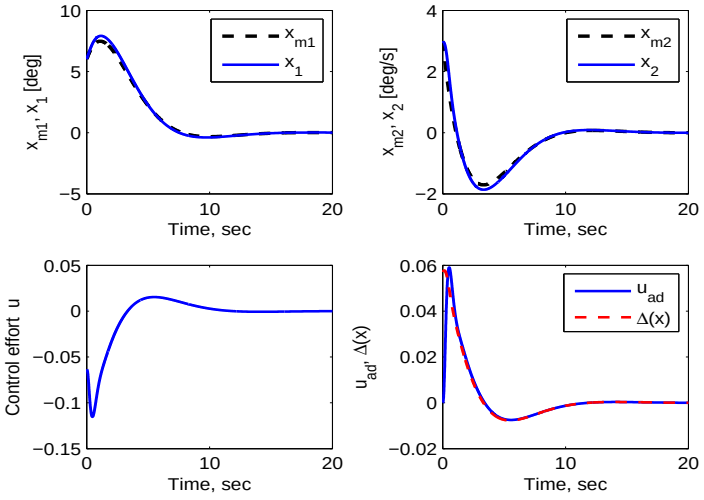

(b) KF-σ-$\mathcal{K}$-AC with $\sigma = 1$, $k = 1$, $T = 0.1$

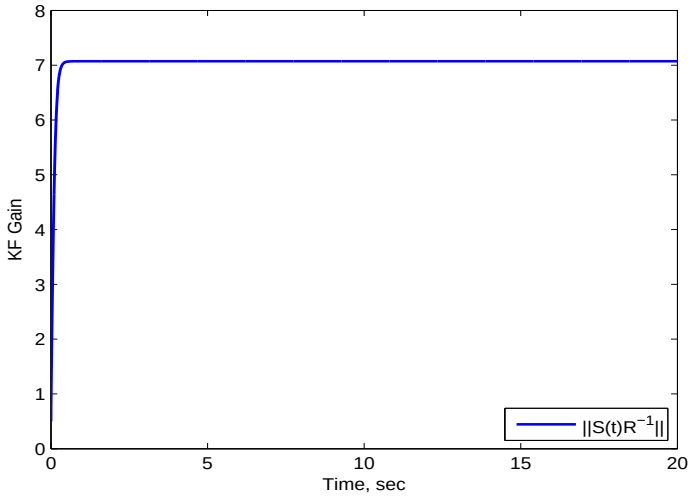

(c) KF Gain

Figure 15: σ-$\mathcal{K}$-modification and KF-σ-$\mathcal{K}$ without time delay.

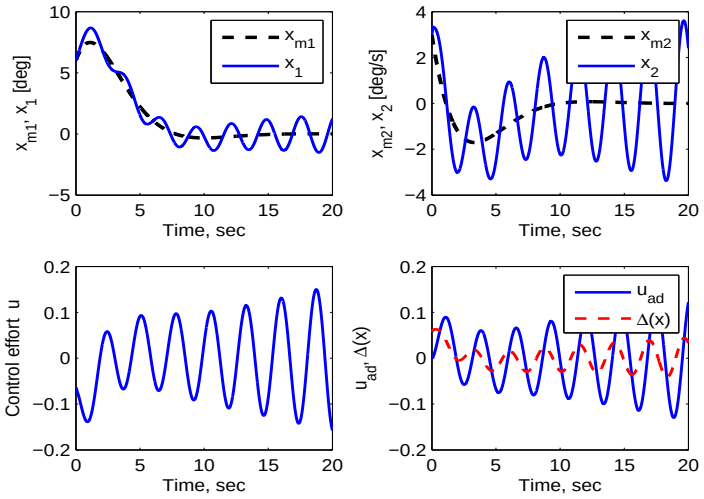

(a) σ-$\mathcal{K}$-mod. with $\gamma = 1$, $\sigma = 1$, $k = 1$, $T = 0.1$, and time delay 0.1 sec

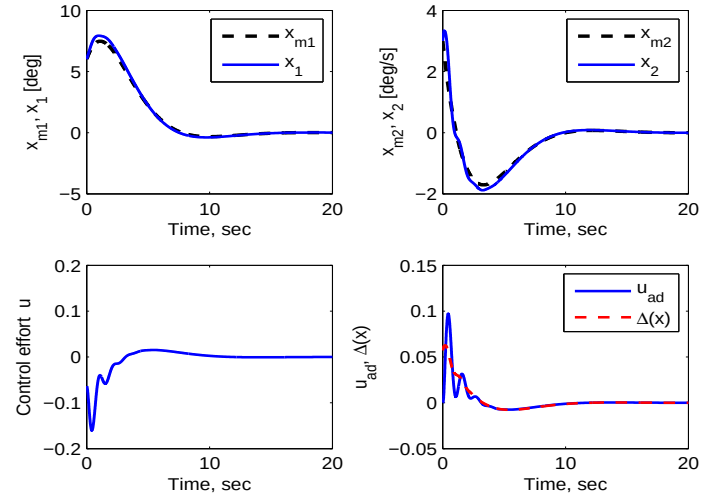

(b) KF-σ-$\mathcal{K}$-AC with $\sigma = 1$, $k = 1$, $T = 0.1$, and time delay 0.1 sec

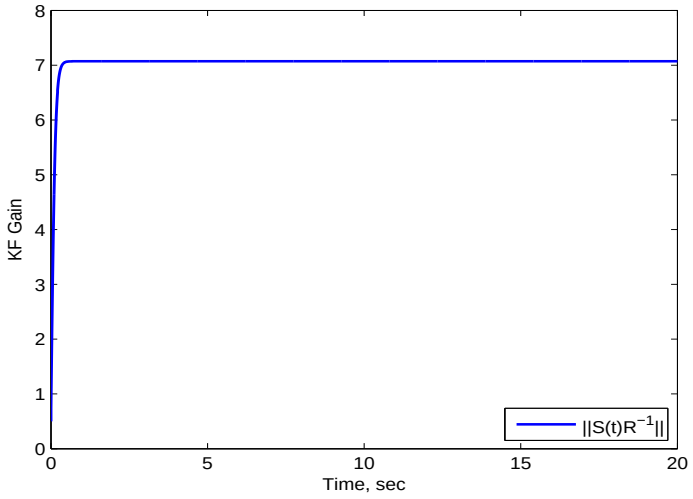

(c) KF Gain

Figure 16: σ-$\mathcal{K}$-modification and KF-σ-$\mathcal{K}$ with time delay 0.1 sec.

2.4 Derivative-Free Model Reference Adaptive Control with $\mathcal{K}$-modification

Conventional MRAC assumes an unknown constant ideal set of weights, and as a result may require a higher adaptation gain than is needed to achieve a prescribed level of performance. High adaptation gain can excite unmodelled dynamics, produce an excessive amount of control activity, and amplify the effect of sensor noise. Recently introduced derivative-free model reference adaptive control (DF-MRAC) in Ref's. [68, 70] uses the information of delayed weight estimates and the information of current system states and errors. In DF-MRAC, the assumption of constant unknown ideal weights is relaxed to the existence of time-varying weights such that fast variation in weights is allowed without assuming the existence of their derivatives.

$\mathcal{K}$-modification is combined with derivative free model reference adaptive control (DF-MRAC). The system error signals are shown to be uniformly ultimately bounded without using additional modification terms. It is shown that $\mathcal{K}$-modification allows better control of the error transient in the DF adaptive law. A spacecraft stabilization example is used to illustrate the benefit of the combined approach.

This section is organized as follows: Subsection 2.4.1 provides a brief background on DF-MRAC. In subsection 2.4.2, DF-MRAC is combined with $\mathcal{K}$-modification. In subsection 2.2.3, a spacecraft stabilization example is used to illustrate the benefit of the combined approach. The example illustrates that DF-$\mathcal{K}$-AC affords greater control of the transient in the error dynamics in the presence of time delay. The results are summarized in subsection 2.2.4.

2.4.1 Derivative-Free MRAC

Consider the uncertain nonlinear dynamical system given in (13) with the following assumption

Assumption 2.4.1 *The matched uncertainty in (13) can be linearly parameterized as*

$$\Delta(x) = W^{\mathrm{T}}(t)\beta(x) \tag{82}$$

where $W(t) \in \mathbb{R}^{s\times m}$ is the unknown time-varying weight matrix that satisfies $\|W(t)\| \leq \omega^*$

and $\beta(\cdot) : \mathbb{R}^n \to \mathbb{R}^s$ *is the bounded basis function vector of the form* $\beta(x) = [\beta_1(x), \beta_2(x), ... , \beta_s(x)]^{\mathrm{T}} \in \mathbb{R}^s$. *With the time-varying weight, the matched uncertainty does not require a residual error* $\varepsilon(x)$.

Furthermore, consider the nominal control in (14), the reference model in (15) with the matching condition in (16), the augmented control form in (18), and the adaptive control in (19).

$\hat{W}(t)$ satisfies the derivative-free adaptive law

$$\hat{W}(t) = \kappa_1 \hat{W}(t-\tau) + \kappa_2 \beta(x(t)) e^{\mathrm{T}}(t) PB \tag{83}$$

where τ is a time delay design value, $e(t) = x(t) - x_{\mathrm{m}}(t)$ is the state tracking error, and P is a positive-definite solution of the Lyapunov equation for any $Q > 0$

$$0 = A_{\mathrm{m}}^{\mathrm{T}} P + P A_{\mathrm{m}} + Q \tag{84}$$

and $\kappa_1 \in \mathbb{R}^{s \times s}$ and $\kappa_2 \in \mathbb{R}$ satisfy

$$\begin{aligned} \kappa_1^{\mathrm{T}} \kappa_1 < I_s \\ \kappa_2 > 0 \end{aligned} \tag{85}$$

Remark 2.4.1 *Let* $\dot{W}_{\mathrm{m}}(t) = 0$ *and apply first order integration to (20) with step size* τ_s. *Then*

$$\hat{W}(t) = \tau_s \gamma \beta(x(t)) e^{\mathrm{T}}(t) PB + \hat{W}(t - \tau_s) \tag{86}$$

This form of weight update law is identical to the DF-MRAC law in (83), if $\kappa_1 = I_s$, $\kappa_2 = \gamma \tau_s$, *and* $\tau = \tau_s$, *and with the exception that the choice of* $\kappa_1 = I_s$ *is not permitted in DF-MRAC. In DF-MRAC,* κ_1 *can be chosen, for example, as* ζI_s *where* $0 < |\zeta| < 1$, *and* τ *is not necessarily equal to* τ_s. *This added dimension in the tuning process provides memory to the adaptive law, and can be employed to improve transient behavior without increasing the effective adaptation gain.*

The state tracking error and weight update error dynamics can be written as:

$$\begin{aligned} \dot{e}(t) &= A_{\mathrm{m}} e(t) + B \tilde{W}^{\mathrm{T}}(t) \beta(x(t)) \\ \tilde{W}(t) &= \kappa_1 \tilde{W}(t-\tau) - \kappa_2 \beta(x(t)) e^{\mathrm{T}} PB + d(t) \end{aligned} \tag{87}$$

where $\tilde{W}(t) = W(t) - \hat{W}(t)$ and $d(t) = W(t) - \kappa_1 W(t-\tau)$.

Theorem 2.4.1 *Consider the controlled nonlinear uncertain dynamical system given by (13) subject to Assumption 2.4.1. In addition, consider the feedback control law given by (18) with the nominal feedback control component given by (14) and with the adaptive control feedback component given by (19) that has a derivative-free weight update law in the form (83). Then $e(t)$ and $\tilde{W}(t)$ given in (87) are UUB.*

Proof: The proof is given in Ref. [68]. ■

Remark 2.4.2 *The assumption in (82) does not place any restriction on the time derivative of the weight matrix. It expands the class of uncertainties that can be represented by a given set of basis functions because time-variation is allowed in the unknown ideal weight matrix. Particularly for time varying disturbances and sudden changes in system dynamics, an adaptive law designed subject to (83) is more effective than an adaptive law that assumes the existence of constant ideal weights, which for example might be expressed as*

$$\Delta(x) = W^{\mathrm{T}}\beta(x) + \varepsilon(x) \tag{88}$$

where W is the unknown constant ideal weight and $\varepsilon(x)$ is the residual error satisfying $|\varepsilon(x)| < \epsilon$ on a sufficiently large bounded set in the state space.

2.4.2 Derivative Free $\mathcal{K}$-modification MRAC

Consider the following DF-MRAC update law from (83) and now with the $\mathcal{K}$-modification.

$$\hat{W}(t) = \kappa_1 \hat{W}(t-\tau) + \kappa_2 \beta(x(t)) e^{\mathrm{T}}(t) PB - \kappa_3 \int_{t-T}^{t} \hat{W}(s) ds \tag{89}$$

This combined weight update law requires the use of a projection operator as in [35] in order to show that the errors are UUB. To avoid the introduction of a projection operator, the integral form of $\mathcal{K}$-modification in (89) is replaced with a numerical integration form. Let's consider two numerical integration forms of $\mathcal{K}$-modification:

$$\begin{aligned} \int_{t_0}^{t_2} \hat{W}(s) ds &\approx \frac{t_2 - t_0}{2} [\hat{W}(t_0) + \hat{W}(t_2)] \\ &\approx \frac{t_2 - t_0}{3} [\hat{W}(t_0) + 4\hat{W}(t_1) + \hat{W}(t_2)] \end{aligned} \tag{90}$$

Remark 2.4.3 *The first expression in (90) uses a Trapezoidal integration rule. When this rule is used for the stiffness term in the update law, the weight update law reduces to a form that is similar to DF-MRAC. The second expression in (90) uses a Simpson's integration rule which is a more accurate integration rule than the Trapezoidal rule, however it is more difficult to analyze.*

The state tracking error dynamics and the weight update error can be written as:

$$\begin{aligned} \dot{e}(t) &= A_{\mathrm{m}} e(t) + B\tilde{W}^{\mathrm{T}}(t)\beta(x(t)) \\ \tilde{W}(t) &= W(t) - \hat{W}(t) \end{aligned} \tag{91}$$

where $e(t) = x(t) - x_{\mathrm{m}}(t)$.

Theorem 2.4.2 *Consider the uncertain nonlinear system given by (13) with the nominal control $u_{\mathrm{n}}(t)$ given by (14) and reference model given by (15), subject to Assumptions 2.1.1 and 2.4.1, and the adaptive control $u_{\mathrm{ad}}(t)$ given by (19) with the weight update law using the Trapezoidal integration rule*

$$\hat{W}(t) = \kappa_1 \hat{W}(t-\tau) + \kappa_2 \beta(x(t)) e^{\mathrm{T}}(t) PB - \kappa_3 \frac{T}{2}\Big[\hat{W}(t) + \hat{W}(t-T)\Big] \tag{92}$$

where $\tau > 0$ and $T > 0$ are updating time intervals for $\hat{W}(t)$ and $\mathcal{K}$-modification term respectively, and the adaptation gains are subject to:

$$\begin{aligned} \kappa_1^{\mathrm{T}} \kappa_1 &< \big(\alpha_1 \Gamma\big)^2 I \\ \kappa_2^{\mathrm{T}} \kappa_2 &= \big(\alpha_2 \Gamma\big)^2 \\ \kappa_3^{\mathrm{T}} \kappa_3 &< \Big(\frac{\alpha_3}{1-\alpha_3}\frac{2}{T}\Big)^2 \end{aligned} \tag{93}$$

where $\kappa_1 \in \mathbb{R}^{s\times s}$, $\kappa_2 \in \mathbb{R}$, $\kappa_3 \in \mathbb{R}$, $\Gamma = 1 + \frac{\kappa_3 T}{2}$ and $0 < \alpha_1 < 1$, $0 < \alpha_2$, $0 < \alpha_3 < 1$. Then the closed loop system errors given by (91) are UUB.

Remark 2.4.4 *Comparing (85) with (93) it can be seen that the upper bound on κ_1 is increased. Also, the Trapezoidal integration rule introduces two additional tuning parameters, κ_3 and T.*

Remark 2.4.5 *$\hat{W}(t)$ appears on both sides of (92) and therefore to implement (92) one must first solve for $\hat{W}(t)$.*

Remark 2.4.6 *When $T = \tau$, (92) reduces to a form that is identical to the derivative-free weight update law in (83).*

Proof of Theorem 2.4.2: The following definitions are introduced to simplify the notation:

$$\begin{aligned} &e \equiv e(t) \\ &\tilde{W} \equiv \tilde{W}(t), \tilde{W}_\tau \equiv \tilde{W}(t-\tau), \tilde{W}_T \equiv \tilde{W}(t-T) \\ &d \equiv d(t), \beta \equiv \beta(x(t)), \Omega \equiv \beta(x(t))e^{\mathrm{T}}(t)PB \end{aligned}$$

With the proposed weight update law in (92), the weight estimation error can be written as

$$\tilde{W} = K_1\tilde{W}_\tau - K_2\beta e^{\mathrm{T}}PB + K_3\tilde{W}_T + d \tag{94}$$

where

$$\begin{aligned} K_1 &= \frac{2\kappa_1}{2+\kappa_3 T} \\ K_2 &= \frac{2\kappa_2}{2+\kappa_3 T} \\ K_3 &= \frac{-\kappa_3 T}{2+\kappa_3 T} \\ d &= W - K_1 W_\tau - K_3 W_T \end{aligned} \tag{95}$$

where $\|d\| \leq \omega^*(1 + \|K_1\| + \|K_3\|)$. Using (94), $\mathrm{tr}\big[\tilde{W}^{\mathrm{T}}\tilde{W}\big]$ can be written as

$$\begin{aligned} \mathrm{tr}\Big[\tilde{W}^{\mathrm{T}}\tilde{W}\Big] = \ &\mathrm{tr}\Big[\tilde{W}_\tau^{\mathrm{T}}K_1^{\mathrm{T}}K_1\tilde{W}_\tau + \Omega^{\mathrm{T}}K_2^{\mathrm{T}}K_2\Omega + \tilde{W}_T^{\mathrm{T}}K_3^{\mathrm{T}}K_3\tilde{W}_T + d^{\mathrm{T}}d \\ &- 2\tilde{W}_\tau^{\mathrm{T}}K_1^{\mathrm{T}}K_2\Omega + 2\tilde{W}_\tau^{\mathrm{T}}K_1^{\mathrm{T}}K_3\tilde{W}_T + 2\tilde{W}_\tau^{\mathrm{T}}K_1^{\mathrm{T}}d \\ &- 2\Omega^{\mathrm{T}}K_2^{\mathrm{T}}K_3\tilde{W}_T - 2\Omega^{\mathrm{T}}K_2^{\mathrm{T}}d + 2\tilde{W}_T^{\mathrm{T}}K_3^{\mathrm{T}}d\Big] \end{aligned} \tag{96}$$

Consider the Lyapunov-Krasovskii functional [23]

$$V(e(t), \tilde{W}(t)) = e^{\mathrm{T}}(t)Pe(t) + \sum_{i=1}^{2} \mathrm{tr}\Big[\rho_i \int_{t-r_i}^{t} \tilde{W}^{\mathrm{T}}(s)\tilde{W}(s)ds\Big] \tag{97}$$

where $r_1 = \tau$, $r_2 = T$, $\rho_1 > 0$, and $\rho_2 > 0$. Differentiating (97) with respect to time, we have

$$\begin{aligned} \dot{V}(e, \tilde{W}) = &- e^{\mathrm{T}}Qe + 2\,\mathrm{tr}\Big[\tilde{W}^{\mathrm{T}}\beta e^{\mathrm{T}}PB\Big] \\ &+ \rho_1\,\mathrm{tr}\Big[\tilde{W}^{\mathrm{T}}\tilde{W} - \tilde{W}_\tau^{\mathrm{T}}\tilde{W}_\tau\Big] + \rho_2\,\mathrm{tr}\Big[\tilde{W}^{\mathrm{T}}\tilde{W} - \tilde{W}_T^{\mathrm{T}}\tilde{W}_T\Big] \end{aligned} \tag{98}$$

where $\dot{V}(e,\tilde{W}) = \dot{V}(e(t),\tilde{W}(t))$. Using $\Omega = \beta e^{\mathrm{T}} PB$ and the expression for $\tilde{W}$ in (91), (98) becomes

$$\begin{aligned}\dot{V}(e,\tilde{W}) =& - e^{\mathrm{T}}Qe + 2\,\mathrm{tr}\Big[\big(K_1\tilde{W}_\tau - K_2\Omega + K_3\tilde{W}_T + d\big)^{\mathrm{T}}\Omega\Big] \\ &+ (\rho_1+\rho_2)\,\mathrm{tr}\Big[\tilde{W}^{\mathrm{T}}\tilde{W}\Big] - \rho\,\mathrm{tr}\Big[\tilde{W}_\tau^{\mathrm{T}}\tilde{W}_\tau\Big] - \rho_2\,\mathrm{tr}\Big[\tilde{W}_T^{\mathrm{T}}\tilde{W}_T\Big]\end{aligned} \tag{99}$$

Define the following:

$$\rho = \rho_1 + \rho_2 > 0$$

$$\eta = 1 + \xi > 1$$

$$\xi > 0$$

$$\lambda > 0$$

Then

$$\begin{aligned}\dot{V}(e,\tilde{W}) =& - e^{\mathrm{T}}Qe + 2\,\mathrm{tr}\Big[\tilde{W}_\tau^{\mathrm{T}}K_1^{\mathrm{T}}\Omega - \Omega^{\mathrm{T}}K_2^{\mathrm{T}}\Omega + \tilde{W}_T^{\mathrm{T}}K_3^{\mathrm{T}}\Omega + d^{\mathrm{T}}\Omega\Big] \\ &- \rho\xi\,\mathrm{tr}\Big[\tilde{W}^{\mathrm{T}}\tilde{W}\Big] + \rho\eta\,\mathrm{tr}\Big[\tilde{W}^{\mathrm{T}}\tilde{W}\Big] - \rho_1\,\mathrm{tr}\Big[\tilde{W}_\tau^{\mathrm{T}}\tilde{W}_\tau\Big] - \rho_2\,\mathrm{tr}\Big[\tilde{W}_T^{\mathrm{T}}\tilde{W}_T\Big]\end{aligned} \tag{100}$$

Using the expression for $\mathrm{tr}\big[\tilde{W}^{\mathrm{T}}\tilde{W}\big]$ in (96), (100) becomes

$$\begin{aligned}\dot{V}(e,\tilde{W}) =& - e^{\mathrm{T}}Qe - \rho\xi\,\mathrm{tr}\Big[\tilde{W}^{\mathrm{T}}\tilde{W}\Big] + 2\,\mathrm{tr}\Big[\tilde{W}_\tau^{\mathrm{T}}K_1^{\mathrm{T}}\Omega - \Omega^{\mathrm{T}}K_2^{\mathrm{T}}\Omega + \tilde{W}_T^{\mathrm{T}}K_3^{\mathrm{T}}\Omega + d^{\mathrm{T}}\Omega\Big] \\ &+ \rho\eta\,\mathrm{tr}\Big[\tilde{W}_\tau^{\mathrm{T}}K_1^{\mathrm{T}}K_1\tilde{W}_\tau + \Omega^{\mathrm{T}}K_2^{\mathrm{T}}K_2\Omega \\ &+ \tilde{W}_T^{\mathrm{T}}K_3^{\mathrm{T}}K_3\tilde{W}_T + d^{\mathrm{T}}d - 2\tilde{W}_\tau^{\mathrm{T}}K_1^{\mathrm{T}}K_2\Omega + 2\tilde{W}_\tau^{\mathrm{T}}K_1^{\mathrm{T}}K_3\tilde{W}_T + 2\tilde{W}_\tau^{\mathrm{T}}K_1^{\mathrm{T}}d \\ &- 2\Omega^{\mathrm{T}}K_2^{\mathrm{T}}K_3\tilde{W}_T - 2\Omega^{\mathrm{T}}K_2^{\mathrm{T}}d + 2\tilde{W}_T^{\mathrm{T}}K_3^{\mathrm{T}}d\Big] \\ &- \rho_1\,\mathrm{tr}\Big[\tilde{W}_\tau^{\mathrm{T}}\tilde{W}_\tau\Big] - \rho_2\,\mathrm{tr}\Big[\tilde{W}_T^{\mathrm{T}}\tilde{W}_T\Big]\end{aligned} \tag{101}$$

Arranging (101) with respect to $\tilde{W}, \tilde{W}_\tau, \tilde{W}_T$, and Ω, then

$$\begin{aligned}\dot{V}(e,\tilde{W}) =& - e^{\mathrm{T}}Qe - \rho\xi\,\mathrm{tr}\Big[\tilde{W}^{\mathrm{T}}\tilde{W}\Big] + \rho\eta\,\mathrm{tr}\Big[d^{\mathrm{T}}d\Big] \\ &+ 2\,\mathrm{tr}\Big[\tilde{W}_\tau^{\mathrm{T}}K_1^{\mathrm{T}}\Omega + \tilde{W}_T^{\mathrm{T}}K_3^{\mathrm{T}}\Omega + d^{\mathrm{T}}\Omega\Big] \\ &+ \mathrm{tr}\Big[\tilde{W}_\tau^{\mathrm{T}}\big(\rho\eta K_1^{\mathrm{T}}K_1 - \rho_1 I\big)\tilde{W}_\tau\Big] \\ &+ \mathrm{tr}\Big[\Omega^{\mathrm{T}}\big(-2K_2^{\mathrm{T}} + \rho\eta K_2^{\mathrm{T}}K_2\big)\Omega\Big] \\ &+ \mathrm{tr}\Big[\tilde{W}_T^{\mathrm{T}}\big(\rho\eta K_3^{\mathrm{T}}K_3 - \rho_2 I\big)\tilde{W}_T\Big] \\ &+ \rho\eta\,\mathrm{tr}\Big[-2\tilde{W}_\tau^{\mathrm{T}}K_1^{\mathrm{T}}K_2\Omega + 2\tilde{W}_\tau^{\mathrm{T}}K_1^{\mathrm{T}}K_3\tilde{W}_T + 2\tilde{W}_\tau^{\mathrm{T}}K_1^{\mathrm{T}}d\Big] \\ &+ \rho\eta\,\mathrm{tr}\Big[-2\Omega^{\mathrm{T}}K_2^{\mathrm{T}}K_3\tilde{W}_T - 2\Omega^{\mathrm{T}}K_2^{\mathrm{T}}d + 2\tilde{W}_T^{\mathrm{T}}K_3^{\mathrm{T}}d\Big]\end{aligned} \tag{102}$$

With the selection of $K_2 = \frac{1}{\rho\eta}$

$$\begin{aligned}\dot{V}(e,\tilde{W}) = &- e^{\mathrm{T}}Qe - \rho\xi \operatorname{tr}\Big[\tilde{W}^{\mathrm{T}}\tilde{W}\Big] - \frac{1}{\rho\eta}\operatorname{tr}\Big[\Omega^{\mathrm{T}}\Omega\Big] + \rho\eta \operatorname{tr}\Big[d^{\mathrm{T}}d\Big] \\ &+ \operatorname{tr}\Big[\tilde{W}_\tau^{\mathrm{T}}\big(\rho\eta K_1^{\mathrm{T}}K_1 - \rho_1 I\big)\tilde{W}_\tau\Big] \\ &+ \operatorname{tr}\Big[\tilde{W}_T^{\mathrm{T}}\big(\rho\eta K_3^{\mathrm{T}}K_3 - \rho_2 I\big)\tilde{W}_T\Big] \\ &+ \rho\eta \operatorname{tr}\Big[2\tilde{W}_\tau^{\mathrm{T}}K_1^{\mathrm{T}}K_3\tilde{W}_T + 2\tilde{W}_\tau^{\mathrm{T}}K_1^{\mathrm{T}}d + 2\tilde{W}_T^{\mathrm{T}}K_3^{\mathrm{T}}d\Big]\end{aligned} \tag{103}$$

Using Young's inequality, the following inequalities hold for $\lambda > 0$.

$$\begin{aligned}\operatorname{tr}\Big[2\rho\eta\tilde{W}_\tau^{\mathrm{T}}K_1^{\mathrm{T}}K_3\tilde{W}_T\Big] \le \operatorname{tr}\Big[\lambda\rho\eta\tilde{W}_\tau^{\mathrm{T}}K_1^{\mathrm{T}}K_1\tilde{W}_\tau\Big] + \operatorname{tr}\Big[\frac{\rho\eta}{\lambda}\tilde{W}_T^{\mathrm{T}}K_3^{\mathrm{T}}K_3\tilde{W}_T\Big] \\ \operatorname{tr}\Big[2\rho\eta\tilde{W}_\tau^{\mathrm{T}}K_1^{\mathrm{T}}d\Big] \le \operatorname{tr}\Big[\lambda\rho\eta\tilde{W}_\tau^{\mathrm{T}}K_1^{\mathrm{T}}K_1\tilde{W}_\tau\Big] + \operatorname{tr}\Big[\frac{\rho\eta}{\lambda}d^{\mathrm{T}}d\Big] \\ \operatorname{tr}\Big[2\rho\eta\tilde{W}_T^{\mathrm{T}}K_3^{\mathrm{T}}d\Big] \le \operatorname{tr}\Big[\lambda\rho\eta\tilde{W}_T^{\mathrm{T}}K_3^{\mathrm{T}}K_3\tilde{W}_T\Big] + \operatorname{tr}\Big[\frac{\rho\eta}{\lambda}d^{\mathrm{T}}d\Big]\end{aligned} \tag{104}$$

Using the three inequalities in (104), (103) can be written as

$$\begin{aligned}\dot{V}(e,\tilde{W}) \le &- e^{\mathrm{T}}Qe - \rho\xi \operatorname{tr}\Big[\tilde{W}^{\mathrm{T}}\tilde{W}\Big] - \frac{1}{\rho\eta}\operatorname{tr}\Big[\Omega^{\mathrm{T}}\Omega\Big] \\ &- \rho\eta \operatorname{tr}\Big[\tilde{W}_\tau^{\mathrm{T}}\Big(-(1+2\lambda)K_1^{\mathrm{T}}K_1 + \frac{\rho_1}{\rho\eta}I\Big)\tilde{W}_\tau\Big] \\ &- \rho\eta \operatorname{tr}\Big[\tilde{W}_T^{\mathrm{T}}\Big(-(1+\frac{1}{\lambda}+\lambda)K_3^{\mathrm{T}}K_3 + \frac{\rho_2}{\rho\eta}I\Big)\tilde{W}_T\Big] \\ &+ \rho\eta \operatorname{tr}\Big[\big(1+\frac{2}{\lambda}\big)d^{\mathrm{T}}d\Big]\end{aligned} \tag{105}$$

From the conditions in (93), define α_1, α_2, and α_3 as:

$$\begin{aligned}\alpha_1 &\equiv \sqrt{\frac{\rho_1}{(1+2\lambda)\rho\eta}} < 1 \\ \alpha_2 &\equiv \frac{1}{\rho\eta} > 0 \\ \alpha_3 &\equiv \sqrt{\frac{\rho_2}{(1+\lambda+\frac{1}{\lambda})\rho\eta}} < 1\end{aligned} \tag{106}$$

With the conditions in (93) and (106), we have that:

$$\begin{aligned}K_1^{\mathrm{T}}K_1 &< \alpha_1^2 I_s \\ K_3^{\mathrm{T}}K_3 &< \alpha_3^2\end{aligned} \tag{107}$$

Finally

$$\begin{aligned}\dot{V}(e(t),\tilde{W}(t)) \leq & -c_1|e(t)|^2 \\ & -c_2\|\tilde{W}(t)\|_F^2 \\ & -c_3\|\tilde{W}(t-\tau)\|_F^2 \\ & -c_4\|\tilde{W}(t-T)\|_F^2 \\ & +c_5\end{aligned} \tag{108}$$

where the constants c_1, c_2, c_3, c_4, and c_5 satisfy the following inequalities:

$$\begin{aligned}c_1 &= \lambda_{\min}(Q) > 0 \\ c_2 &= \rho\xi \\ c_3 &= \rho\eta(1+2\lambda)\lambda_{\min}\Big(\alpha_1^2 I - K_1^{\mathrm{T}}K_1\Big) > 0 \\ c_4 &= \rho\eta(1+\lambda+\frac{1}{\lambda})\lambda_{\min}\Big(\alpha_3^2 I - K_3^{\mathrm{T}}K_3\Big) > 0 \\ c_5 &= \rho\eta\big(1+\frac{2}{\lambda}\big)\|d\|^2\end{aligned} \tag{109}$$

Thus, $|e(t)| > \sqrt{c_5/c_1}$ or $\|\tilde{W}(t)\|_F > \sqrt{c_5/c_2}$ or $\|\tilde{W}(t-\tau)\|_F > \sqrt{c_5/c_3}$ or $\|\tilde{W}(t-T)\|_F > \sqrt{c_5/c_4}$ renders $\dot{V}(e(t),\tilde{W}(t)) < 0$. Therefore it follows that $e(t)$ and $\tilde{W}(t)$ are UUB. ■

2.4.3 Example Simulation with Rigid Spacecraft

Consider the nonlinear dynamical system representing a controlled rigid spacecraft given by Ref. [64]

$$\dot{x}(t) = Ax(t) + B\big[u(t) + \Delta(x(t)) + \delta(t)\big] \tag{110}$$

where $x(t) = [x_1(t), x_2(t), x_3(t)]^{\mathrm{T}}$ represents the angular velocities of the spacecraft with respect to the body-fixed frame, $A = 0_{3\times3}$, $B = I_b^{-1}$, $I_b \in \mathbb{R}^{3\times3}$ is an unknown positive-definite inertia matrix of the spacecraft, $u(t) = [u_1(t), u_2(t), u_3(t)]^{\mathrm{T}}$ is a control input providing body-fixed torques about three mutually perpendicular axes defining the body-fixed frame of the spacecraft, $\delta(t)$ is a disturbance applied to three states as $[10\sin(0.5t), 5\sin(t), 2.5\sin(5t)]^{\mathrm{T}}$, $\Delta(x(t)) = -XI_b x(t)$ is uncertainty, and X denotes the skew-symmetric matrix

$$X \equiv \begin{bmatrix} 0 & -x_3 & x_2 \\ x_3 & 0 & -x_1 \\ -x_2 & x_1 & 0 \end{bmatrix} \tag{111}$$

For our simulation, the initial condition $x(0) = [3, -1, -2]^{\mathrm{T}}$(deg/sec) and

$$I_b \equiv \begin{bmatrix} 40 & -5 & -20 \\ -5 & 80 & -10 \\ -20 & -10 & 60 \end{bmatrix} \tag{112}$$

are used, and the nominal control feedback gain $K_x = \mathrm{diag}[10, 10, 10]$ is used. From the DF-$\mathcal{K}$-AC law in (92), the following adaptation parameters are used: $\kappa_1 = 0.98$, $\kappa_2 = 250$, $\tau = 0.01$ second, $\kappa_3 = 1$, and $T = 0.2$ second.

Figure 17 shows the nominal control responses without uncertainty and disturbance, whereas Figure 18 shows the nominal control responses with both uncertainty and disturbance. Figure 19 through Figure 21 show responses of the standard MRAC in (20) with adaptation gains of $\gamma = 10^3$, 10^4, and 10^5 without modification term. As the gain increases, performance gets better, but the control signal exhibits higher frequency oscillations. Figure 22 shows the comparison between $u_{\mathrm{ad}}(t)$ and $\Delta(x) + \delta(t)$ in MRAC with adaptation gain set to 10^5. The response of the DF-MRAC with uncertainty and disturbance is shown in Figure 23. It achieves the same level of performance as the nominal control response in Figure 17 that was obtained without uncertainty and disturbance, but the control efforts are smaller than the standard MRAC results in Figures 19-21. Figure 24 shows the comparison between $u_{\mathrm{ad}}(t)$ and $\Delta(x) + \delta(t)$ in DF-MRAC.

Figure 25 shows the response of the DF-MRAC with uncertainty, disturbance, and with a time delay of 0.05 seconds introduced in the control channels. Note the oscillations that appear in both the state and control responses. Figure 26 shows the comparison between $u_{\mathrm{ad}}(t)$ and $\Delta(x) + \delta(t)$ in the corresponding environment of DF-MRAC.

Figure 27 shows that these oscillations are significantly reduced when employing DF-$\mathcal{K}$-MRAC, which affords greater control of the error transient through the introduction of a stiffness term in the adaptive law. Figure 28 shows the comparison between $u_{\mathrm{ad}}(t)$ and $\Delta(x) + \delta(t)$ in the corresponding environment of DF-$\mathcal{K}$-MRAC. It achieves the similar level of performance shown in Figure 24 which is the comparison of $u_{\mathrm{ad}}(t)$ and $\Delta(x) + \delta(t)$ in DF-MRAC without time delay.

2.4.4 Conclusion

The proposed DF-$\mathcal{K}$-MRAC combines all the benefits provided by each of individual methods. The system error signals are proven to be uniformly ultimately bounded using a Lyapunov-Krasovskii functional without the need of additional modification terms or a projection operator. A simple spacecraft example shows that the proposed controller provides better performance with less control effort than conventional MRAC and $\mathcal{K}$-MRAC when uncertainty, disturbances, and time delay are applied to the model.

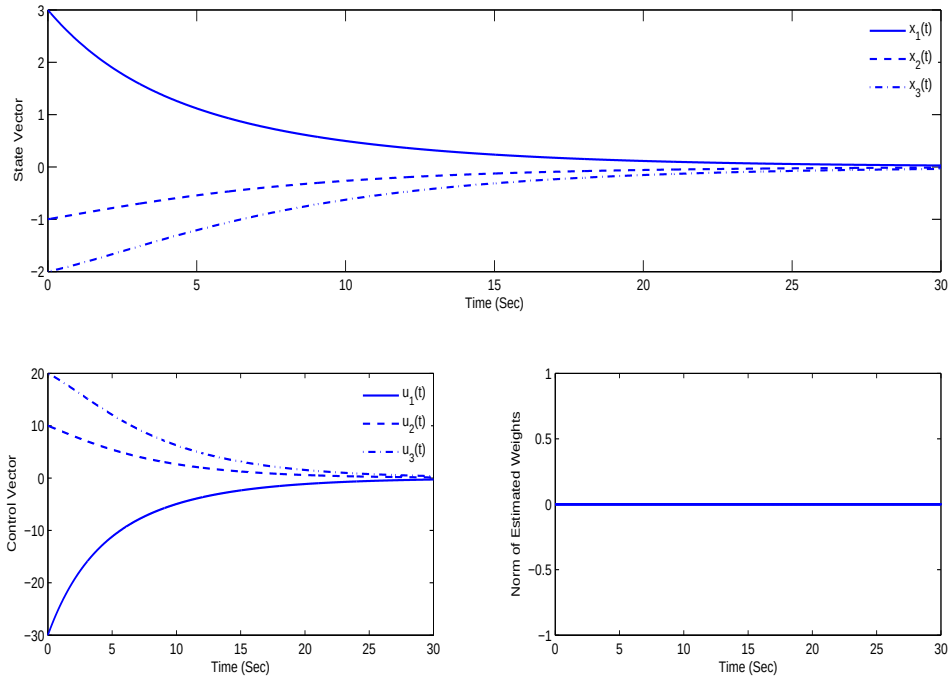

Figure 17: Responses with nominal control, without uncertainty and disturbance.

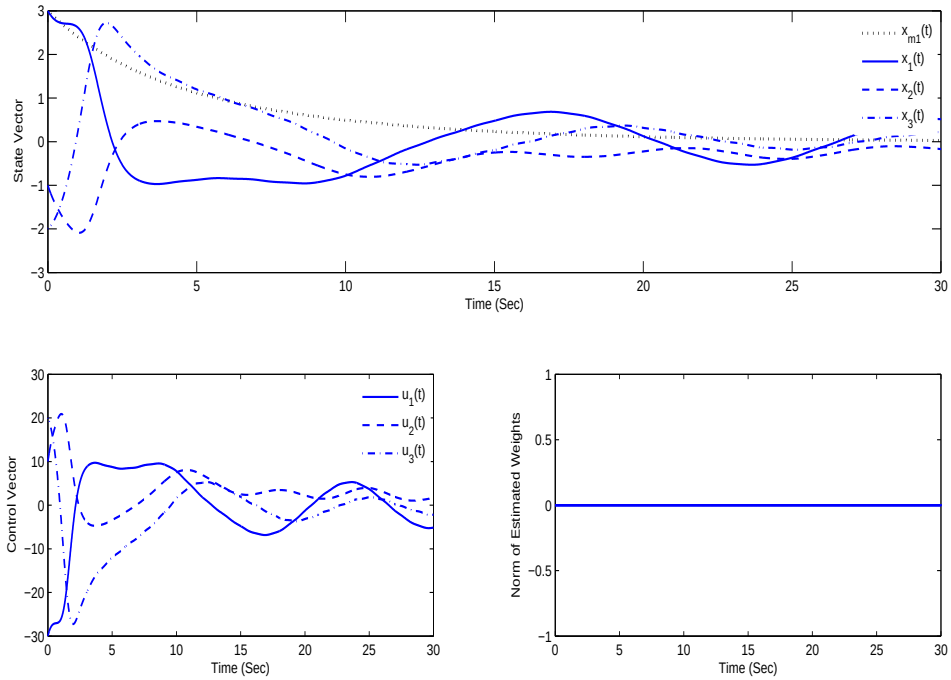

Figure 18: Responses with nominal control, with uncertainty and disturbance.

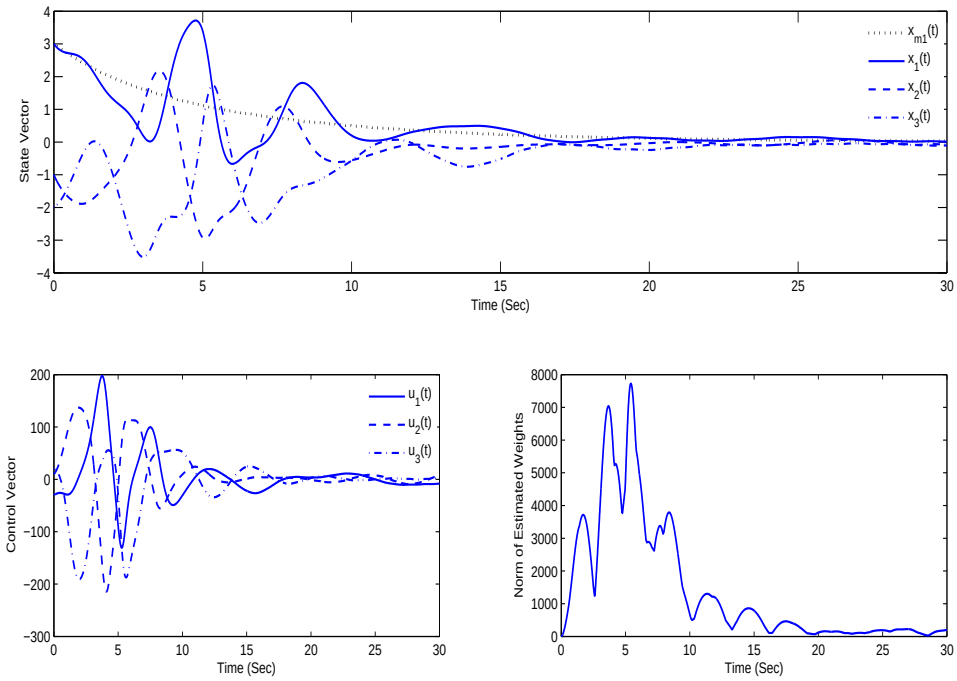

Figure 19: Response with MRAC with adaptation gain set to 10^3, with uncertainty and disturbance.

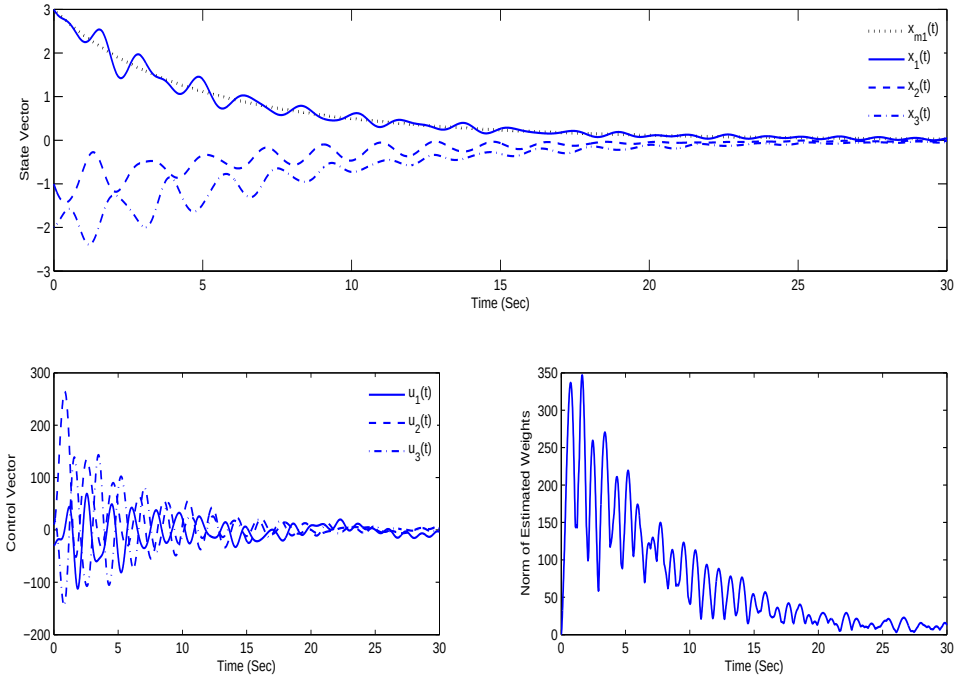

Figure 20: Response with MRAC with adaptation gain set to 10^4, with uncertainty and disturbance.

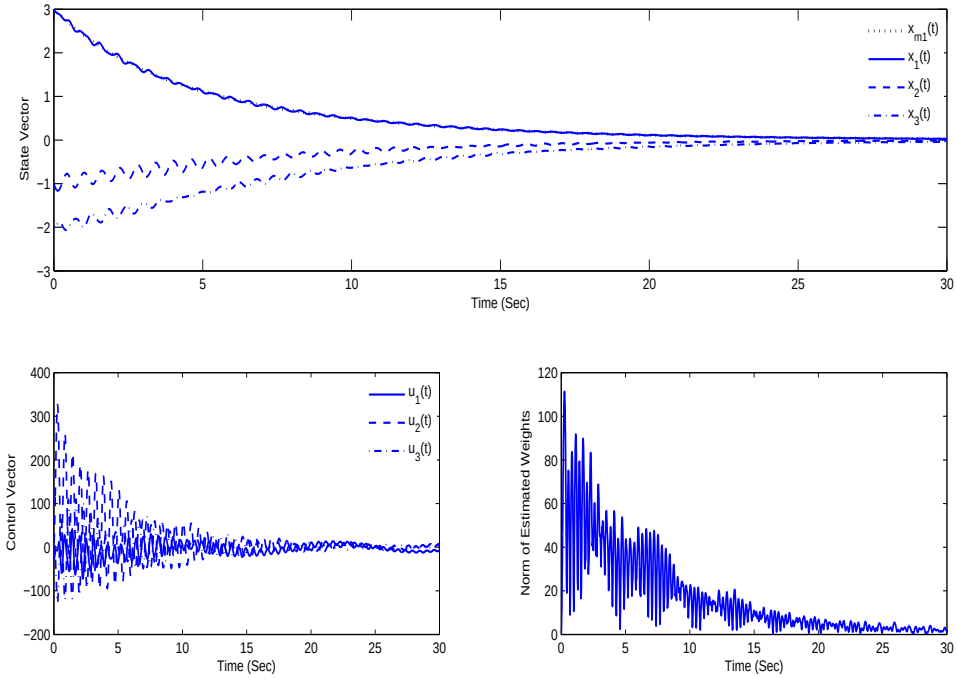

Figure 21: Response with MRAC with adaptation gain set to 10^5, with uncertainty and disturbance.

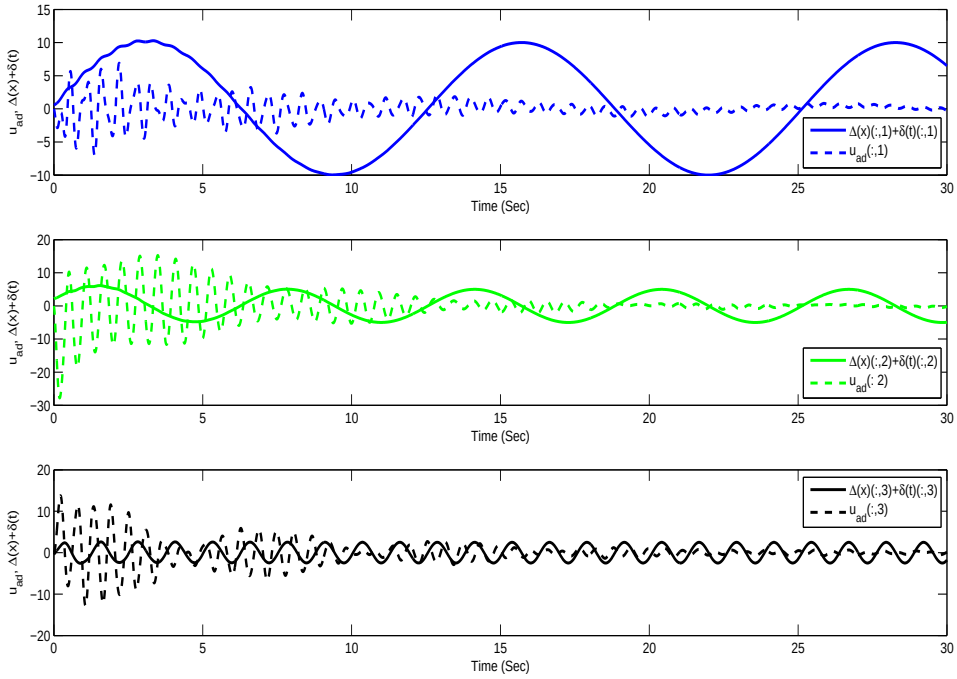

Figure 22: $u_{\text{ad}}(t)$ vs $\Delta(x)+\delta(t)$ in MRAC with adaptation gain set to 10^5, with uncertainty and disturbance.

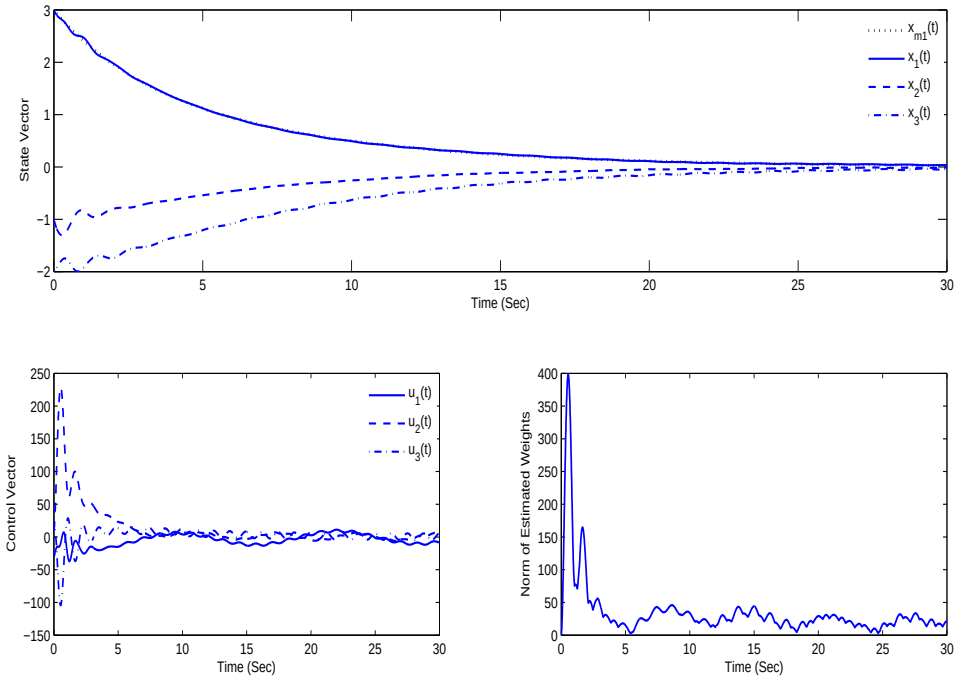

Figure 23: Responses with DF-MRAC, with uncertainty and disturbance.

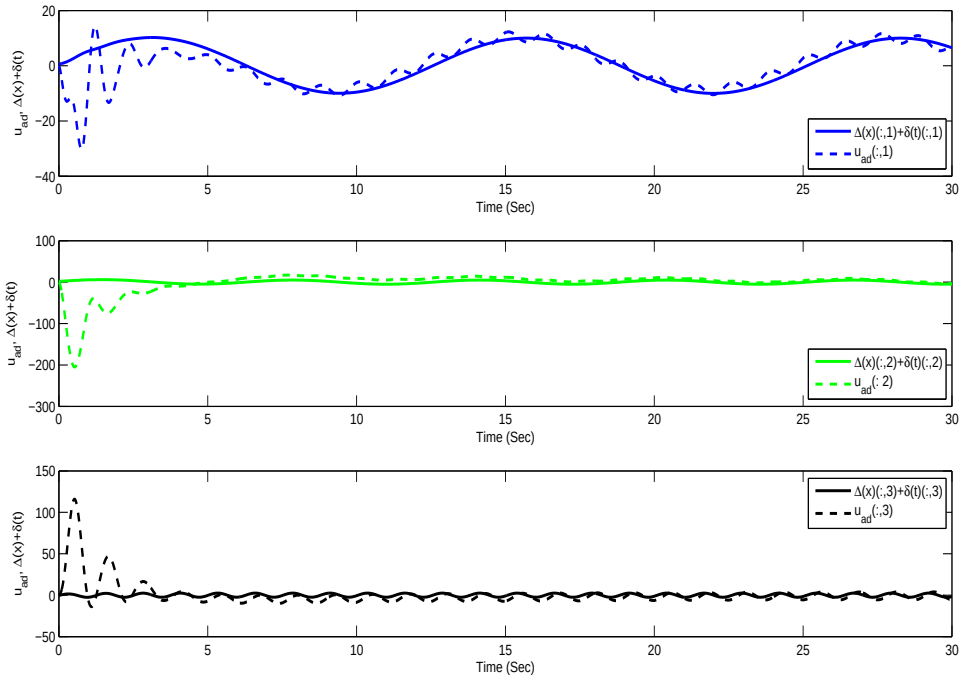

Figure 24: $u_{\text{ad}}(t)$ vs $\Delta(x) + \delta(t)$ in DF-MRAC with uncertainty and disturbance.

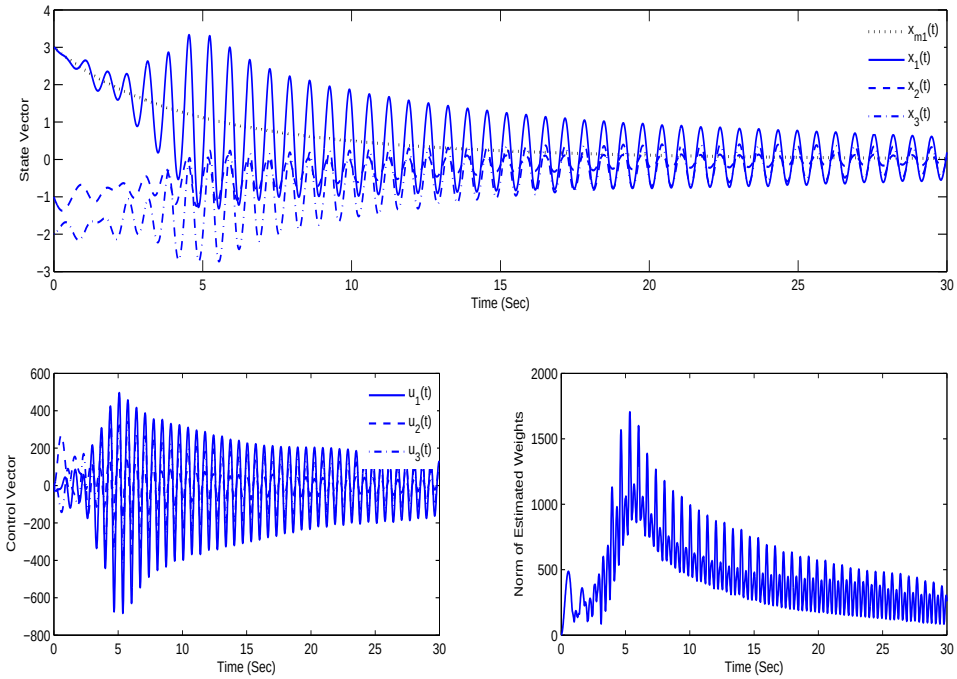

Figure 25: Responses with DF-MRAC with uncertainty, disturbance, and time delay 0.05 sec.

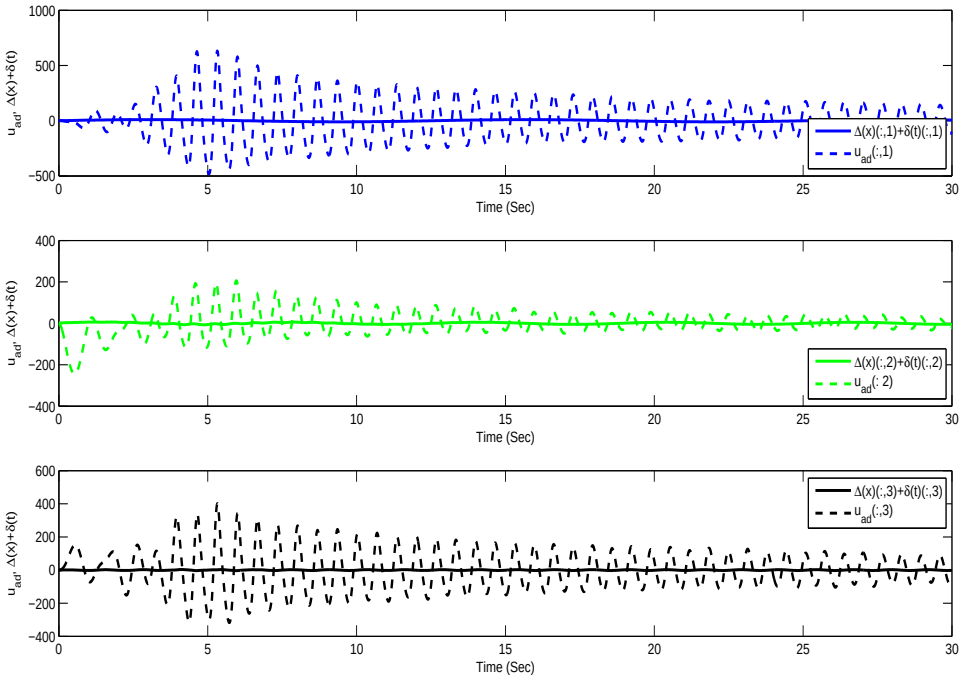

Figure 26: $u_{\rm ad}(t)$ vs $\Delta(x)+\delta(t)$ in DF-MRAC with uncertainty and disturbance, and time delay 0.05 sec.

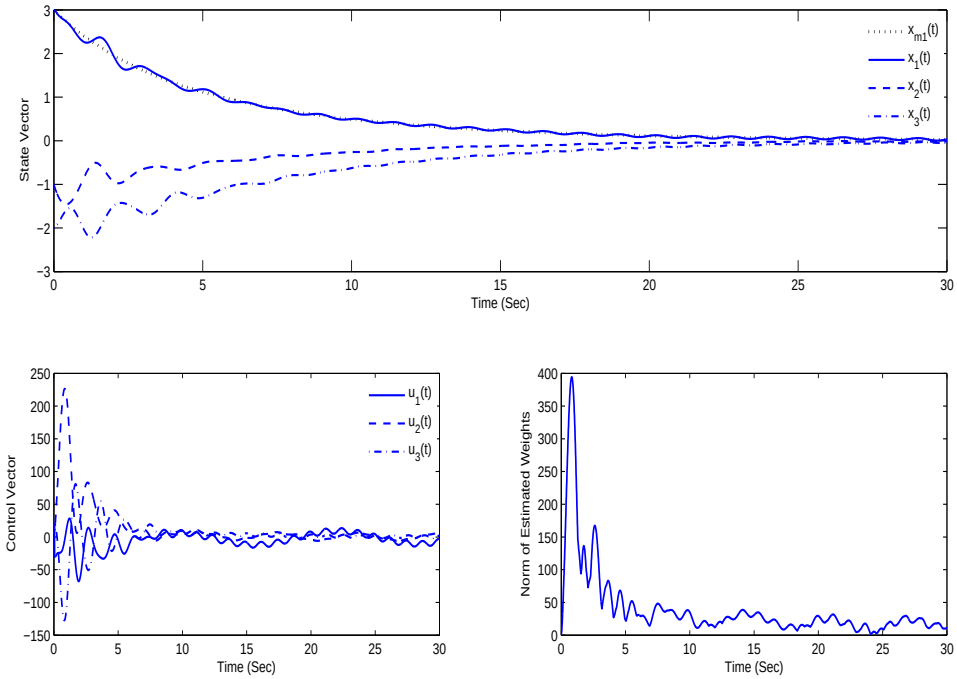

Figure 27: Responses with DF-$\mathcal{K}$-MRAC with uncertainty, disturbance, and time delay 0.05 sec.

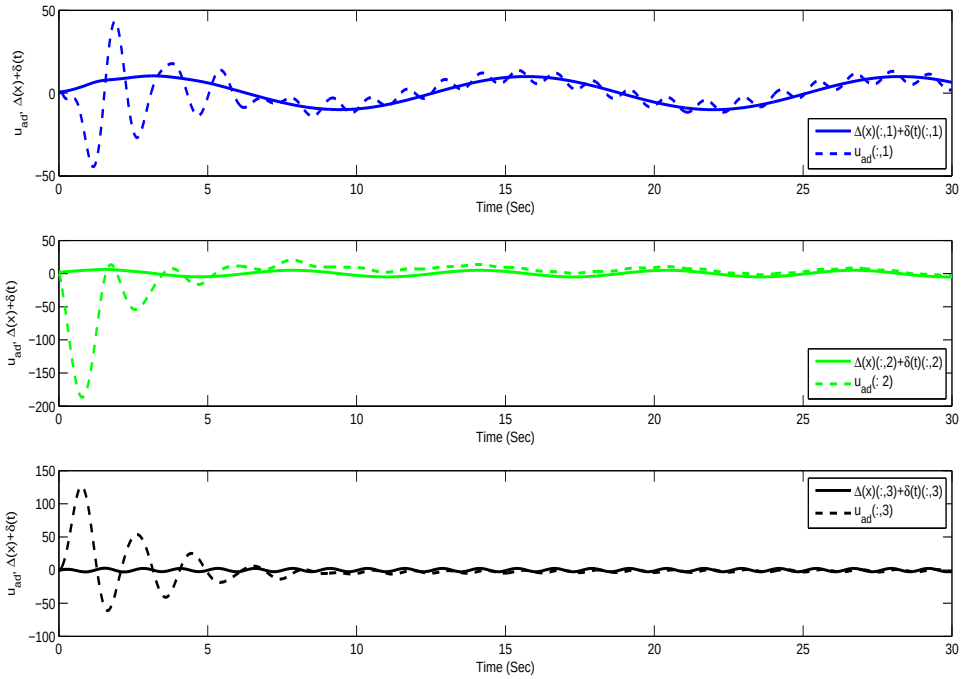

Figure 28: $u_{\text{ad}}(t)$ vs $\Delta(x) + \delta(t)$ in DF-$\mathcal{K}$-MRAC with uncertainty, disturbance, and time delay 0.05 sec.

Chapter III

A PARAMETER DEPENDENT RICCATI EQUATION APPROACH TO OUTPUT FEEDBACK ADAPTIVE CONTROL

A parameter dependent Riccati equation approach is taken to analyze the stability properties of an output feedback adaptive control law. The adaptive controller is intended to augment a nominal, fixed gain, observer based output feedback control law. Although the formulation is in the setting of model following adaptive control, the realization of the adaptive controller does not require implementing the reference model. In this regard, the cost of implementing the adaptive controller above that of a fixed gain control law is far less than that of other methods. The error signals are shown to be uniformly ultimately bounded and an expression for the ultimate bound is provided. The control design process and theoretical results are illustrated using a model for wing-rock dynamics.

The stability analysis employs a Lyapunov candidate function that entails the solution of a parameter dependent Riccati equation (rather than a Lyapunov equation) to show that all error signals are uniformly ultimately bounded (UUB). It is shown how the upper limit for the Riccati equation parameter is employed in the design of the adaptive law, and also influences the ultimate bounds for the state estimate error and the adapted weight error.

This Chapter is organized as follows: Section 3.1 defines the architecture of the adaptive output feedback control design, the nominal, observer based controller design, and the weight update law for the output feedback adaptive control design. This section also defines the parameter dependent Riccati equation, and the properties of its associated Hamiltonian matrix. Section 3.2 proves a theorem and corollaries that state the conditions under which the error signals are UUB and provide expressions for the ultimate bounds. Section 3.3 provides a numerical example to illustrate the proposed approach. Conclusions are given in Section 3.4.

3.1 Output Feedback Adaptive Control Design

Consider the uncertain system given by:

$$\begin{aligned} \dot{x}(t) &= Ax(t) + B[u(t) + \Delta(x(t))] \\ y(t) &= Cx(t) \end{aligned} \tag{113}$$

where $A \in \mathbb{R}^{n\times n}$, $B \in \mathbb{R}^{n\times m}$, and $C \in \mathbb{R}^{m\times n}$ are known system matrices; $x(t) \in \mathbb{R}^n$ is the state vector; $u(t) \in \mathbb{R}^m$ is the control input; $\Delta(\cdot) : \mathbb{R}^n \to \mathbb{R}^m$ is the unknown matched uncertainty; $y(t) \in \mathbb{R}^m$ is the regulated output vector, m elements of which are to be regulated; and the triple $\{A, B, C\}$ is minimal.

Remark 3.1.1 *The system given by (113) assumes that the control input vector and the regulated output vector have the same dimension. For the case when the dimension of the control input vector is larger than the dimension of the regulated output vector, due to redundant actuation, one can use matrix inverse and pseudo-inverse approaches, constrained control allocation, pseudo-controls, and daisy chaining [5, 18, 65] to reduce the dimension of the control input vector to the dimension of the regulated output vector. Furthermore, the system can have a sensed output vector denoted by*

$$y_s(t) = C_s x(t) \tag{114}$$

where $y_s(t) \in \mathbb{R}^p$, $C_s \in \mathbb{R}^{p\times n}$, $p \geq m$ such that the elements of $y(t)$ are a subset of the elements of $y_s(t)$.

Consider the following nominal control law

$$u_{\rm n}(t) = -K_x\hat{x}(t) + K_r r(t) \tag{115}$$

where $K_x \in \mathbb{R}^{m\times n}$ and $K_r \in \mathbb{R}^{m\times m}$ with $m \leq p$ are given feedback and feedforward gain matrices, respectively, $\hat{x}(t)$ is an estimate of $x(t)$ in an observer based design, and $r(t) \in \mathbb{R}^m$ is a bounded reference command. Define the reference model:

$$\begin{aligned} \dot{x}_{\rm m}(t) &= A_{\rm m}x_{\rm m}(t) + B_{\rm m}r(t) \\ y_{\rm m}(t) &= Cx_{\rm m}(t) \end{aligned} \tag{116}$$

where $x_{\mathrm{m}}(t) \in \mathbb{R}^n$ is the model state, $y_{\mathrm{m}}(t) \in \mathbb{R}^p$ is the model output, $A_{\mathrm{m}} = A - BK_x$ is Hurwitz by design, and $B_{\mathrm{m}} = BK_r$. The gains of the nominal control law are designed for the system in (113) assuming full state feedback, with $\Delta(x(t)) = 0$, so that a subset of the elements in $y_{\mathrm{m}}(t)$ tracks $r(t)$ to within some set of specifications on both the transient and steady state performance.

Assumption 3.1.1 *The matched uncertainty in (113) can be linearly parameterized as*

$$\Delta(x) = W^{\mathrm{T}}\beta(x) + \varepsilon(x), \quad \forall x \in D \tag{117}$$

where $W \in \mathbb{R}^{s\times m}$ is an unknown constant ideal weight matrix that satisfies $\|W\| = \omega^*$, $\beta(\cdot) : \mathbb{R}^n \to \mathbb{R}^s$ is a known basis vector of the form $\beta(x) = [\beta_1(x), \beta_2(x), ..., \beta_s(x)]^{\mathrm{T}}$ with $|\beta(x)| \leq \bar{\beta}$, and $\varepsilon(x)$ is the residual error satisfying $|\varepsilon(x)| < \overline{\varepsilon}$ for a sufficiently large domain $D \subset \mathbb{R}^n$.

Assumption 3.1.2 *The basis function $\beta(\cdot)$ in (117) is Lipschitz continuous on D*

$$|\beta(x) - \beta(\hat{x})| \leq L_\beta |x - \hat{x}|, \quad \forall x, \hat{x} \in D \tag{118}$$

The adaptive control objective is to design a control law $u(\cdot)$ for the dynamics in (113) so that the output $y(t)$ tracks the reference model output $y_{\mathrm{m}}(t)$ with bounded error. The nominal control law $u_{\mathrm{n}}(t)$ given by (115) is augmented by an adaptive control $u_{\mathrm{ad}}(t)$

$$u(t) = u_{\mathrm{n}}(t) - u_{\mathrm{ad}}(t) \tag{119}$$

where

$$u_{\mathrm{ad}}(t) = \hat{W}^{\mathrm{T}}(t)\beta(\hat{x}(t)) \tag{120}$$

where $\hat{x}(t)$ is an estimate of $x(t)$ obtained using a state observer given by:

$$\begin{aligned} \dot{\hat{x}}(t) &= A\hat{x}(t) + Bu_{\mathrm{n}}(t) + L[y(t) - \hat{y}(t)] \\ \hat{y}(t) &= C\hat{x}(t) \end{aligned} \tag{121}$$

where $L \in \mathbb{R}^{n\times p}$ is an observer gain matrix designed such that $A - LC$ is Hurwitz. The state observer in (121) is regarded as a part of the nominal control design. However, our viewpoint

is that L may be altered for purposes of adaptively augmenting the nominal controller. Denote the state estimation error, the estimated state tracking error, the tracking error, and the weight estimate error as:

$$\begin{aligned} \tilde{x}(t) &= x(t) - \hat{x}(t) \\ \hat{e}(t) &= \hat{x}(t) - x_{\mathrm{m}}(t) \\ e(t) &= x(t) - x_{\mathrm{m}}(t) \\ \tilde{W}(t) &= W - \hat{W}(t) \end{aligned} \tag{122}$$

The dynamics for the state estimation error, $\tilde{x}(t)$, and the estimated state tracking error, $\hat{e}(t)$, are described as:

$$\begin{aligned} \dot{\tilde{x}}(t) &= A_e \tilde{x}(t) + B\tilde{\Delta}(t) \\ \dot{\hat{e}}(t) &= A_{\mathrm{m}} \hat{e}(t) + LC\tilde{x}(t) \end{aligned} \tag{123}$$

where $A_e = A - LC$ and $\tilde{\Delta}(t) = \Delta(x) - u_{\mathrm{ad}}(t)$.

Consider the parameter dependent Riccati equation

$$\begin{aligned} 0 &= A_e^{\mathrm{T}} P + P A_e + Q_0 + \mu N N^{\mathrm{T}} \\ N &= C^{\mathrm{T}} - PB \end{aligned} \tag{124}$$

where $Q_0 > 0$ and $0 < \mu < \bar{\mu}$ defines the set within which there exists a positive definite solution for P. Note that $N = 0$ corresponds to the situation in which $\{A_e, B, C\}$ is positive real. The asymptotic approach in Ref. [39] is aimed at reducing the size of N, whereas in our approach $N \neq 0$ is treated as giving rise to a parameter dependent Riccati equation. Furthermore, consider the following weight update law

$$\dot{\hat{W}}(t) = \gamma \Big[\beta(\hat{x}(t)) \tilde{y}^{\mathrm{T}}(t) - \big(\sigma I_s + \beta(\hat{x}(t)) \beta(\hat{x}(t))^{\mathrm{T}} / 2\mu \big) \hat{W}(t) \Big] \tag{125}$$

where $\gamma \in \mathbb{R}$, $\sigma \in \mathbb{R}$ are positive adaptation gains, and $\tilde{y}(t) = y(t) - \hat{y}(t)$.

Remark 3.1.2 *The structure of the adaptive law in (125) is novel in that it contains an additional term depending on μ, the parameter in the Riccati equation in (124).*

Figure 29 shows the overall adaptive output feedback control system architecture. It should be noted that the reference model is not used in the adaptive output feedback design.

The observer serves as the reference model. Its dynamics are the same as the reference model if $u_{\rm ad}(t)$ cancels $\Delta(x)$, and in this case the observer error transient $\tilde{y}(t)$ goes to zero. So in the end the components that are added to the nominal controller design in order to realize the adaptive control consist of computing the basis functions, forming the adaptive law, and integration of $\dot{\hat{W}}(t)$.

Remark 3.1.3 *An expression for the upper bound on γ in (125) is given in Remark 3.2.2 in the subsection 3.2.*

Remark 3.1.4 *$P > 0$ for $\mu = 0$ and P depends continuously on μ. Therefore the existence of $\bar{\mu} > 0$ is assured.*

Remark 3.1.5 *If $A_{\rm m}$ has no repeated eigenvalues and the observer gain matrix, L, is designed using pole placement such that $\lambda(A_e) = {\rm k}\lambda(A_{\rm m})$, then for a given $\mu < \bar{\mu}$ we can denote $P({\rm k})$ as the corresponding positive definite solution for P. In this case we can state the following Lemma.*

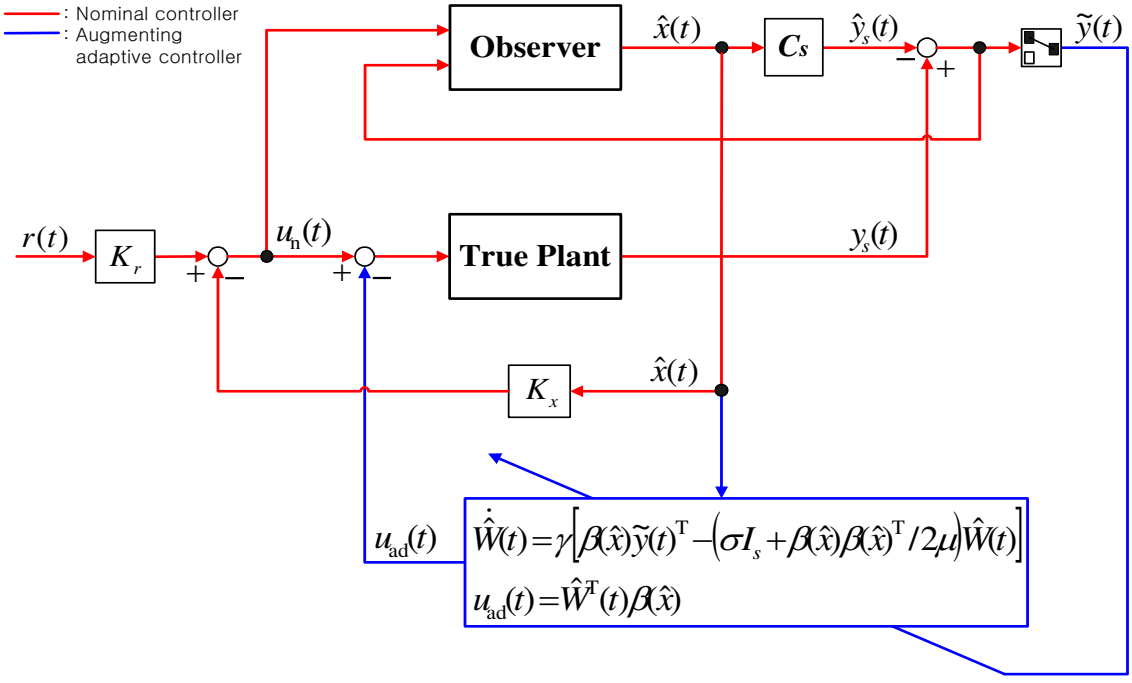

Figure 29: Overall Control System Architecture.

Lemma 3.1.1 ${\rm Lim}_{{\rm k}\to\infty} P({\rm k}) = 0$.

Proof: Let T_m and T_e denote diagonalizing transformations for A_{m} and A_e, so that:

$$\begin{aligned} A_{\mathrm{m}} &= T_m \mathrm{diag}[\lambda(A_{\mathrm{m}})] T_m^{-1} \\ A_e &= \mathrm{k} T_e \mathrm{diag}[\lambda(A_{\mathrm{m}})] T_e^{-1} \end{aligned} \tag{126}$$

and let $T_s = T_e T_m^{-1}$. Then

$$A_e = \mathrm{k} T_s A_{\mathrm{m}} T_s^{-1} \equiv \mathrm{k} A_s \tag{127}$$

Defining $P_{\mathrm{k}} \equiv \mathrm{k} P(\mathrm{k})$ and $N_{\mathrm{k}} \equiv C^{\mathrm{T}} - \mathrm{k}^{-1} P_{\mathrm{k}} B$, (124) can be written as

$$0 = A_s^{\mathrm{T}} P_{\mathrm{k}} + P_{\mathrm{k}} A_s + Q_0 + \mu N_{\mathrm{k}} N_{\mathrm{k}}^{\mathrm{T}} \tag{128}$$

Taking the $\lim_{\mathrm{k}\to\infty}$ of (128), it follows that

$$0 = A_s^{\mathrm{T}} P_\infty + P_\infty A_s + Q_0 + \mu C C^{\mathrm{T}} \tag{129}$$

Since the solution of (129) ($P_\infty > 0$) is finite, it follows that

$$\lim_{\mathrm{k}\to\infty} P(\mathrm{k}) = \lim_{\mathrm{k}\to\infty} \frac{P_{\mathrm{k}}}{\mathrm{k}} = 0 \qquad \blacksquare \tag{130}$$

The next lemma shows that (124) can be solved for $P > 0$ using Potter's method [55]. This also means that $\bar{\mu}$ can be determined by searching for the boundary value that results in a failure of the algorithm to converge. We employ the notation $\mathrm{Ric}(\cdot)$ and $\mathrm{dom}(\mathrm{Ric})$ as defined in Ref. [17].

Lemma 3.1.2 *Define the Hamiltonian matrix*

$$H \equiv \begin{bmatrix} A_e - \mu B C & \mu R \\ -Q & -\big(A_e - \mu B C\big)^{\mathrm{T}} \end{bmatrix} \tag{131}$$

where $Q \equiv Q_0 + \mu C C^{\mathrm{T}}$ *and* $R \equiv B B^{\mathrm{T}}$. *Then for all* $0 < \mu < \bar{\mu}$, $H \in \mathrm{dom}(\mathrm{Ric})$ *and* $P = \mathrm{Ric}(H)$.

Proof: The proof follows directly from Lemmas 3 and 4 in Ref. [17]. ■

Remark 3.1.6 *It can and often does happen that the Ricatti equation in (129) will have more than one positive definite solution. However, since all we require is that a solution exists and that a unique solution can be reliably computed using Potter's method, the fact that other solutions exist seems to have no bearing on the design approach. Therefore the implication of multiple solutions was not pursued in this thesis.*

The uncertainty estimation error $\tilde{\Delta}(t)$ can be written as

$$\begin{aligned}\tilde{\Delta}(t) &= \Delta(x) - u_{\mathrm{ad}}(t) = W^{\mathrm{T}}\beta(x(t)) + \varepsilon(x) - \hat{W}^{\mathrm{T}}(t)\beta(\hat{x}(t)) \\ &= \tilde{W}^{\mathrm{T}}(t)\beta(\hat{x}(t)) + W^{\mathrm{T}}\big(\beta(x(t)) - \beta(\hat{x}(t))\big) + \varepsilon(x)\end{aligned} \tag{132}$$

Hence the system error dynamics (123) can be rewritten as:

$$\begin{aligned}\dot{\tilde{x}}(t) &= A_c\tilde{x}(t) + B[\,\tilde{W}^{\mathrm{T}}(t)\beta(\hat{x}(t)) + W^{\mathrm{T}}\big(\beta(x(t)) - \beta(\hat{x}(t))\big) + \varepsilon(x)\,] \\ \dot{\hat{e}}(t) &= A_{\mathrm{m}}\hat{e}(t) + LC\tilde{x}(t)\end{aligned} \tag{133}$$

3.2 Boundedness of the Error Dynamics

The following definitions are introduced to simplify the notation throughout this section:

$$\begin{aligned}&\tilde{x} \equiv \tilde{x}(t), \tilde{y} \equiv \tilde{y}(t), \tilde{W} \equiv \tilde{W}(t), \\ &\beta \equiv \beta(x), \hat{\beta} \equiv \beta(\hat{x}), \tilde{\beta} \equiv \beta(x) - \beta(\hat{x}), \\ &\Omega \equiv \tilde{x}^{\mathrm{T}}(t)PB, \varepsilon \equiv \varepsilon(x) \\ &e \equiv e(t), \hat{e} \equiv \hat{e}(t), \hat{e}_{\mathrm{m}} \equiv \hat{e}_{\mathrm{m}}(t), \hat{W} \equiv \hat{W}(t) \\ &Q \equiv Q_0 + \mu NN^{\mathrm{T}}\end{aligned} \tag{134}$$

The next theorem states the main result.

Theorem 3.2.1 *Consider the system comprised of the plant dynamics in (113) and the control law given in (119), made up of the nominal control law in (115) and the adaptive control law in (120), together with the state observer in (121) and the weight update law in (125) with $\mu < \bar{\mu}$. Under Assumptions 3.1.1 and 3.1.2, for a sufficiently large D, and if $\lambda_{\min}(Q_0) > 2\|PB\|\omega^* L_\beta$, then $\tilde{x}(t)$ and $\tilde{W}(t)$ are UUB.*

Proof: Consider the Lyapunov candidate given by

$$V(\tilde{x}, \tilde{W}) = \tilde{x}^{\mathrm{T}}P\tilde{x} + \gamma^{-1}\,\mathrm{tr}\Big[\tilde{W}^{\mathrm{T}}\tilde{W}\Big] \tag{135}$$

where P is a positive definite solution of (124) for $0 < \mu < \bar{\mu}$. The time derivative of (135) along closed loop solutions of (113) is given by

$$\dot{V} = -\tilde{x}^{\mathrm{T}}Q\tilde{x} + 2\tilde{x}^{\mathrm{T}}PB\tilde{\Delta} - 2\gamma^{-1}\,\mathrm{tr}\Big[\tilde{W}^{\mathrm{T}}\dot{\hat{W}}\Big] \tag{136}$$

where $\dot{V} \equiv \dot{V}(\tilde{x}, \tilde{W})$. With the proposed weight update law in (125) and $\tilde{\Delta}(t)$ in (132), (136) can be written as

$$\begin{aligned}\dot{V} =& -\tilde{x}^{\mathrm{T}} Q \tilde{x} + 2\Omega\Big[\tilde{W}^{\mathrm{T}}\hat{\beta} + W^{\mathrm{T}}\tilde{\beta} + \varepsilon\Big] \\ & - 2\,\mathrm{tr}\Big[\tilde{W}^{\mathrm{T}}\hat{\beta}\tilde{y}^{\mathrm{T}} - \sigma\tilde{W}^{\mathrm{T}}\hat{W} - \tilde{W}^{\mathrm{T}}\hat{\beta}\hat{\beta}^{\mathrm{T}}\hat{W}/2\mu\Big] \\ =& -\tilde{x}^{\mathrm{T}} Q \tilde{x} + 2\Omega\Big[\tilde{W}^{\mathrm{T}}\hat{\beta} + W^{\mathrm{T}}\tilde{\beta} + \varepsilon\Big] \\ & - 2\,\mathrm{tr}\Big[\tilde{W}^{\mathrm{T}}\hat{\beta}\tilde{y}^{\mathrm{T}} - \sigma\tilde{W}^{\mathrm{T}}W + \sigma\tilde{W}^{\mathrm{T}}\tilde{W} - \tilde{W}^{\mathrm{T}}\hat{\beta}\hat{\beta}^{\mathrm{T}}W/2\mu + \tilde{W}^{\mathrm{T}}\hat{\beta}\hat{\beta}^{\mathrm{T}}\tilde{W}/2\mu\Big]\end{aligned} \tag{137}$$

Using the expression for N in (124), the definition of Ω in (134), and the trace property $a^{\mathrm{T}}b = \mathrm{tr}[ba^{\mathrm{T}}]$ for $a, b \in \mathbb{R}^m$, (137) becomes

$$\begin{aligned}\dot{V} =& -\tilde{x}^{\mathrm{T}} Q \tilde{x} + 2\Omega\Big[W^{\mathrm{T}}\tilde{\beta} + \varepsilon\Big] \\ & - 2\tilde{x}^{\mathrm{T}} N\tilde{W}^{\mathrm{T}}\hat{\beta} - 2\sigma\,\mathrm{tr}\Big[\tilde{W}^{\mathrm{T}}\tilde{W}\Big] + 2\sigma\,\mathrm{tr}\Big[\tilde{W}^{\mathrm{T}}W\Big] + \hat{\beta}^{\mathrm{T}}W\tilde{W}^{\mathrm{T}}\hat{\beta}/\mu - \hat{\beta}^{\mathrm{T}}\tilde{W}\tilde{W}^{\mathrm{T}}\hat{\beta}/\mu\end{aligned} \tag{138}$$

From Young's inequality [3], we have $2a^{\mathrm{T}}b \leq \nu a^{\mathrm{T}}a + b^{\mathrm{T}}b/\nu, \nu > 0$ for any vectors a and b. This can be generalized to matrices as $2\,\mathrm{tr}\big[A^{\mathrm{T}}B\big] \leq \nu\,\mathrm{tr}\big[A^{\mathrm{T}}A\big] + \mathrm{tr}\big[B^{\mathrm{T}}B\big]/\nu$, for any matrices A and B with compatible dimensions. Applying the vector form to the third term in (138) and the matrix form with $\nu = 1$ to the sixth term in (138), we obtain

$$\dot{V} \leq -\tilde{x}^{\mathrm{T}} Q \tilde{x} + 2\Omega\Big[W^{\mathrm{T}}\tilde{\beta} + \varepsilon\Big] + \mu\tilde{x}^{\mathrm{T}} N N^{\mathrm{T}}\tilde{x} + \frac{1}{\mu}\hat{\beta}^{\mathrm{T}}\, W\tilde{W}^{\mathrm{T}}\hat{\beta} - \sigma\,\mathrm{tr}\Big[\tilde{W}^{\mathrm{T}}\tilde{W}\Big] + \sigma\,\mathrm{tr}\Big[W^{\mathrm{T}}W\Big] \tag{139}$$

Using Assumptions 3.1.1 and 3.1.2,

$$2\Omega\Big[W^{\mathrm{T}}\tilde{\beta} + \varepsilon\Big] \leq 2|\Omega|\|W\|L_\beta|x - \hat{x}| + 2|\Omega||\varepsilon| \leq 2\|PB\|\omega^* L_\beta|\tilde{x}|^2 + 2\|PB\|\bar{\varepsilon}|\tilde{x}| \tag{140}$$

Also

$$\frac{1}{\mu}\hat{\beta}^{\mathrm{T}}\, W\tilde{W}^{\mathrm{T}}\hat{\beta} \leq \frac{1}{\mu}\bar{\beta}^2\|W\|_F\|\tilde{W}\|_F \tag{141}$$

With (140) and (141), it follows from (139) that

$$\begin{aligned}\dot{V} \leq & -\tilde{x}^{\mathrm{T}}\Big(Q - \mu N N^{\mathrm{T}}\Big)\tilde{x} + 2\|PB\|\omega^* L_\beta|\tilde{x}|^2 + 2\|PB\|\bar{\varepsilon}|\tilde{x}| \\ & - \sigma\|\tilde{W}\|_F^2 + \frac{1}{\mu}\bar{\beta}^2\|W\|_F\|\tilde{W}\|_F + \sigma\|W\|_F^2\end{aligned} \tag{142}$$

Substituting for Q from (134), (142) can be expressed as

$$\begin{aligned}\dot{V} \leq & -\tilde{x}^{\mathrm{T}} Q_0 \tilde{x} + 2\|PB\|\omega^* L_\beta |\tilde{x}|^2 + 2\|PB\|\overline{\varepsilon}|\tilde{x}| \\ & -\sigma\|\tilde{W}\|_F^2 + \frac{1}{\mu}\bar{\beta}^2\|W\|_F\|\tilde{W}\|_F + \sigma\|W\|_F^2\end{aligned} \tag{143}$$

Using

$$\lambda_{\min}(Q)|\tilde{x}|^2 \leq \tilde{x}^{\mathrm{T}} Q \tilde{x} \leq \lambda_{\max}(Q)|\tilde{x}|^2 \tag{144}$$

it follows from (143) that

$$\dot{V} \leq -\Big(\lambda_{\min}\big(Q_0\big) - 2\|PB\|\omega^* L_\beta\Big)|\tilde{x}|^2 + 2\|PB\|\overline{\varepsilon}|\tilde{x}| - \sigma\|\tilde{W}\|_F^2 + \frac{1}{\mu}\bar{\beta}^2\|W\|_F\|\tilde{W}\|_F + \sigma\|W\|_F^2 \tag{145}$$

Defining:

$$\begin{aligned} c &\equiv \lambda_{\min}\big(Q_0\big) - 2\|PB\|\omega^* L_\beta > 0 \\ d_1 &\equiv \|PB\|\overline{\varepsilon} \\ d_2 &\equiv \frac{1}{2\mu}\bar{\beta}^2\|W\|_F \\ \mathbf{e}^2 &\equiv d_1^2/c + d_2^2/\sigma + \sigma\|W\|_F^2 > 0 \end{aligned} \tag{146}$$

(145) can be written as

$$\dot{V} \leq -c\Big(|\tilde{x}| - \frac{d_1}{c}\Big)^2 - \sigma\Big(\|\tilde{W}\|_F - \frac{d_2}{\sigma}\Big)^2 + \mathbf{e}^2 \tag{147}$$

Consequently, we can conclude that either of the following conditions:

$$|\tilde{x}| > \Psi_1, \;\; \|\tilde{W}\| > \Psi_2 \tag{148}$$

renders $\dot{V}(\tilde{x}, \tilde{W}) < 0$, where $\Psi_1 = \mathbf{e}/\sqrt{c} + d_1/c$ and $\Psi_2 = \mathbf{e}/\sqrt{\sigma} + d_2/\sigma$, and it follows that $\tilde{x}$ and $\tilde{W}$ are UUB. ■

Remark 3.2.1 *From Lemma 3.1.1, the condition $c > 0$ can be satisfied by choosing* k *sufficiently large.*

Corollary 3.2.1 *Under the conditions of Theorem 3.2.1, an estimate for the ultimate bound is given by*

$$r = \sqrt{\frac{\lambda_{\max}(P){\Psi_1}^2 + \gamma^{-1}\Psi_2^2}{\lambda_{\min}(\tilde{P})}} \tag{149}$$

where $\tilde{P} = \mathrm{diag}[P, \gamma^{-1} I]$.

Proof: Define $\zeta = [\tilde{x}^{\mathrm{T}}, \mathrm{vec}(\tilde{W})^{\mathrm{T}}]^{\mathrm{T}}$ and denote the following sets:

$$\begin{aligned} B_r &= \{\zeta : |\zeta| \leq r\} \\ \Omega_\alpha &= \{\zeta \in B_r : \zeta^{\mathrm{T}} \tilde{P} \zeta \leq \alpha\} \end{aligned} \tag{150}$$

where $B_r \subset D_\zeta$ for a sufficiently large compact set D_ζ and $\alpha = \min_{|\zeta=r|}\left(\zeta^{\mathrm{T}} \tilde{P} \zeta\right) = r^2 \lambda_{\min}(\tilde{P})$. A geometric description of these sets is given in Figure 30. From

$$V(\tilde{x}, \tilde{W}) = \zeta^{\mathrm{T}} \tilde{P} \zeta = \tilde{x}^{\mathrm{T}} P \tilde{x} + \gamma^{-1} \operatorname{tr}\left[\tilde{W}^{\mathrm{T}} \tilde{W}\right] \tag{151}$$

and it follows that Ω_α is an invariant set if and only if

$$\alpha \geq \lambda_{\max}(P) \Psi_1^2 + \gamma^{-1} \Psi_2^2 \tag{152}$$

Therefore the minimum size of B_r is defined by (149). ■

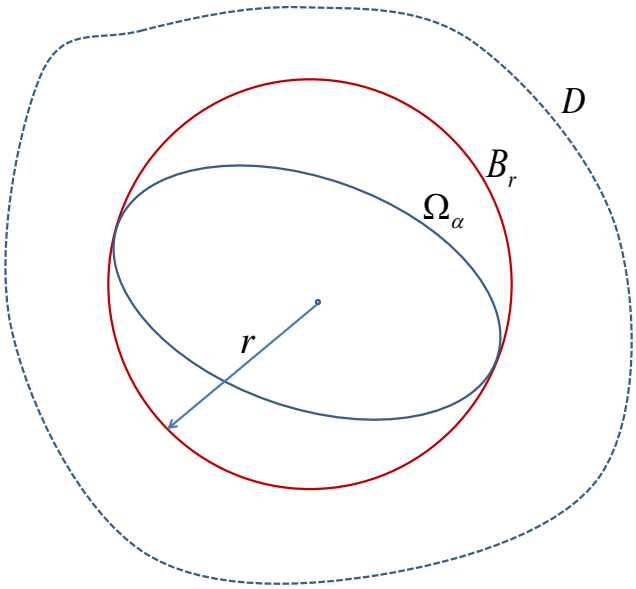

Figure 30: Geometric representation of sets.

Remark 3.2.2 *The proofs of Theorem 3.2.1 and Corollary 3.2.1 assume the sets D and D_ζ are sufficiently large. If we define B_R as the largest ball $\subset D_\zeta$, and assume the initial conditions are such that $\zeta(0) \in B_R$, then from Figure 30 we have added the condition that $r < R$, which implies an upper bound on γ. It can be shown that in this case the upper*

bound must be such that $\lambda_{\min}(\tilde{P}) = \gamma^{-1}$. *With* r *defined by (149) and* $\lambda_{\min}(\tilde{P}) = \gamma^{-1}$, *the condition* $r < R$ *implies*

$$\gamma < \frac{R^2 - \Psi_2^2}{\lambda_{\max}(P)\Psi_1^2} \tag{153}$$

Therefore, the meaning of 'D_ζ *sufficiently large' in Corollary 3.1 is that* $R > \sqrt{\gamma\lambda_{\max}(P)\Psi_1^2 + \Psi_2^2}$ *and* $\zeta(0) \in B_R$. *The meaning of 'D sufficiently large' is difficult to characterize since* $x(t)$ *depends on both* $r(t)$ *and* $x(0)$.

Corollary 3.2.2 *If* $\tilde{x}$ *is bounded, then the state tracking error* e *is bounded.*

Proof: The state tracking error e can be expressed as a sum of the state estimation error $\hat{e}$ and the estimated state tracking error $\hat{e}_{\mathrm{m}}$:

$$\begin{aligned} |e| &= |x - x_{\mathrm{m}}| = |x - \hat{x} + \hat{x} - x_{\mathrm{m}}| \\ &\leq |x - \hat{x}| + |\hat{x} - x_{\mathrm{m}}| = |\tilde{x}| + |\hat{e}| \end{aligned} \tag{154}$$

From (123) it follows that if $\tilde{x}$ is bounded, then $\hat{e}$ is bounded, and therefore e is bounded. ■

Corollary 3.2.3 *Consider the system of equations in (123). If* $\tilde{x}$ *is UUB by* $\mathbf{r}$ *then* e *is UUB by* $\mathbf{r}(1 + \mathbf{v})$, *where*

$$\mathbf{v} \equiv \frac{2\|P_{\mathrm{m}}LC\|}{\lambda_{\min}(Q_{\mathrm{m}})} \tag{155}$$

Proof: Consider the positive semi-definite function

$$V(\hat{e}) = \hat{e}^{\mathrm{T}} P_{\mathrm{m}} \hat{e} \tag{156}$$

From (123), there exists $P_{\mathrm{m}} > 0$ for any $Q_{\mathrm{m}} > 0$ such that

$$0 = A_{\mathrm{m}}^{\mathrm{T}} P_{\mathrm{m}} + P_{\mathrm{m}} A_{\mathrm{m}} + Q_{\mathrm{m}} \tag{157}$$

Then the time derivative of (156) along the trajectories of (123) can be written as

$$\begin{aligned} \dot{V}(\hat{e}, \tilde{x}) &= -\hat{e}^{\mathrm{T}} Q_{\mathrm{m}} \hat{e} + 2\hat{e}^{\mathrm{T}} P_{\mathrm{m}} LC\tilde{x} \\ &\leq -|\hat{e}|\Big[\lambda_{\min}(Q_{\mathrm{m}})|\hat{e}| - 2\|P_{\mathrm{m}}LC\||\tilde{x}|\Big] \\ &= -|\hat{e}|\lambda_{\min}(Q_{\mathrm{m}})\Big[|\hat{e}| - \frac{2\|P_{\mathrm{m}}LC\|}{\lambda_{\min}(Q_{\mathrm{m}})}|\tilde{x}|\Big] \end{aligned} \tag{158}$$

From (123) it follows that $\hat{e}$ is bounded so long as $\tilde{x}$ is bounded. It therefore follows that once $\tilde{x}$ reaches its ultimate bound that $\dot{V}(\hat{e},\tilde{x}) < 0$ for all $|\hat{e}| > \mathbf{rv}$, and from (154) that $|e|$ is UUB by $\mathbf{r}(1+\mathbf{v})$. ■

3.3 Illustrative Examples with Wing Rock Dynamics

Consider wing-rock dynamics presented in (61) with one output measurement $y(t) = \phi(t)$. It can be written in the form of (113):

$$\begin{aligned} \begin{bmatrix} \dot{\phi}(t) \\ \ddot{\phi}(t) \end{bmatrix} &= \begin{bmatrix} 0 & 1 \\ 0 & 0 \end{bmatrix} \begin{bmatrix} \phi(t) \\ \dot{\phi}(t) \end{bmatrix} + \begin{bmatrix} 0 \\ 1 \end{bmatrix} \Big[u(t) + \Delta(x) \Big] \\ y(t) &= \begin{bmatrix} 1 & 0 \end{bmatrix} \begin{bmatrix} \phi(t) \\ \dot{\phi}(t) \end{bmatrix} \end{aligned} \tag{159}$$

where

$$\Delta(x) = \big[b_0 + b_1\phi(t) + b_2\dot{\phi}(t) + b_3|\phi(t)|\dot{\phi}(t) + b_4|\dot{\phi}(t)|\dot{\phi}(t) + b_5\phi^3(t) \big] \tag{160}$$

where $b_0 = 0$, $b_1 = -0.0186$, $b_2 = 0.0152$, $b_3 = 0.6245$, $b_4 = -0.0095$, and $b_5 = 0.0215$ are aerodynamic coefficients. The control objective is to track a reference roll angle command. A bias term and five sigmoidal basis functions $\beta_i(x)$ are used to form the basis vector, so $\beta_1 = 1$ and

$$\beta_i(x) = \frac{1 - e^{-ax_i}}{1 + e^{-ax_i}}, \qquad i = 2, 3, ..., 6 \tag{161}$$

with $a = 3$ and normalized $x_i = [\phi_n, \dot{\phi}_n, \phi_n^2, \dot{\phi}_n^2, \phi_n\dot{\phi}_n]$, where $\phi_n = \hat{\phi}/\pi$ and $\dot{\phi}_n = \dot{\hat{\phi}}/\pi$.

3.3.1 Augmentation of a Proportional Nominal Controller

We will first illustrate a typical result when augmenting a nominal control design based on proportional control. The reference model is second order with a natural frequency of 1.5 rad/sec and a damping ratio of 0.707. This amounts to choosing $K_x = [2.25, 2.121]$ and $K_r = 2.25$. The observer gain $L = [7.07, 25]^{\mathrm{T}}$ so that $\lambda(A_e) = 4\lambda(A_{\mathrm{m}})$ (k = 4).

Figure 31 shows the $\bar{\mu}$ boundary versus k for $Q_0 = I_2$. For k = 4, $\bar{\mu} = 23.8$. Figure 32 shows the ultimate bound for $\tilde{x}$ and $\tilde{W}$ versus μ for the case k = 4 in the observer design, $\sigma = 0.01$, and assuming $\omega^* = 0.1$. Note that the ultimate bounds are minimized by choosing μ close to $\bar{\mu}$. Figure 33 confirms that $c > 0$ for the complete range for μ, for k = 4.

Simulation results are given in Figures 34 - 37 for k = 4 in the observer design. These were generated using $\gamma = 100$, $\sigma = 0.01$, $\mu = 23.7$, and randomly selected initial conditions $\phi(0) = 6^\circ$ and $\dot{\phi}(0) = 3^\circ/\text{sec}$. Figure 34 shows a typical step response. Note that the system is unstable without adaptation, but it tracks the reference response reasonably well with adaptation. However there is a significant steady state error. Figure 35 shows the response for a sequence of pulse commands. The comparison between $u_{\text{ad}}(t)$ and $\Delta(x)$ is given in Figure 36 and the corresponding weight histories are shown in Figure 37.

3.3.2 Augmentation of a PI Nominal Controller

The previous results highlight the fact that we cannot rely on the adaptive controller to provide zero steady state error when $\Delta(x) \neq 0$. If zero steady state error in the presence of constant uncertainty or constant disturbances is a requirement, then this requirement should be reflected in the design of the nominal control law. This point in illustrated in the remainder of this section.

A third state variable is added to the dynamics that represents the integral of $r(t) - \phi(t)$. The new system becomes

$$\begin{aligned} \dot{x}(t) &= Ax(t) + B[u(t) + \Delta(x(t))] + B_r r(t) \\ y(t) &= Cx(t) \end{aligned} \tag{162}$$

where $x(t) = [\phi(t), \dot{\phi}(t), \int (r(t) - \phi(t))]^{\text{T}}$ and

$$A = \begin{bmatrix} 0 & 1 & 0 \\ 0 & 0 & 0 \\ -1 & 0 & 0 \end{bmatrix}, \quad B = \begin{bmatrix} 0 \\ 1 \\ 0 \end{bmatrix}, \quad B_r = \begin{bmatrix} 0 \\ 0 \\ 1 \end{bmatrix}, \quad C = \begin{bmatrix} 1 & 0 & 0 \end{bmatrix} \tag{163}$$

The feedback gain matrix in the nominal controller was designed as a linear quadratic regulator (LQR). The weighting matrices in the design were chosen as $Q = \text{diag}[20, 3, 1]$ and $R = 0.5$. This leads to $K_x = [7.2675, 4.5316, -1.4142]$ as the PI feedback gain and $K_r = 7.2675$ as the feedforward gain. In this case the form of the observer dynamics in (121) becomes

$$\dot{\hat{x}}(t) = A\hat{x}(t) + Bu_{\text{n}}(t) + B_r r(t) + L[y(t) - \hat{y}(t)] \tag{164}$$

and the form of the error dynamics in (123) remains the same. Therefore the theorem and corollaries of the previous section still apply.

Figure 38 shows the $\bar{\mu}$ boundary versus k for $Q_0 = I_3$. The value of $\bar{\mu}$ for k = 4 in this case is 71.2. It was again verified that the value of μ that minimizes the ultimate bounds for $\tilde{x}$ and $\tilde{W}$ is very close to this value. Step responses for the the case of PI nominal control design are given in Figures 39. These were generated using the same adaptation gains used previously, $\mu = 71$, and initial conditions $[6^\circ, 3^\circ/\text{sec}, 0]^{\text{T}}$. The system shows a significant oscillation without adaptation, but it tracks the reference response reasonably well with adaptation. Furthermore, the steady state error is zero.

3.4 Conclusion

This section presents an architecture for output feedback model reference adaptive control that augments a nominal fixed gain controller. It is assumed that the nominal controller employs an observer. The observer is used in the adaptive part of the design in place of a reference model. The level of complexity for realization of proposed architecture, above that of the nominal controller, is far less than other methods. The error signals including state estimation error, estimated state tracking error, and weight estimate error are proven to be uniformly ultimately bounded. The stability analysis employs a Lyapunov candidate based on the existence of a positive definite solution of a parameter dependent Riccati equation. The upper limit for this parameter is employed in the design of the adaptive law, and also influences the ultimate bounds for the state estimate error and the weight error. Simulation examples illustrate the computation of parameter bound, computation of its influence on the ultimate error bounds, and a set of typical simulation results highlighting the attainable performance.

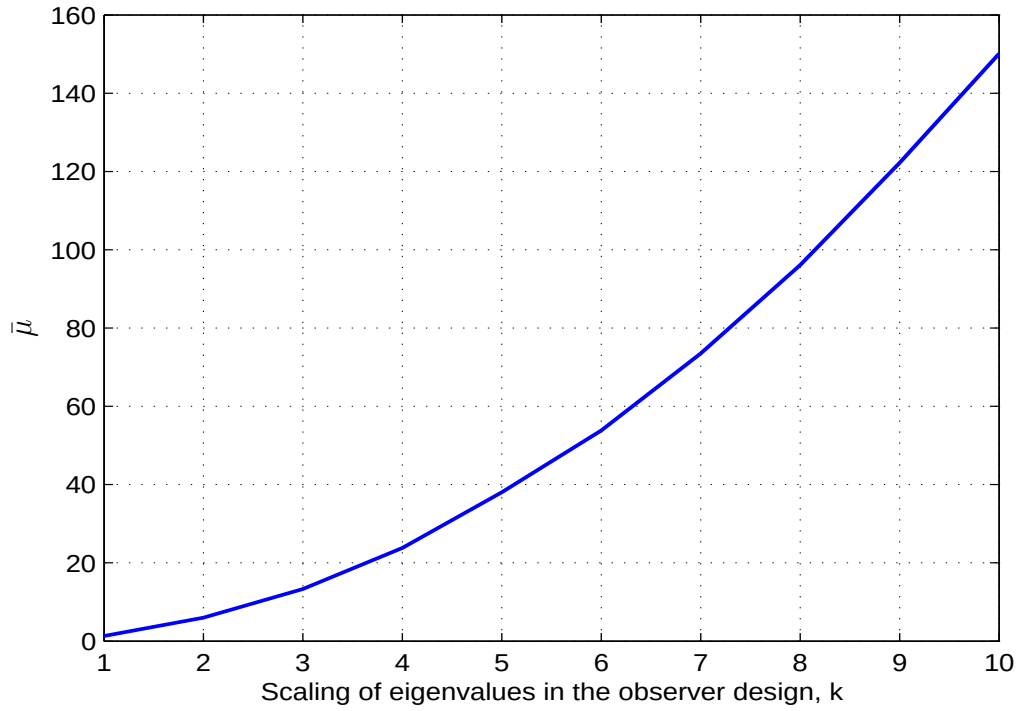

Figure 31: Limit value of μ for $Q_0 = I_2$ using a proportional nominal controller.

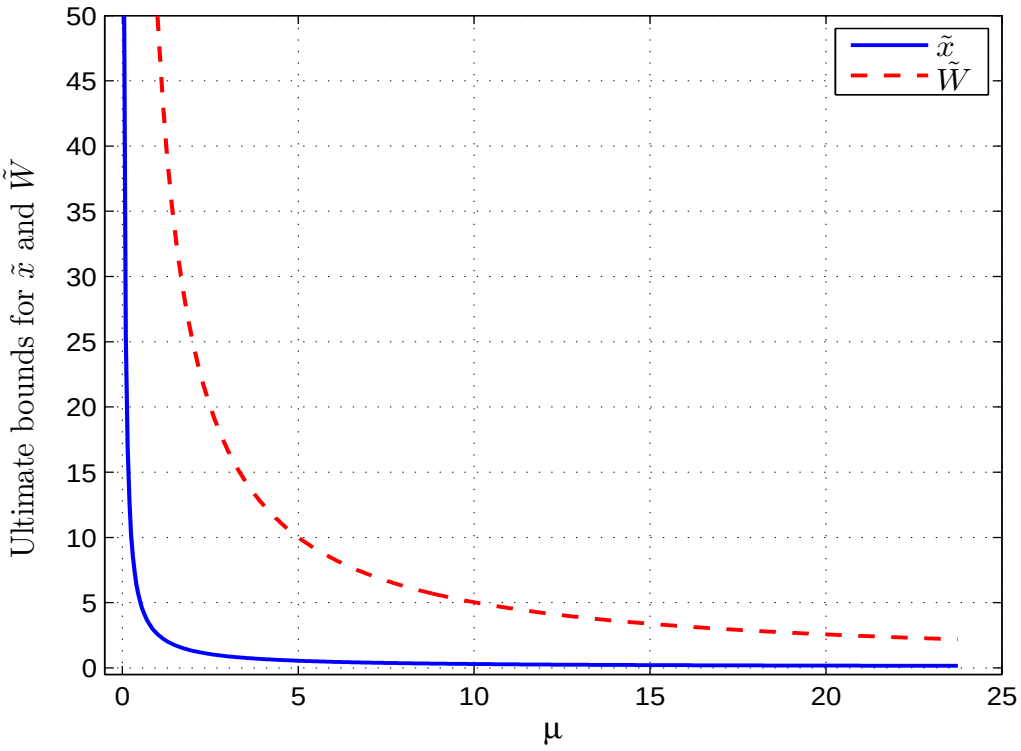

Figure 32: Ultimate bounds for k = 4.

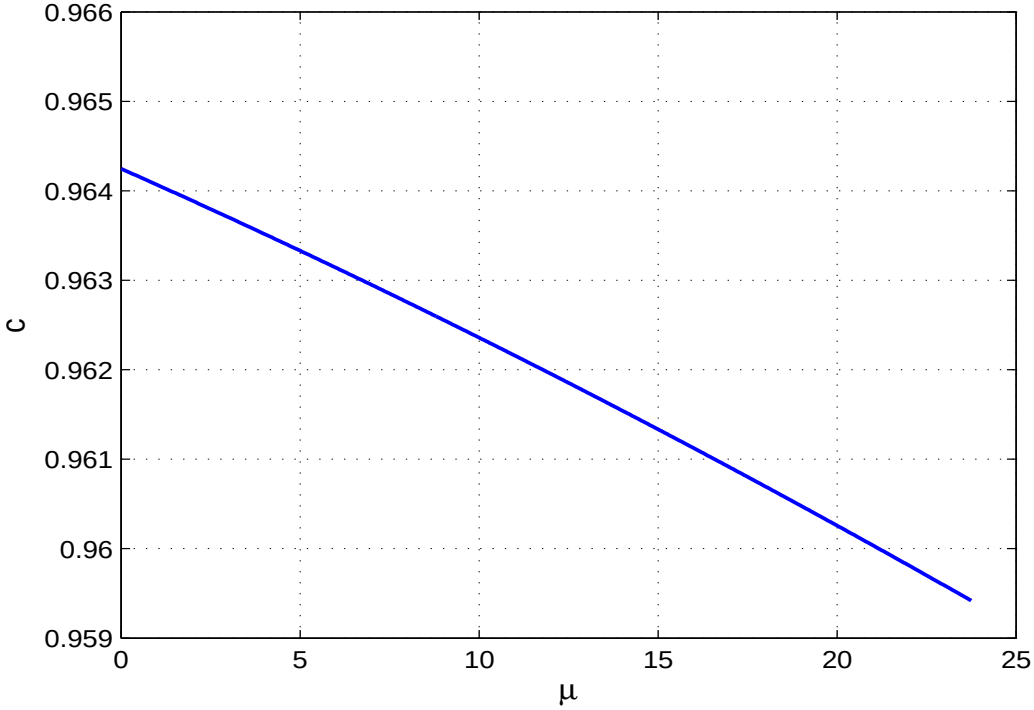

Figure 33: The value of $c(\mu)$ for k = 4.

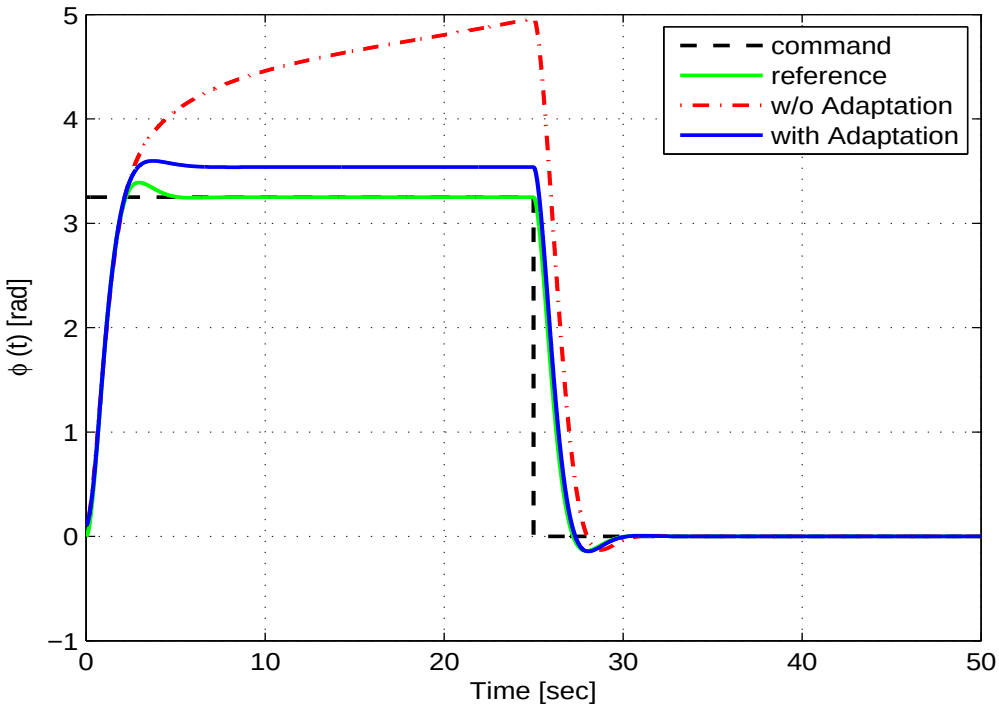

Figure 34: Step responses with and without adaptation using a proportional nominal controller.

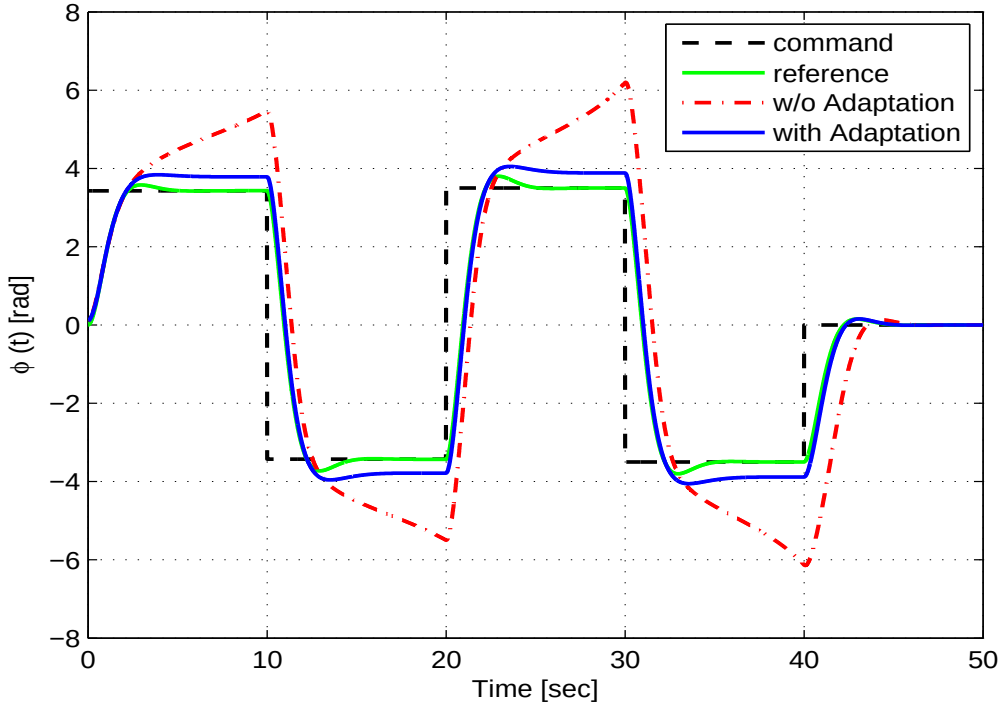

Figure 35: Tracking responses with and without adaptation using a proportional nominal controller.

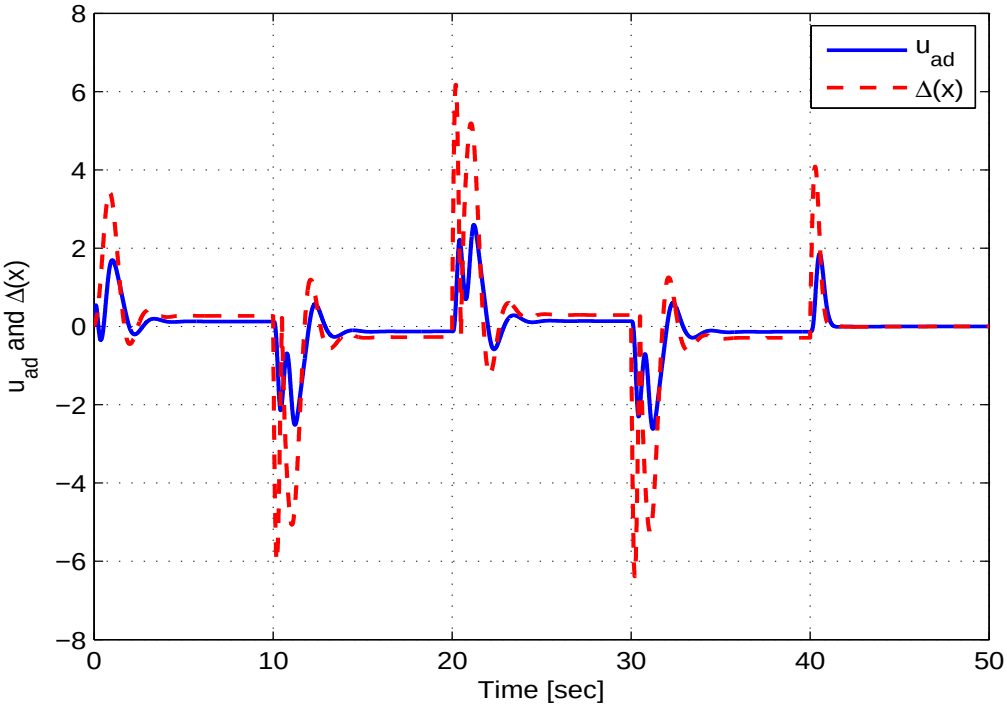

Figure 36: $u_{\text{ad}}(t)$ vs $\Delta(x)$.

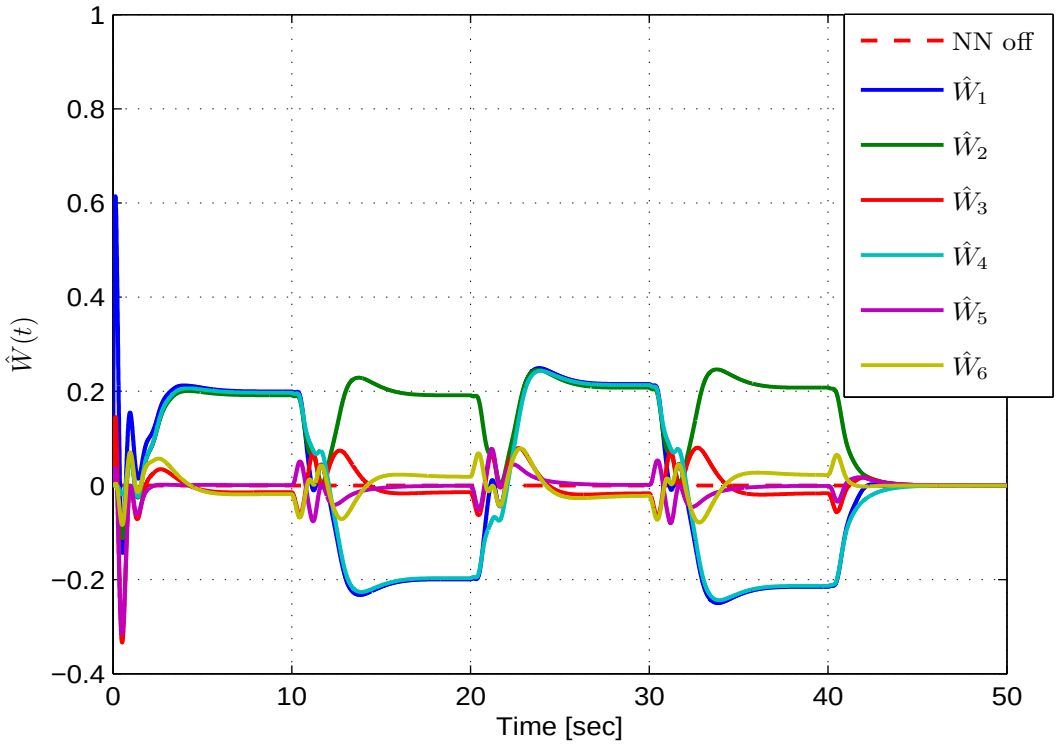

Figure 37: History of the estimated weight in tracking responses.

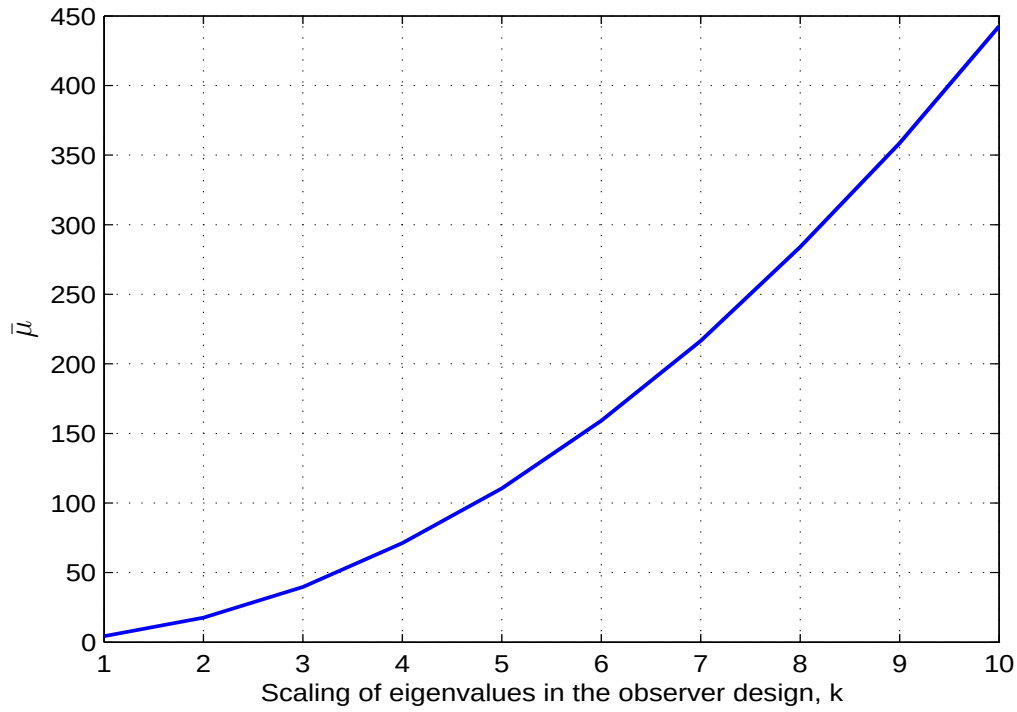

Figure 38: Limit value of μ for $Q_0 = I_3$ using a PI nominal controller.

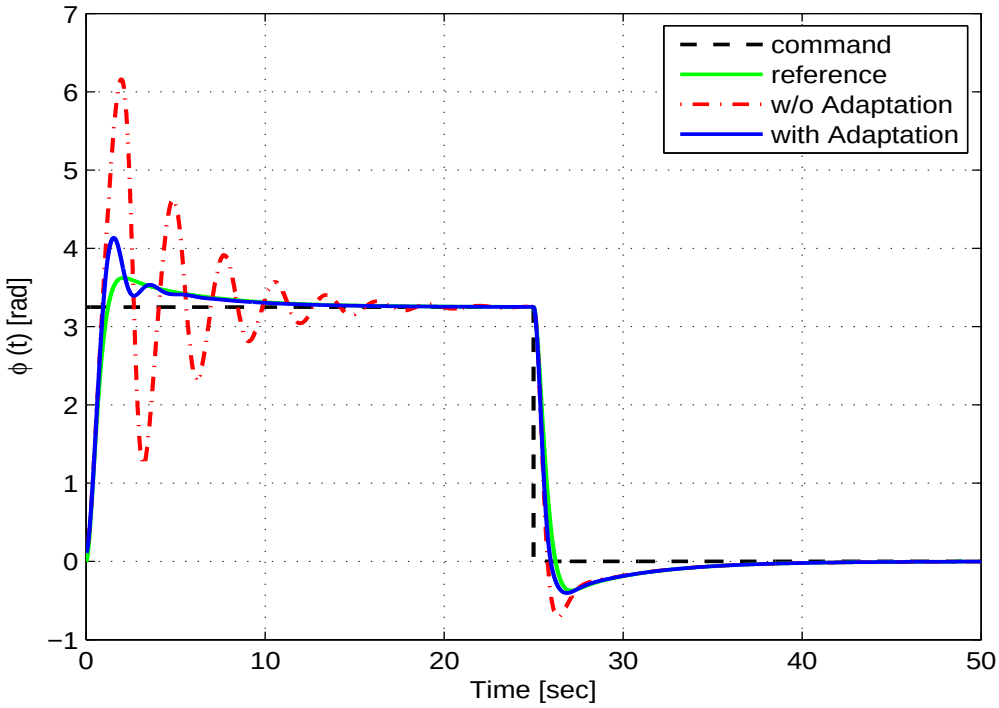

Figure 39: Step responses with and without adaptation using a PI nominal controller.

Chapter IV

OUTPUT FEEDBACK ADAPTIVE CONTROL OF AN AEROELASTIC GENERIC TRANSPORT MODEL

This Chapter presents the application of the output feedback adaptive control theory developed in Chapter III to an aeroelastic generic transport model. An aeroelastic model of the longitudinal dynamics of a generic transport model (GTM) is developed in Ref. [52]. This model accounts for interactions between wing bending and torsion and rigid body longitudinal aircraft dynamics. The structural dynamics are modeled using Galerkin's method [25]. This Chapter is organized as follows. Section 4.1 describes the application and presents the numerical results. Conclusions are given in Section 4.2.

4.1 Application to Aeroelastic GTM

The frequencies and damping ratios of the first bending (1B) and the first torsion (1T) modes, taken from Ref. [52], are given in Table 2. These values correspond to having 80% of the total fuel capacity.

	Frequency [rad/sec]	Damping Ratio
Mode 1B	7.3183	0.3718
Mode 1T	11.2201	0.0188

Table 2: Aeroelastic Modal Properties at 80% fuel capacity.

Figures 40 and 41 show the dependence of modal frequency and damping ratio on the ratio of fuel remaining to total fuel capacity. Note that there is a large dependence on the fuel ratio, and that the first torsional mode is lightly damped and the damping decreases as the fuel ratio decreases.

A linearized aeroelastic longitudinal flight dynamics model is obtained for a fuel ratio of 0.8, at an altitude of 3×10^4 feet, and a Mach number of 0.8. The state vector $x(t)$, the

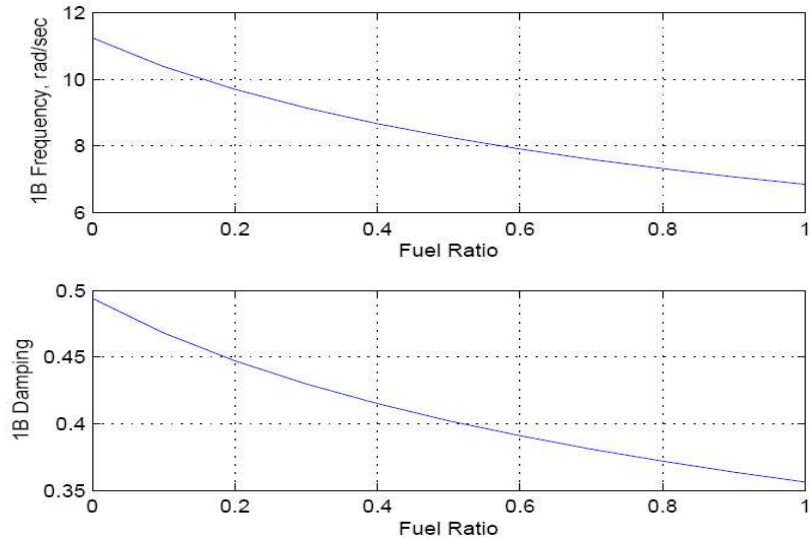

Figure 40: Frequency and Damping of Mode 1B as function of fuel ratio.

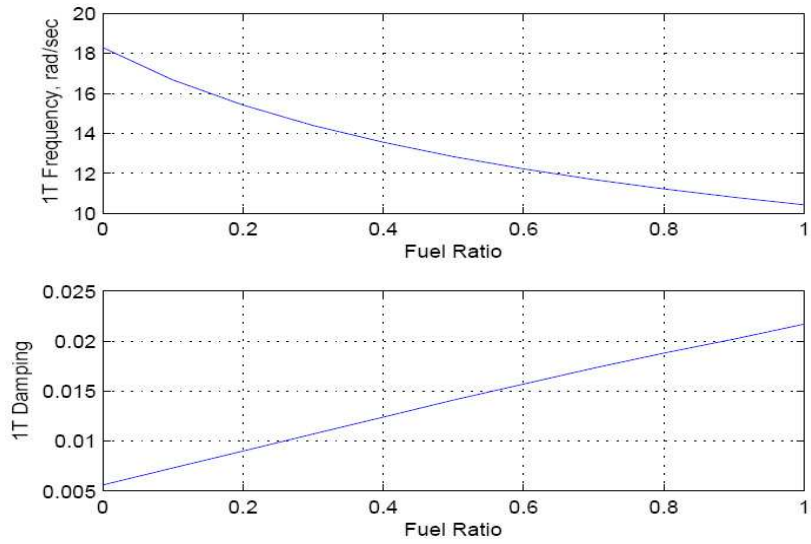

Figure 41: Frequency and Damping of Mode 1T as function of fuel ratio.

control input $u(t)$, the regulated output $y(t)$, and the sensed output $y_s(t)$ are expressed as:

$$\begin{aligned} x(t) &= \{\alpha(t), q(t), w(t), \theta(t), \dot{w}(t), \dot{\theta}(t)\}^{\mathrm{T}} \\ u(t) &= \delta_e \\ y(t) &= q(t) \qquad y_s(t) = [q(t), A_z(t)]^{\mathrm{T}} \end{aligned} \tag{165}$$

where $\alpha(t)$ denotes the angle of attack, $q(t)$ the pitch rate, $w(t)$ denotes the wing bending modal amplitude, $\theta(t)$ denotes the wing torsional modal amplitude, δ_e denotes the elevator deflection, and $A_z(t)$ denotes the normalized acceleration at the aircraft center of gravity.

The measurement equation for $A_z(t)$ was obtained using the relationship

$$A_z(t) = \frac{U_o}{G}\left(\frac{d\alpha}{dt} - q(t)\right) \tag{166}$$

where U_o is the equilibrium speed and G is the acceleration due to gravity. The system matrices in the form of (113) and (114) are written as:

$$A = \begin{bmatrix} -8.01 \times 10^{-1} & 9.65 \times 10^{-1} & 1.26 \times 10^{-2} & 5.09 \times 10^{-1} & 5.46 \times 10^{-4} & -2.42 \times 10^{-3} \\ -2.45 & -9.14 \times 10^{-1} & 1.75 \times 10^{-1} & 7.39 & 9.11 \times 10^{-3} & -3.11 \times 10^{-2} \\ 0 & 0 & 0 & 0 & 1 & 0 \\ 0 & 0 & 0 & 0 & 0 & 1 \\ 1.42 \times 10^{3} & 3.96 \times 10^{1} & -3.13 \times 10^{1} & -1.40 \times 10^{3} & -3.25 & -8.26 \\ -2.62 \times 10^{2} & -5.63 & 3.78 & -1.89 \times 10^{2} & 2.52 \times 10^{-1} & -3.75 \end{bmatrix}$$

$$B = \begin{bmatrix} 6.50 \times 10^{-2} & 3.52 & 0 & 0 & 0 & 0 \end{bmatrix}^{\mathrm{T}}$$

$$C = \begin{bmatrix} 0 & 1 & 0 & 0 & 0 & 0 \end{bmatrix}$$

$$C_s = \begin{bmatrix} 0 & 1 & 0 & 0 & 0 & 0 \\ -1.98 \times 10^{1} & -8.47 \times 10^{-1} & 3.11 \times 10^{-1} & 1.26 \times 10^{1} & 1.35 \times 10^{-2} & -6.00 \times 10^{-2} \end{bmatrix} \tag{167}$$

If the eigenvalues of the rigid aircraft's short period mode are computed from the 2 by 2 upper left matrix partition of the A matrix in (167) and if the eigenvalues of the aeroelastic modes are computed from the 4 by 4 lower right matrix partition, then this results in the following values:

$$\begin{aligned} \lambda_{SP} &= -0.8580 \pm 1.5380i \\ \lambda_{1B} &= -3.3212 \pm 7.5617i \\ \lambda_{1T} &= -0.1807 \pm 12.8379i \end{aligned} \tag{168}$$

However, the eigenvalues of the entire A matrix are:

$$\begin{aligned} \lambda_{SP} &= 1.5626, -2.6393 \\ \lambda_{1B} &= -4.5338 \pm 8.0733i \\ \lambda_{1T} &= 0.7122 \pm 13.0840i \end{aligned} \tag{169}$$

This suggests that the primary cause of instability in the aeroelastic model is coupling of the rigid body dynamics with the lightly damped torsional mode, and that it is necessary to take into account the aeroelastic modes to stabilize the airframe.

The frequency response for this model is given in Figure 42. The notch in the bode plot of the transfer function $\delta_e(i\omega)$ to $q(i\omega)$ is due to a near pole/zero cancelation associated with the torsional mode, indicating that this mode is not observable from $q(t)$ alone. However, the torsional mode resonance is evident in the transfer function from $\delta_e(i\omega)$ to $A_z(i\omega)$.

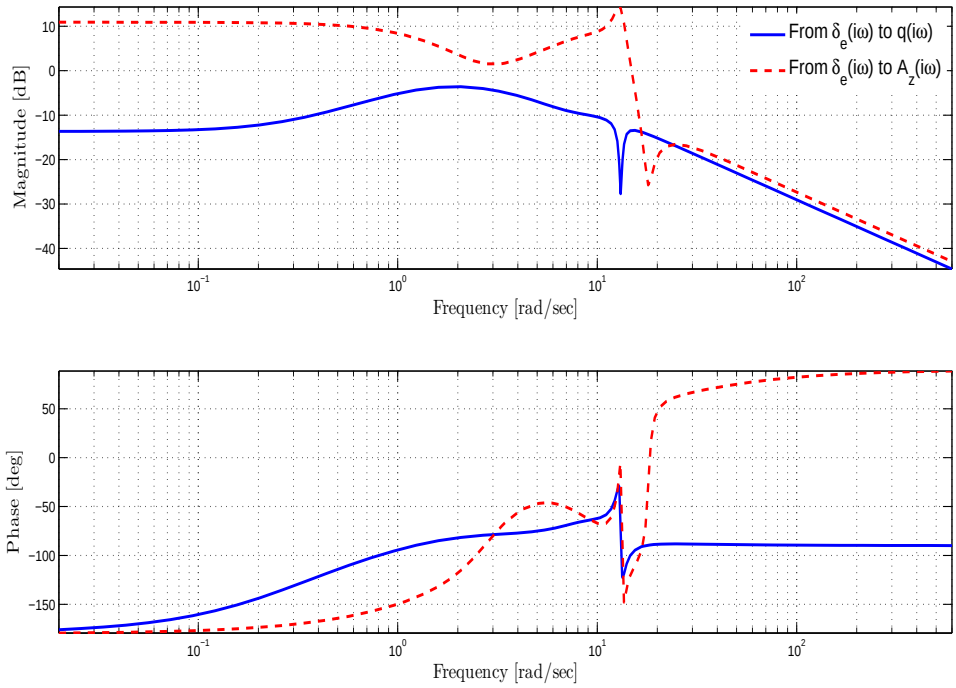

Figure 42: Selected frequency responses of the linearized GTM.

4.1.1 Nominal Controller Design

In the following design we consider augmenting a state observer based nominal controller in which the controller is designed with integral action by defining

$$\dot{x}_{\text{int}}(t) = -y(t) + r(t) \tag{170}$$

where $y(t) = q(t)$. The augmented dynamics can be put in the form of (113) by defining:

$$\begin{aligned}
\dot{x}_*(t) &= \underbrace{\begin{bmatrix} A & 0 \\ -C & 0 \end{bmatrix}}_{A_*} x_*(t) + \underbrace{\begin{bmatrix} B \\ 0 \end{bmatrix}}_{B_*} \big[u(t) + \Delta(x)\big] + \underbrace{\begin{bmatrix} 0_{6\times 1} \\ 1 \end{bmatrix}}_{B_r} r(t) \\
y_*(t) &= \underbrace{\begin{bmatrix} C & 0 \end{bmatrix}}_{C_*} x_*(t), \qquad y_{s*}(t) = \underbrace{\begin{bmatrix} C_s & 0_{2\times 1} \\ 0_{1\times 6} & 1 \end{bmatrix}}_{C_{s*}} x_*(t)
\end{aligned} \tag{171}$$

where $x_*(t) = \big[x(t), x_{\text{int}}(t)\big]^{\text{T}}$. In this case the form of observer dynamics in (121) becomes

$$\dot{\hat{x}}_*(t) = A_*\hat{x}_*(t) + B_*u_{\text{n}}(t) + B_r r(t) + L_*[y_{s*}(t) - C_{s*}\hat{x}_*(t)] \tag{172}$$

and the nominal control law in (115) becomes

$$u_{\text{n}*}(t) = K_{x_*}\hat{x}_*(t) + K_r r(t) \tag{173}$$

where $K_{x_*} \in \mathbb{R}^{m\times n_*}$ such that $A_{\text{m}*} = A_* - B_*K_{x_*}$ is Hurwitz. Since the form of the error dynamics in (123) remains the same, the theorem and corollaries of the previous section still apply.

The nominal control design was performed using LQG/LTR theory [16]. The controller gain matrix (K_{x_*}) was obtained using $Q_K = \text{diag}[1,\, 25,\, 0.0001,\, 5,\, 0.0001,\, 5,\, 125]$ to penalize $x_*(t)$ and $R_K = 10$ to penalize $u(t)$. The observer gain matrix (L) was obtained using $Q_L = \kappa^2 BB^{\text{T}}$ as the process noise matrix where $\kappa = 6$ is the LTR gain, and $R_L = \text{diag}[I_2, 0.01]$ as the measurement noise matrix. The resulting gain matrices for this design are:

$$\begin{aligned}
K_{x_*} &= \begin{bmatrix} 18.5583 & 3.0926 & -0.2406 & 12.4516 - 0.0244 & 0.0192 & -3.5355 \end{bmatrix} \\
L_* &= \begin{bmatrix} 0.4568 & 12.4859 & 1.4554 & 0.2120 & 5.4207 & -2.2599 & -0.2314 \\ -0.8144 & -16.2959 & 1.7348 & 0.2937 & -42.1016 & 10.7795 & 0.5333 \\ -3.5836 & -23.1385 & -105.4518 & -0.0173 & -168.1133 & 31.8997 & 3.5324 \end{bmatrix}^{\text{T}}
\end{aligned} \tag{174}$$

Figure 43 shows the frequency response of the loop transfer functions with the loop broken at the plant input for both full-state feedback and LQG/LTR loops, where it can be seen that the margins of the full-state feedback loop are nearly recovered.

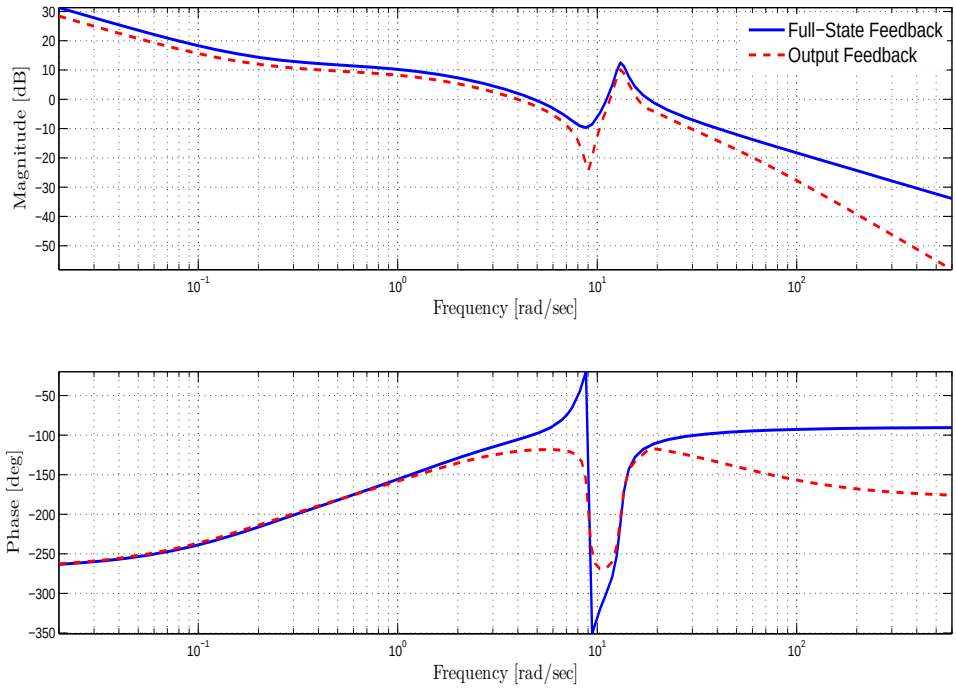

Figure 43: Selected Frequency responses of the loop transfer functions for both full-state feedback and LQG-LTR.

In what follows, we consider the command tracking problem with the initial conditions set to zero. Our simulation includes the effect of actuator dynamics, measurement noise, and sensor analog pre-filter. The actuator model for the elevator has a bandwidth of 12Hz, an amplitude saturation of $\pm 30^\circ$, and a rate saturation of $\pm 100^\circ$/sec. To model sensor noise, we assume that $q(t)$ and $A_z(t)$ are corrupted with a band-limited white noise process with a correlation time constant of 0.001 seconds and noise power levels of 1×10^{-8} and 1×10^{-6} respectively. Pre-filters for $q(t)$ and $A_z(t)$ have a bandwidth of 8Hz.

Figures 44 and 45 show the responses with nominal control (adaptation off) in the absence of uncertainty. The upper part of Figure 44 compares the pitch rate command $(q_{\rm cmd}(t))$, the reference model response $(q_{\rm m}(t))$, and the actual plant response $(q(t))$. The lower portion compares the command to the actuator $(\delta_{e-{\rm cmd}}(t))$ with the actuator response. The difference cannot be distinguished at this scale. The upper left portion of Figure 45 shows the relative amounts of sensor noise. The remainder of this figure shows the performance of the observer. The effect of sensor noise is most evident in the rate of change

of the torsional amplitude.

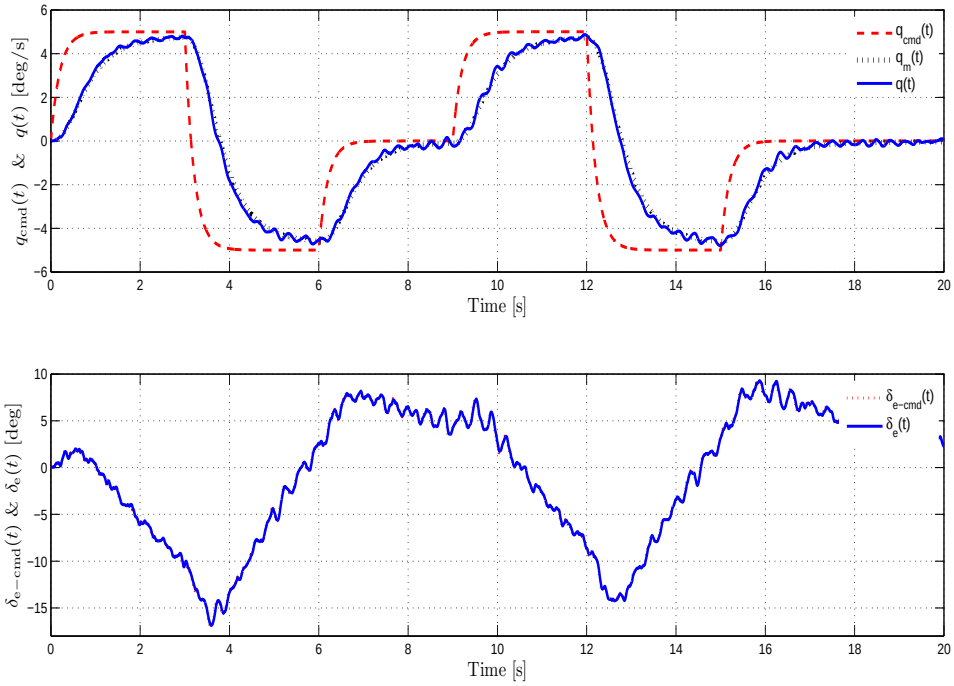

Figure 44: Nominal control responses without uncertainty.

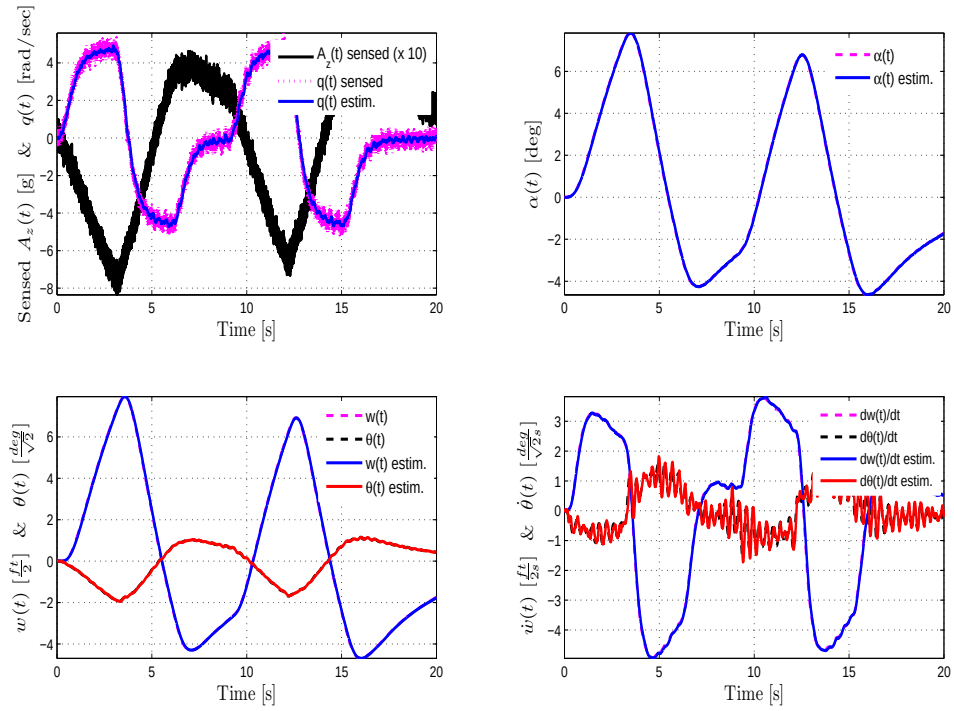

Figure 45: Measurements, state responses, and their estimates with nominal control in the absence of uncertainty.

4.1.2 Adaptive Controller Design

For the adaptive control design we used a combination of bias term and sigmoidal basis functions of the form

$$\begin{aligned} \beta(\hat{x}) =& [1, \beta_1(\hat{x}), \ldots, \beta_6(\hat{x})] \\ \beta_i(\hat{x}) =& \frac{1 - e^{-\hat{x}_i}}{1 + e^{-\hat{x}_i}}, \qquad i = 1, 2, ..., 6 \end{aligned} \tag{175}$$

For $Q_0 = 1.2I$ the upper bound $\bar{\mu} = 238.4$ is computed using the Lemma 2.2. From the weight update law in (125), the following selected adaptation gains are used for all cases of uncertainty.

$$\gamma = 200, \quad \sigma = 0.008 \times \gamma, \quad \mu = 238 \tag{176}$$

4.1.3 Nonlinear Uncertainty

We consider the case when there exists a nonlinear uncertainty of the form

$$\begin{aligned} \Delta(x) = & 2.5\alpha(t)q(t) + 2.5\alpha^2(t) + 1.5q^2(t) + 1.25w(t)\theta(t) \\ & + 0.25\dot{w}(t)\dot{\theta}(t) + 2.5\theta(t)\dot{\theta}(t) - 2.5\dot{\theta}^2(t) + 0.00025\dot{w}^2(t) \end{aligned} \tag{177}$$

in the system dynamics (113). Figure 46 shows the responses with nominal control and Figure 47 shows the responses with adaptive control. The response with nominal control eventually goes unstable, whereas the response with adaptation is stable, and the tracking performance is nearly as good as that observed in Figure 44 without uncertainty. Also, the level of noise present in the elevator command for the adaptive result is comparable to that observed for the nominal control without uncertainty in Figure 44. Figure 48 shows the comparison between $u_{\text{ad}}(t)$ and $\Delta(x)$ in the case of nonlinear uncertainty and sensor noise.

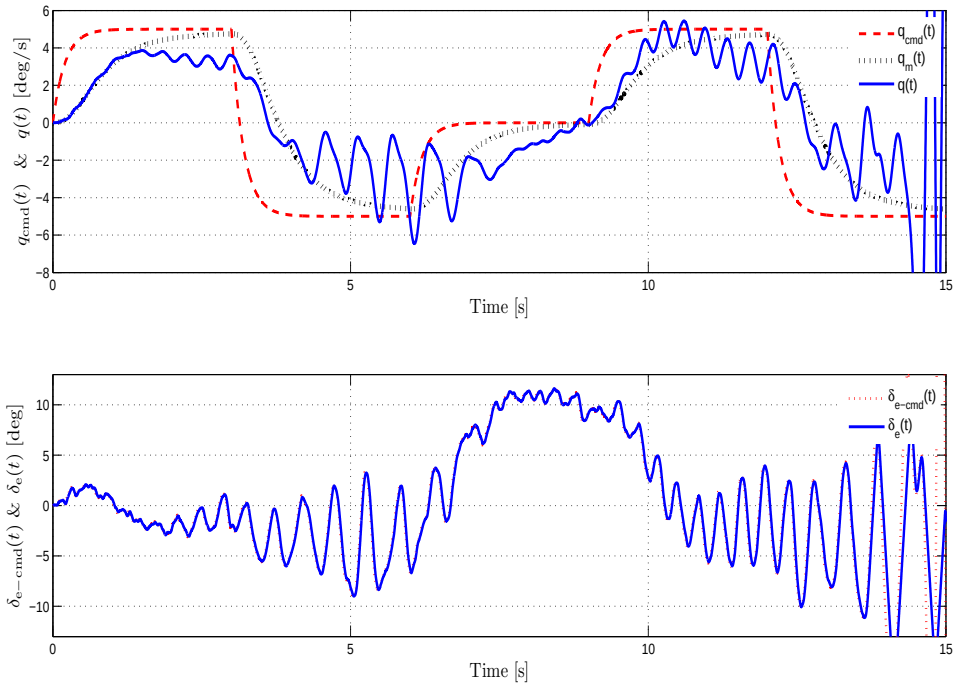

Figure 46: Pitch rate and elevator responses with nominal control for the case of nonlinear uncertainty and no sensor noise.

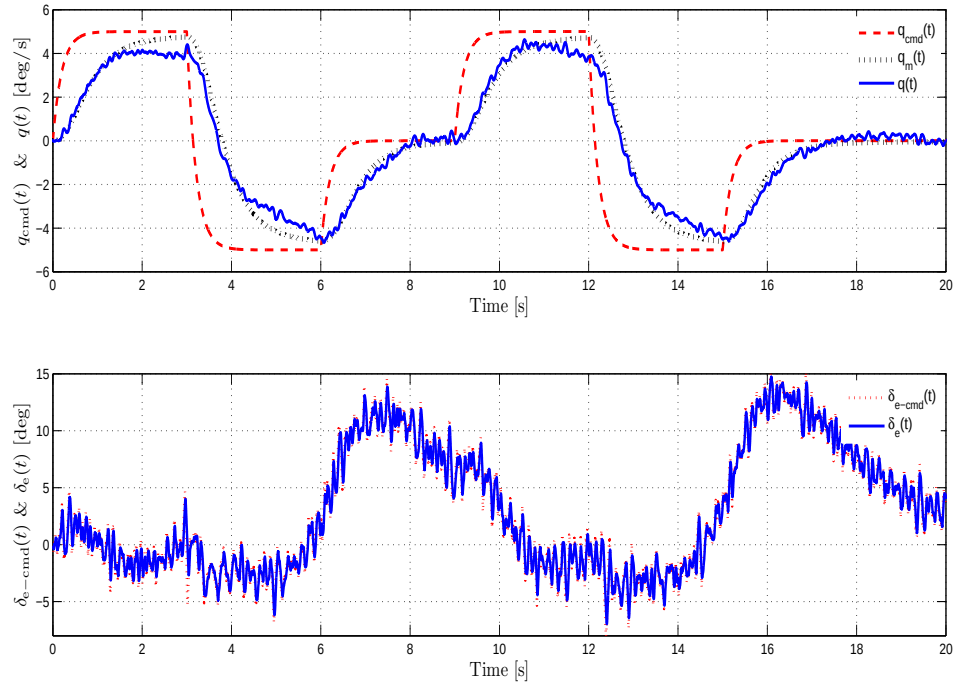

Figure 47: Pitch rate and elevator responses with adaptive control for the case of nonlinear uncertainty and sensor noise.

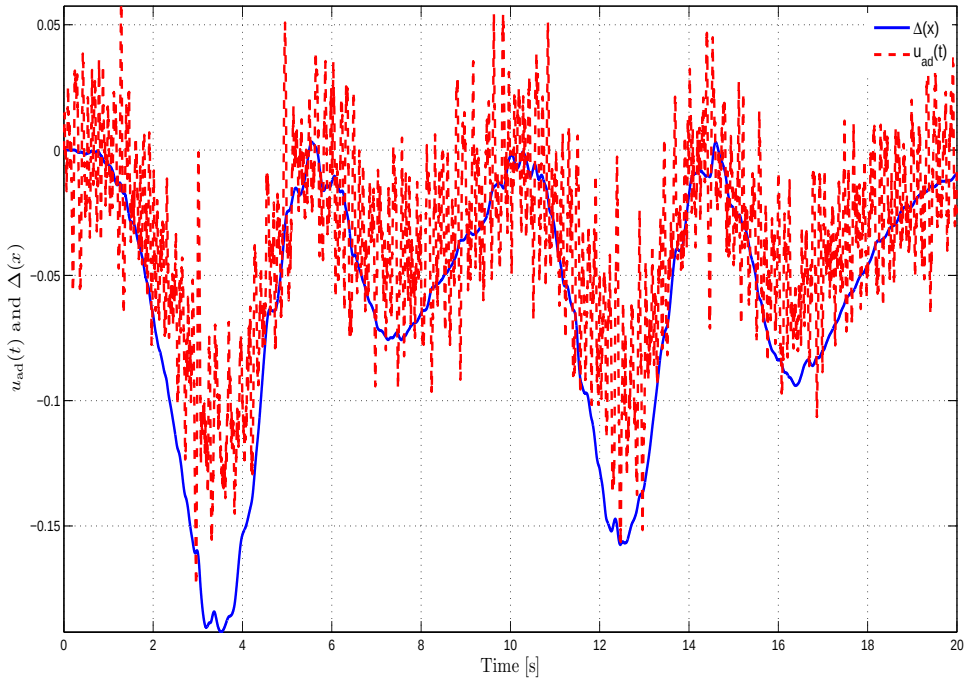

Figure 48: $u_{\text{ad}}(t)$ vs $\Delta(x)$ for the case of nonlinear uncertainty and sensor noise.

4.1.4 External Disturbance

We consider the case when a disturbance $d(t) = 4\sin(3t)$ is applied to the system through the control input. Figure 49 shows the nominal control response and Figure 50 shows the adaptive control response, in which the tracking performance is improved with adaptation. Figure 51 shows the comparison between $u_{\text{ad}}(t)$ and $\Delta(x)$ in the case of external disturbance and sensor noise.

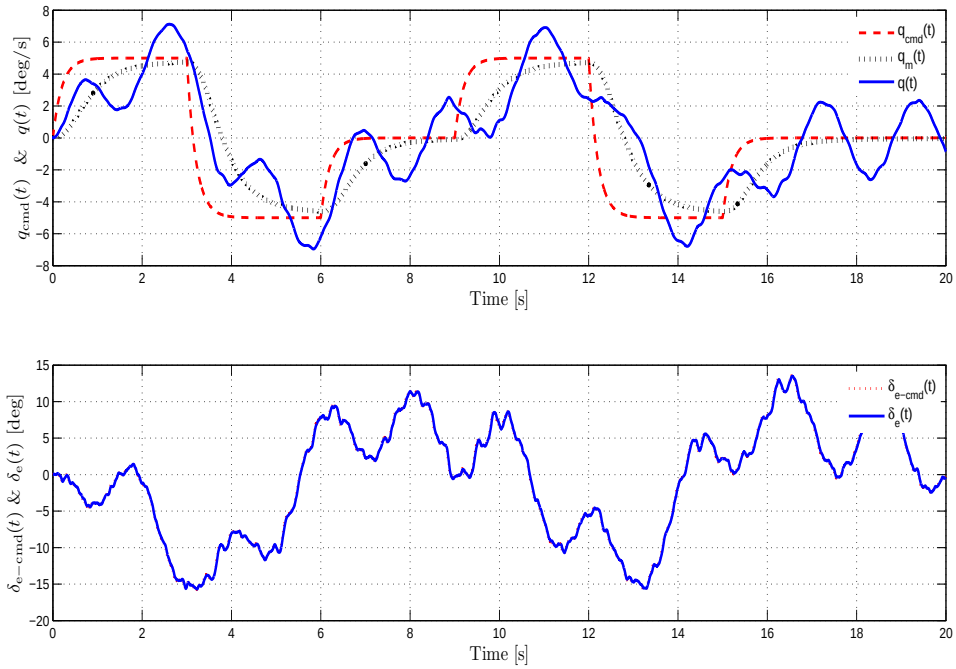

Figure 49: Pitch rate and elevator responses with nominal control for the case of external disturbance and no sensor noise.

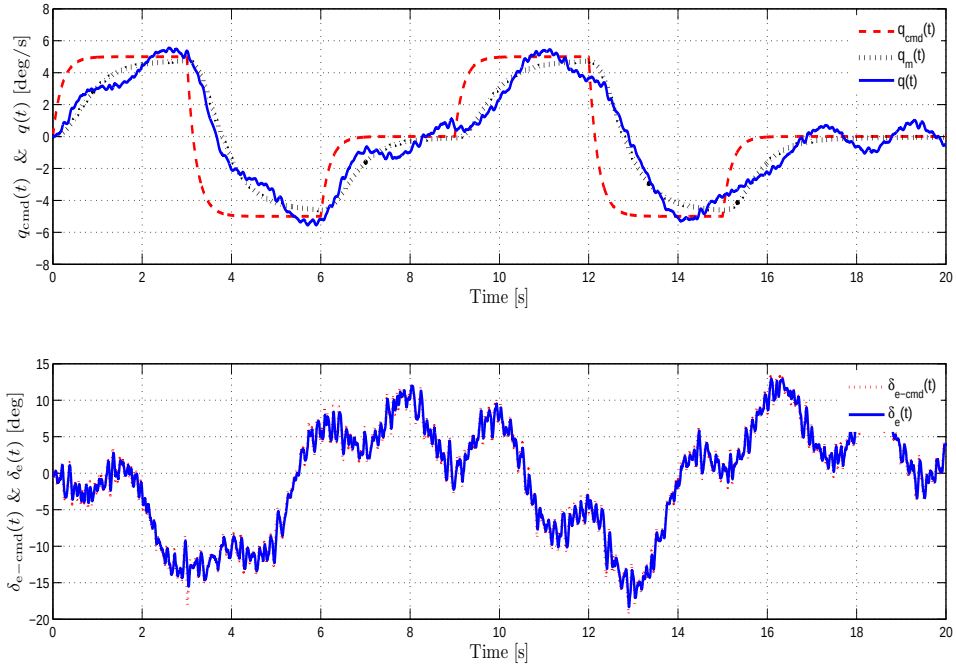

Figure 50: Pitch rate and elevator responses with adaptive control for the case of external disturbance and sensor noise.

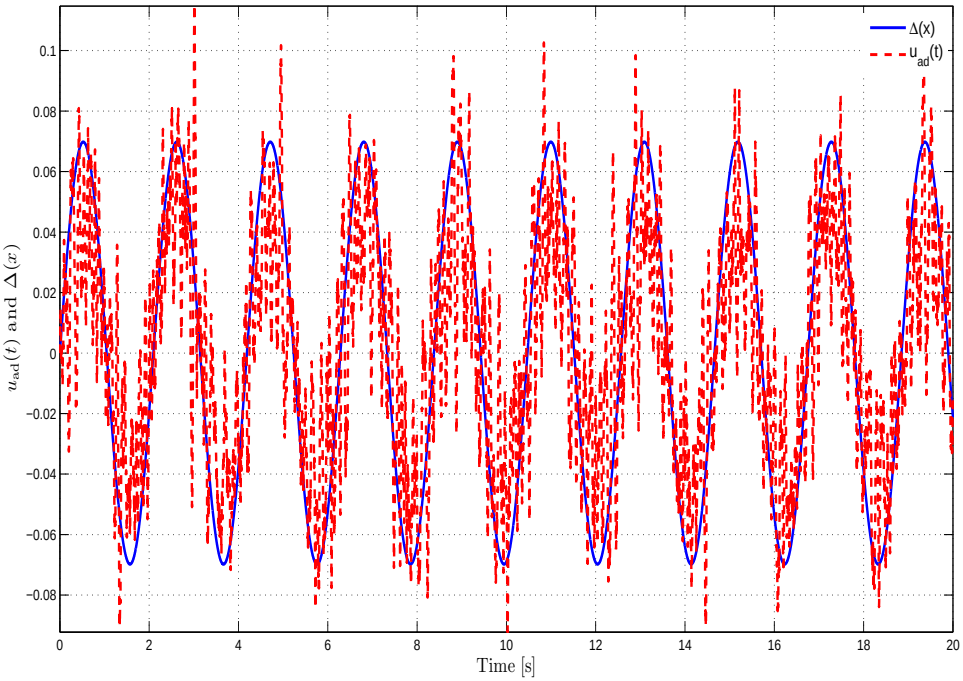

Figure 51: $u_{\text{ad}}(t)$ vs $\Delta(x)$ for the case of external disturbance and sensor noise.

4.1.5 Nonlinear Uncertainty and External Disturbance

The nonlinear uncertainty and external disturbance considered previously are combined in this case. Figure 52 shows that the adaptive control response remains stable and its tracking performance is still reasonably well maintained. Figure 53 shows the comparison between $u_{\text{ad}}(t)$ and $\Delta(x)$ in the case of nonlinear uncertainty, external disturbance, and sensor noise.

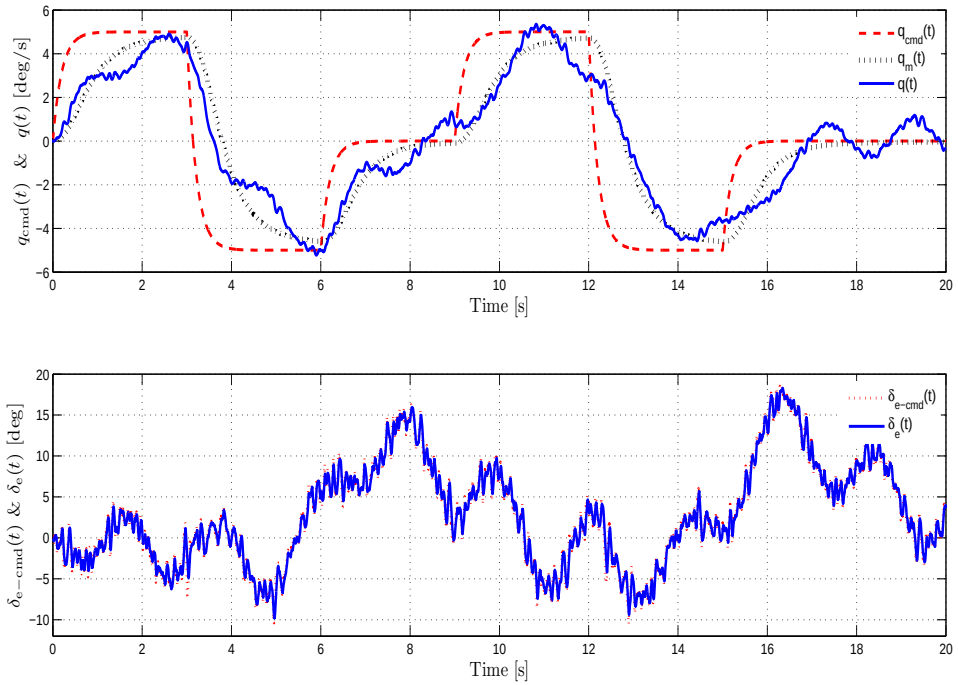

Figure 52: Pitch rate and elevator responses with adaptive control for the case of nonlinear uncertainty and external disturbance.

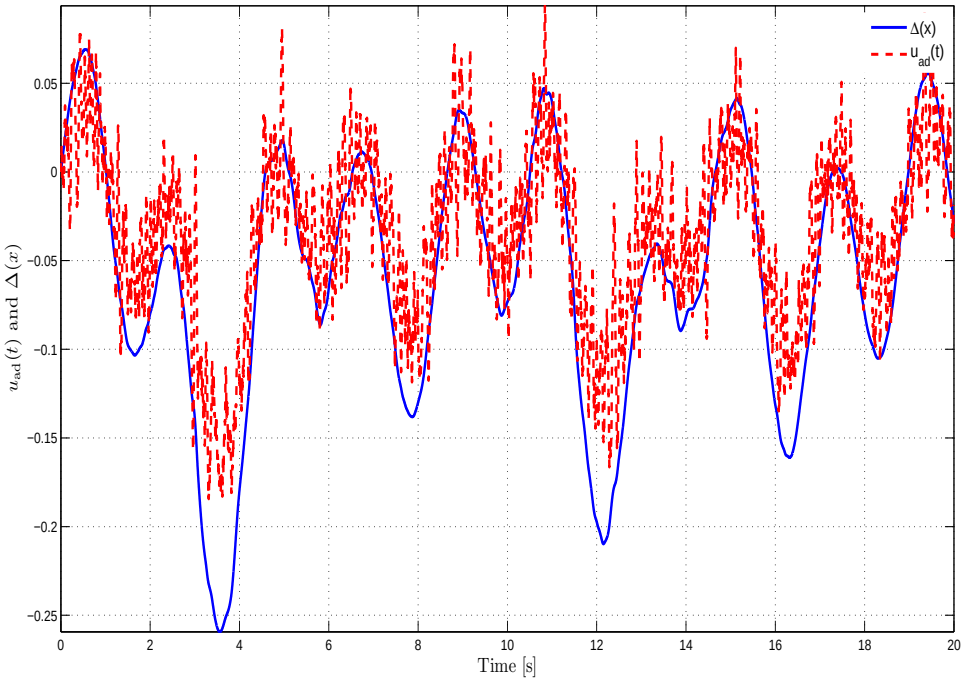

Figure 53: $u_{\text{ad}}(t)$ vs $\Delta(x)$ for the case of nonlinear uncertainty and external disturbance with sensor noise.

4.1.6 Change of Inertia

Next we illustrate an example of parameter change, as might be caused by structural damage, in which the moment of inertia (I_{xx}) is reduced to 70% of its nominal value. The resulting change in modal properties is shown in Table 3.

λ_{SP}	1.5626, -2.6393	1.48, -3.6938
	Frequency [rad/sec]	Damping Ratio
Mode 1B	$9.26 \rightarrow 9.8$	$4.9 \times 10^{-1} \rightarrow 6.65 \times 10^{-1}$
Mode 1T	$13.1 \rightarrow 12.1$	$-5.44 \times 10^{-2} \rightarrow -2.7 \times 10^{-1}$

Table 3: Modal Properties change.

Figure 54 shows that the response with nominal control becomes unstable, whereas Figure 55 shows that the tracking performance is nearly as good as that observed in Figure 44 without uncertainty. Also, the level of noise present in the elevator command for the adaptive result is comparable to that observed for the nominal control without uncertainty in Figure 44. Figure 56 shows that the estimation performance of the observer is also as good as that observed in Figure 45 without uncertainty.

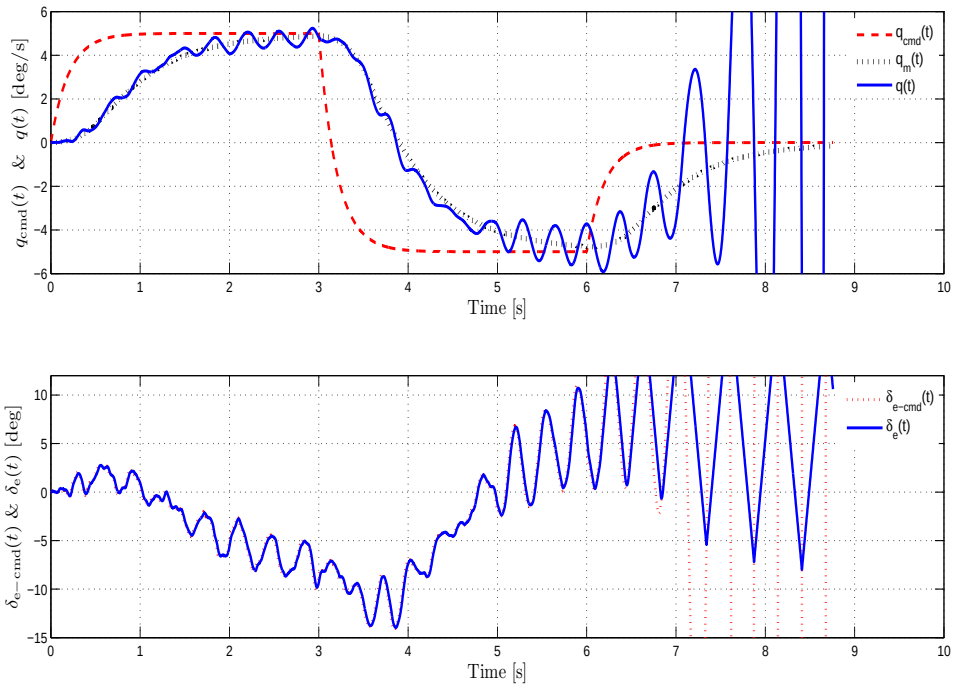

Figure 54: Pitch rate and elevator responses with nominal control for the case of inertia change.

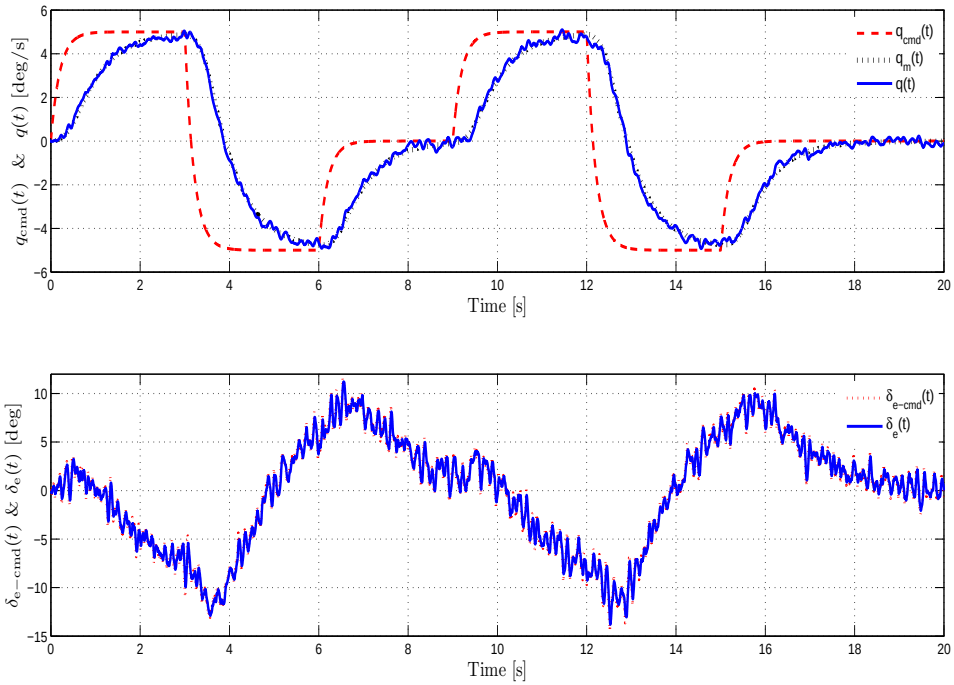

Figure 55: Pitch rate and elevator responses with adaptive control for the case of inertia change and sensor noise.

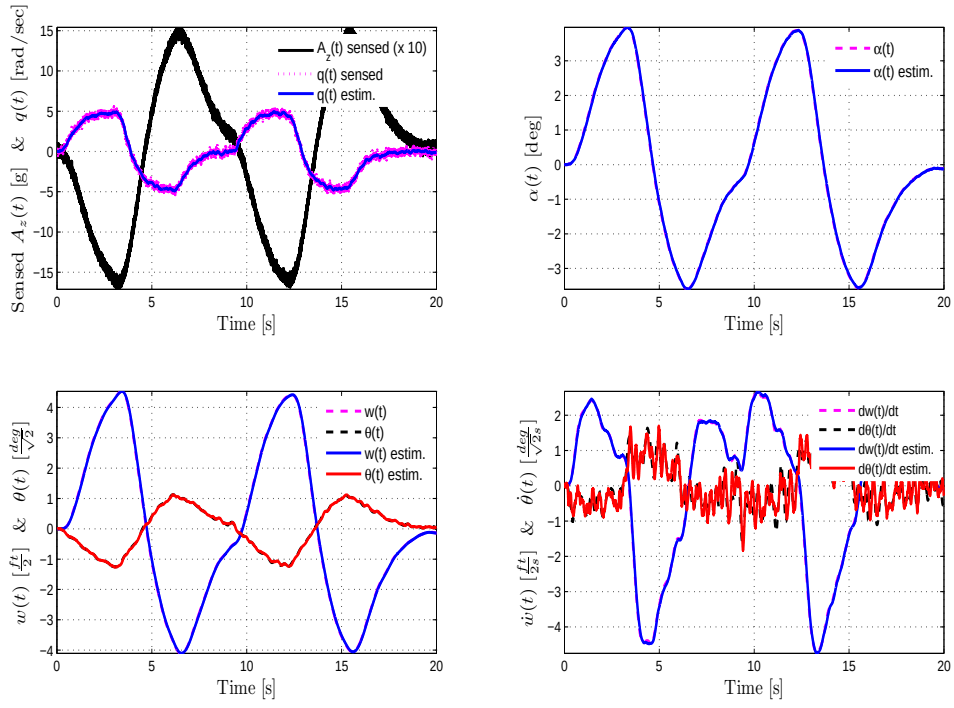

Figure 56: Measurements, state responses, and their estimates with adaptive control for the case of inertia change and sensor noise.

4.1.7 Uncertainty in an Elastic Property

Finally we illustrate an example of parameter change in which Young's modulus and shear modulus of the wing section are reduced to 70% of their nominal values. The resulting change in modal properties is shown in Table 4.

λ_{SP}	1.5626, -2.6393	1.49, -3.68
	Frequency [rad/sec]	Damping Ratio
Mode 1B	$9.26 \rightarrow 9.04$	$4.9 \times 10^{-1} \rightarrow 6.73 \times 10^{-1}$
Mode 1T	$13.1 \rightarrow 11$	$-5.44 \times 10^{-2} \rightarrow -2.98 \times 10^{-1}$

Table 4: Modal Properties change.

Figure 57 shows that the response with nominal control becomes unstable, whereas Figure 58 shows that the tracking performance is nearly as good as that observed in Figure 44 without uncertainty. Also, the level of noise present in the elevator command for the adaptive result is comparable to that observed for the nominal control without uncertainty in Figure 44. Figure 59 shows that the estimation performance of the observer is also as good as that observed in Figure 45 without uncertainty.

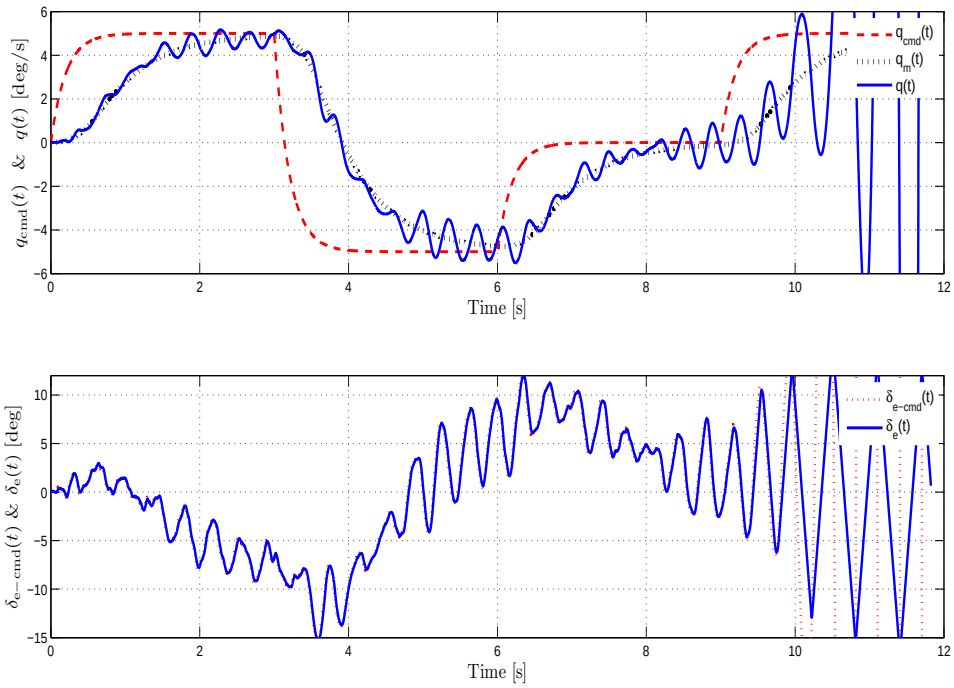

Figure 57: Pitch rate and elevator responses with nominal control for the case of elastic property change.

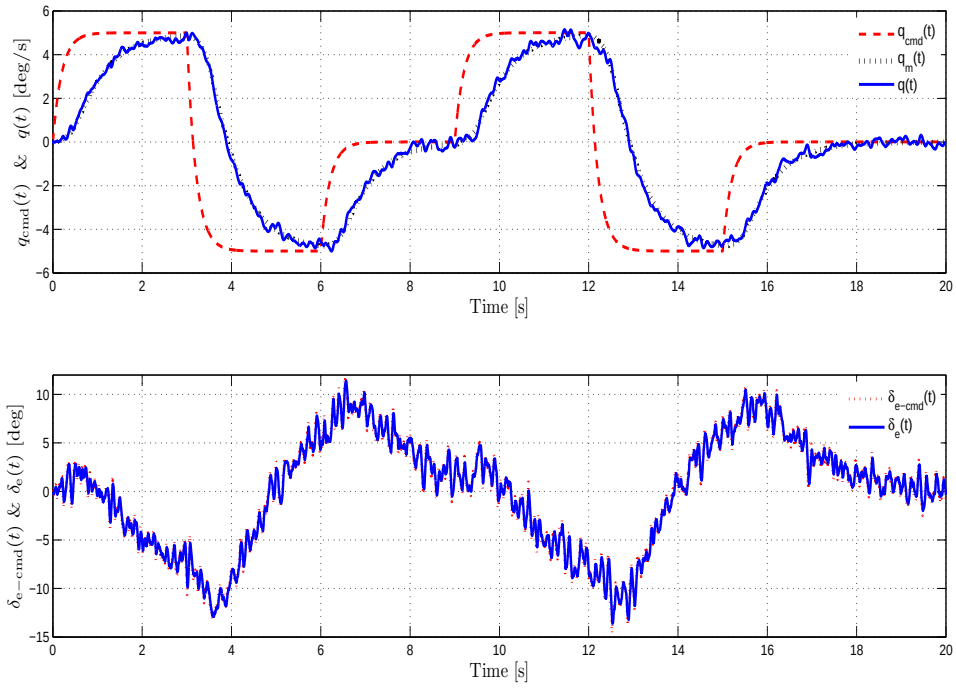

Figure 58: Pitch rate and elevator responses with adaptive control for the case of elastic property change and sensor noise.

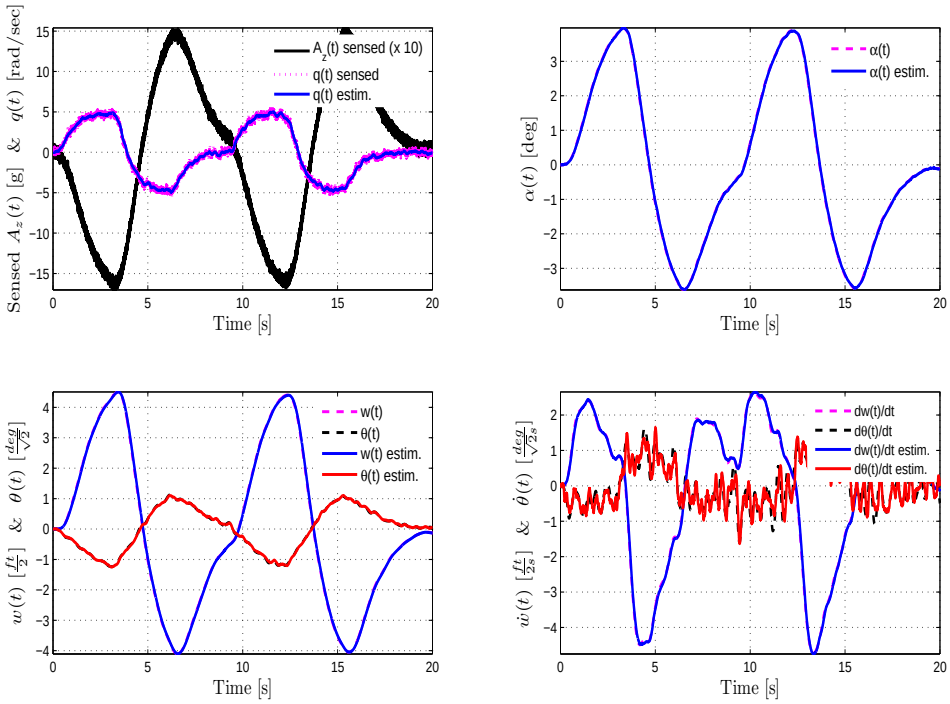

Figure 59: Measurements, state responses, and their estimates with adaptive control for the case of elastic property change and sensor noise.

4.2 Conclusion

A parameter dependent Riccati equation approach to output feedback adaptive control architecture has been applied to an aeroelastic model of longitudinal dynamics of a generic transport model including actuator dynamics, measurement noise, and sensor analog pre-filtering. The method of LQG-LTR design was used to obtain a nominal controller, and four different cases of uncertainty are investigated in simulation. The results show that the proposed output feedback adaptive approach is effective in treating modeling uncertainty in flight control design for a flexible aircraft.

Chapter V

CONCLUSIONS AND FUTURE RESEARCH

5.1 Conclusions

This thesis provides novel approaches to both state feedback and output feedback adaptive control. In the case of state feedback adaptive control, $\mathcal{K}$-modification and its combination with Kalman Filter based adaptive control and derivative-free adaptive control are developed.

The proposed $\mathcal{K}$-modification prescribes a way to introduce a tunable stiffness term in the weight update law of an adaptive control system such that smooth transient characteristics can be obtained. The system error signals are proven to be uniformly ultimately bounded using the projection based weight update law. $\mathcal{K}$-modification can be interpreted as a feedback of time delayed values of the weights and filters inputs of the uncertainty according to the tuned damping ratio and natural frequency. The examples also illustrate that robustness to time delay is improved, however there is no theoretical results in this direction were obtained.

The example of wing rock dynamics illustrates that oscillations in adaptive systems can be significantly reduced through the appropriate choice of the stiffness parameter in combination with other adaptation gains. $\mathcal{K}$-modification can be also used in combination with other modification methods that provide damping.

KF based σ- and $\mathcal{K}$ adaptive control law combines the benefits provided by each of these individual methods. The system error signals are proven to be uniformly ultimately bounded using the projection based weight update law. The main advantage of this approach is that less effort is required in tuning the parameters in the adaptive law, while at the same time it provides a way to control damping and stiffness associated with error transients. Also, the KF based σ- and $\mathcal{K}$ adaptive control law significantly reduces oscillations in the wing rock example when a time delay was inserted in the control channel.

DF-$\mathcal{K}$-MRAC also combines all the benefits provided by each of individual methods. The system error signals are proven to be uniformly ultimately bounded using a Lyapunov-Krasovskii functional without the need of additional modification terms or a projection operator. It is also shown that greater flexibility is introduced in tuning the adaptive controller. A simple spacecraft example shows that the proposed controller provides better performance with less control effort than conventional MRAC when uncertainty, disturbances, and time delay are applied to the model.

In the setting of output feedback adaptive control, a parameter dependent Riccati equation approach is developed and is applied to an aeroelastic generic transport model. The architecture for output feedback model reference adaptive control that augments a nominal fixed gain controller is presented. It is assumed that the nominal controller employs an observer. The observer is used in the adaptive part of the design in place of a reference model. The level of complexity for realization of proposed architecture, above that of the nominal controller, is far less than other methods [8, 27, 64, 73]. The error signals including state estimation error, estimated state tracking error, and weight estimate error are proven to be uniformly ultimately bounded. The stability analysis employs a Lyapunov candidate based on the existence of a positive definite solution of a parameter dependent Riccati equation. The upper limit for this parameter is employed in the design of the adaptive law, and also influences the ultimate bounds for the state estimate error and the weight error. Simulation examples illustrate the computation of the parameter bound, computation of its influence on the ultimate error bounds, and a set of typical simulation results highlighting the attainable performance. The approach is applied to an aeroelastic model of longitudinal dynamics of a generic transport model. The results show that the proposed output feedback adaptive approach is effective in treating modeling uncertainty in flight control design for a flexible aircraft.

5.2 Future Research

Three cases for future research appear promising:

1. $\mathcal{K}$-modification has an additional tuning parameter, T, which is defined as updating time

interval. As shown in the wing rock simulation with time delay insertion, $\mathcal{K}$-modification seems to improve robustness to time delay significantly, but no theoretical basis for this simulation result is given. Therefore one topic of future research interest will be developing an analysis of the potential benefits of $\mathcal{K}$-modification in this regard.

2. $\mathcal{K}$-modification is perhaps most useful when it comes to adaptive control of flexible systems. Since that falls with the setting of output feedback adaptive control, it is of interest to extend $\mathcal{K}$-modification to the output feedback case, employing the parameter depending Riccati equation approach developed in Chapter III. This would also bring together and unify the theory developed in Chapters II and III.

3. It is of interest for practical application to extend the theory developed in this thesis to the case of uncertainty in control effectiveness, and in the case of redundant actuation, to also consider the case of actuator failure. A suitable formulation for the system dynamics would have the form

$$\begin{aligned} \dot{x}(t) &= Ax(t) + B\Lambda\big[Gu_{\mathrm{n}}(t) - u_{\mathrm{ad}}(t) + \Delta(x(t))\big] \\ y(t) &= Cx(t) \end{aligned} \tag{178}$$

where G is a control allocation matrix, and $\Lambda \in \mathbb{R}^{m\times m}$ is a diagonal matrix with entries $\lambda_i \geq 0$. Uncertainty in control effectiveness is modeled using $\lambda_i > 0$, which actuator failure is treated by letting $\lambda_i = 0$. Examples illustrating when this has been done for other approaches to adaptive control appear in Ref. [69].

REFERENCES

[1] Ananthakrishnan, S., "Adaptive tachometer feedback augmentation of the shuttle remote manipulator control system," 1995.

[2] Anderson, C., Hittle, D., Katz, A., and Kretchmar, R., "Synthesisof reinforcement learning, neural networks and pi control applied to a simulated heating coil," *Artificial Intelligence in Engineering*, vol. 11, pp. 421–429, 1997.

[3] Bernstein, D., *Matrix mathematics: theory, facts, and formulas.* New York, NJ: Princetion, 2nd ed., 2009.

[4] Bodson, M. and Groszkiewicz, J., "Multivariable adaptive algorithms for reconfigurable flight control," *IEEE Transactions on Control Systems Technology*, vol. 5, no. 2, pp. 217–229, 1997.

[5] Bordignon, K. and Durham, W., "Closed form solutions to the constrained control allocation problem," 1993.

[6] Calise, A. and Rysdyk, R., "Nonlinear adaptive flight control using neural networks," *IEEE Control Systems Magazine*, vol. 18, no. 6, 1998.

[7] Calise, A., Yucelen, T., Muse, J., and Yang, B., "A loop recovery method for adaptive control," in *AIAA Guidance Navigation and Control Conference*, 2009.

[8] Calise, A. J., Hovakimyan, N., and Idan, M., "Adaptive output feedback control of nonlinear systems using neural networks," *Automatica*, vol. 37, no. 8, pp. 1201–1211, 2001.

[9] Cao, C. and Hovakimyan, N., "Design and analysis of a novel adaptive control architecture with guaranteed transient performance," *IEEE Transactions on Automatic Control*, vol. 53, no. 2, pp. 586–591, 2008.

[10] Chen, F.-C. and Liu, C.-C., "Adatively controlling nonlinear continous-time systems using multilayer neural networks," *IEEE Transactions on Automatic Control*, vol. 39, no. 6, pp. 1306–1310, 1994.

[11] Chen, W. and Chowdhury, F. N., "Simultaneous identification of time-varying parameters and estimation of system states using iterative learning observers," *International Journal of Systems Science*, vol. 38, no. 1, pp. 39–45, 2007.

[12] Choi, J. and Farrell, J., "Observer-based backstepping control using on-line approximation," in *Proceedings of the American Control Conference*, pp. 3646–3650, 2000.

[13] Chowdhury, F., Wahi, R., and Kaminedi, S., "A survey of neural networks applications in automatic control," in *Proceedings of the 33rd Southeastern Symposium on System Theory*, pp. 349–353, 2001.

[14] Dash, P., Elangovan, S., and Liew, A., "Design of nonlinear expert supervisory controllers for power system stabilization," *Eleictric Power Systems Research*, vol. 33, pp. 25–32, 1995.

[15] Davis, L., Hyland, D., Yen, G., and Das, A., "Adaptive neural control for space structure vibration suppression," *Smart Materials and Structures*, vol. 8, pp. 753–766, 1999.

[16] Doyle, J. and Stein, G., "Robustness with observers," *IEEE Transactions on Automatic Control*, vol. 24, pp. 607–611, 1979.

[17] Doyle, J., Glover, K., Khargonekar, P., and Francis, B., "State-space solutions to standard h_2 and h_∞ control problems," *IEEE Transactions on Automatic Control*, vol. 34, no. 8, pp. 831–847, 1989.

[18] Durham, W., "Constrained control allocation," *AIAA Journal of Guidance, Control, and Dynamics*, vol. 16, no. 4, pp. 717–725, 1993.

[19] Elzebda, J. M., Nayfeh, A. H., and Mook, D. T., "Development of an analytical model of wing rock for slender delta wings," *Journal of Aircraft*, vol. 26, no. 8, 1989.

[20] Esfandiari, F. and Khalil, H. K., "Output-feedback stabilization of fully linearizable systems," *International Journal of Control*, vol. 56, no. 5, pp. 1007–1037, 1992.

[21] Funahashi, K., "On the approximate realization of continuous mappings by neural networks," *Neural Networks*, vol. 2, pp. 183–192, 1989.

[22] Ge, S., Hang, C., Lee, T., and Zhang, T., *Stable Adaptive Neural Network Control*. Boston: Kluwer Academic Publishers, 2002.

[23] Gu, K. and Niculescu, S., "Stability analysis of time-delay systems: A lyapunov approach," in *Advanced Topics in Control Systems Theory*, vol. 328, pp. 139–170, London: Springer-Verlag, 2006.

[24] Gutierrez, L., Lewis, F., and Lowe, A., "Implementation of a neural network tracking controller for a single flexible link: Comparison with pd and pid controllers," *IEEE Transactions on Industrial Electronics*, vol. 45, no. 2, April 1998.

[25] Hodges, D. and Pierce, A., *Introduction to structural dynamics and aeroelasticity*. Cambridge University Press, 2002.

[26] Hornik, N., Stinchcombe, M., and White, H., "Multilayer feedforward networks are universal approximators," *Neural Networks*, vol. 2, pp. 359–366, 1989.

[27] Hovakimyan, N., Nardi, F., Calise, A., and Kim, N., "Adaptive output feedback control of uncertain nonlinear systems using single-hidden-layer neural networks," *IEEE Transactions on Neural Networks*, vol. 13, no. 6, pp. 1420–1431, 2002.

[28] Hovakimyan, N., Nardi, F., Calise, A., and Lee, H., "Adaptive output feedback control of a class of nonlinear systems using neural networks," *International Journal of Control*, vol. 74, no. 12, pp. 1161–1169, 2001.

[29] Hsu, C. and Lan, C., "Theory of wing rock," *Journal of Aircraft*, vol. 22, no. 10, pp. 920–924, 1985.

[30] Hyland, D. C., "Neural network architecture for on-line system identification and adaptively optimized control," in *Proceedings of the Conference on Decision and Control*, (Brighton, England), pp. 2552–2557, 1991.

[31] Hyland, D. C., "Adaptive neural control for flexible aerospace systems: Progress and prospects," *10th IEEE International Symposium on Intelligent Control*, pp. 3–8, 1995.

[32] Ioannou, O. and Sun, J., *Robust Adaptive Control*. Englewood Cliff, NJ: Prentice-Hall, 1996.

[33] Ioannou, P. and Kokotovic, P., "Instability analysis and improvement of robustness of adaptive control," *Automatica*, vol. 20, no. 5, pp. 583–594, 1984.

[34] Johnson, E. and Oh, S., "Adaptive control using combined online and background learning neural network," in *AIAA Guidance, Navigation and Control Conference*, 2004.

[35] Kim, K., Yucelen, T., and Calise, A., "K-modification in adaptive control," in *AIAA InfoTech@Aerospace*, (Atlanta, GA), 2010.

[36] Kim, Y. and Lewis, F., *High Level Feedback Control with Neural Networks*. NJ: World Scientific, 1998.

[37] Krishnakumar, K. and Montgomery, L., "Adaptive neuro-control for large flexible structures," *Smart Materials and Structures*, vol. 1, pp. 312–323, 1992.

[38] Krstic, M., Kanellakopoulos, I., and Kokotovic, P., *Nonlinear and Adaptive Control Design*. New York: Wiley, 1995.

[39] Lavretsky, E., "Adaptive output feedback design using asymptotic properties of lqg/ltr controllers," in *AIAA Guidance, Navigation, and Control Conference*, (Toronto, Canada), 2010.

[40] Lewis, F., Jagannathan, S., and Yesildirek, A., *Neural Network Control of Robot Manipulators and Nonlinear Systems*. Taylor and Francis, 1999.

[41] Lewis, F. L., Yesildirek, A., and Liu, K., "Multilayer neural-net robot controller with guaranteed tracking performance," *IEEE Transactions on Neural Networks*, vol. 7, no. 2, pp. 388–399, 1996.

[42] Luo, J. and Lan, E. C., "Control of wing-rock motion of slender delta wings," *Journal of Guidance, Control and Dynamics*, vol. 16, no. 2, pp. 225–231, 1993.

[43] Marino, R. and Tomei, P., *Nonlinear Control Design: Geometric, Adaptive and Robust*. Englewood Cliffs, NJ: Prentice-Hall, 1995.

[44] Narendra, K., *Adaptive control using neural networks*. Neural Networks for Control, Cambridge, MA: MIT Press, 1990.

[45] Narendra, K., *Adaptive Control of Dynamical Systems Using Neural Networks, Handbook of Intelligent Control ,*. 1992.

[46] Narendra, K., "Neural networks for control: Theory and practice," in *Proceedings of the IEEE*, vol. 84, pp. 1385–1996, 1996.

[47] Narendra, K. and Annaswamy, A., "A new adaptive law for robust adaptation without persistent excitation," *IEEE Transactions on Automatic Control*, vol. 32, no. 2, pp. 134–145, 1987.

[48] Narendra, K. and Annaswamy, A., *Stable Adaptive Control*. Englewood Cliff, NJ: Prentice-Hall, 1989.

[49] Narendra, K. and Parthasarathy, K., "Identification and control of dynamical systems using neural networks," *IEEE Transactions on Neural Networks*, vol. 1, pp. 4–27, 1990.

[50] Nayfeh, A. H., Elzebda, J. M., and Mook, D. T., "Analytical study of the subsonic wing-rock phenomenon for slender delta wings," *Journal of Aircraft*, vol. 26, no. 9, pp. 805–809, 1989.

[51] Nguyen, N., Krishnakumar, K., and Boskovic, J., "An optimal control modification to model-reference adaptive control for fast adaptation," in *AIAA Guidance, Navigation and Control Conference*, 2008.

[52] Nguyen, N., T. I., "Longitudinal dynamics and adaptive control application for an aeroelastic generic transport model," in *AIAA Guidance, Navigation, and Control*, (Portland, Oregon), To appear in 2011.

[53] Polycarpou, M., "Stable adaptive neural control scheme for nonlinear systems," *IEEE Transactions on Automatic Control*, vol. 41, no. 3, pp. 447–451, 1996.

[54] Pomet, J.-B. and Praly, L., "Adaptive nonlinear regulation: Estimation from lyapunov equation," *IEEE Transactions on Automatic Control*, vol. 37, no. 6, pp. 729–740, 1992.

[55] Potter, J. E., "Matrix quadratic solutions," *SIAM Journal on Applied Mathematics*, vol. 14, no. 3, pp. 496–501, 1966.

[56] Rao, V., Damle, R., Tebbe, C., and Kern, F., "The adaptive control of smart structures using neural networks," *Smart Materials and Structures*, vol. 3, pp. 354–366, 1994.

[57] Rovithakis, G. A. and Christodoulou, M. A., *Adaptive Control with Recurrent Highorder Neural Networks*. London: Springer-Verlag, 2000.

[58] Rysdyk, R. and Calise, A., "Robust nonlinear adaptive flight control for consistent handling qualitites," *IEEE Transactions on Control Systems Technology*, vol. 13, no. 6, pp. 896–910, 2005.

[59] Seshagiri, S. and Khalil, H. K., "Output feedback control of nonlinear systems using rbf neural networks," *IEEE Transactions on Neural Networks*, vol. 11, no. 1, pp. 69–79, 2000.

[60] Singh, S., Yim, W., and Wells, W., "Direct adaptive and neural control of wing-rock motion of slender delta wings," *Journal of Guidance, Control, and Dyanmics*, vol. 18, pp. 25–30, 1995.

[61] Spooner, J. T., Maggiore, M., Ordonez, R., and Passino, K. M., *Stable Adaptive Control and Estimation for Nonlinear Systems - Neural and Fuzzy Approximator Techniques*. New York, NY: John Wiley and Sons, 2002.

[62] Suare, C. J., Kramer, B. R., Ayers, B., and Malcolm, G. N., "Forebody vortex control for suppressing wing rock on a highly-swept wing configuration," *AIAA Paper*, 1992.

[63] Tao, G., *Adaptive Control Design and Analysis*. New York, NY: Wiley, 2003.

[64] Volyanskyy, K. Y., Haddad, W. M., and Calise, A. J., "A new neuroadaptive control architecture for nonlinear uncertain dynamical systems: Beyond sigma- and e-modifications," *IEEE Transactions on Neural Networks*, vol. 20, pp. 1707–1723, 2009.

[65] Wise, K. A., "Applied controls research topics in the aerospace industry," 1995.

[66] Wohletz, J., Paduano, J., and Annaswamy, A., "Retrofit systems for reconfiguration in civil aviation," in *Proceedings of the AIAA Guidance, Navigation, and Control Conference*, (Portland, OR), 1999.

[67] Yucelen, T. and Calise, A., "A kalman filter optimization approach to direct adaptive control," in *AIAA Guidance, Navigation and Control Conference*, (Cicago, IL), 2009.

[68] Yucelen, T. and Calise, A., "Derivative-free model reference adaptive control," in *AIAA, Guidance, Navigation and Control Conference*, (Toronto, Canada), 2010.

[69] Yucelen, T. and Calise, A., "A derivative free model reference adaptive control law," *AIAA Journal of Guidance Control and Dynamics*, 2010.

[70] Yucelen, T. and Calise, A., "Derivative-free model reference adaptive control of a generic transport model," in *AIAA, Guidance, Navigation and Control Conference*, (Toronto, Canada), 2010.

[71] Yucelen, T. and Calise, A., "A kalman filter modification in adaptive conrol," *Journal of Guidance, Control, and Dyanmics*, vol. 33, no. 2, pp. 426–439, 2010.

[72] Yucelen, T. and Calise, A., "Adaptive control with loop transfer recovery: A kalman filter approach," in *Proceedings of IEEE American Control Conference*, To appear in 2011.

[73] Yucelen, T., Haddad, W., and Calise, A., "Output feedback adaptive command following for nonminimum phase uncertain dynamical systems," in *American Control Conference*, (Baltimore, MD), 2010.

VITA

Kilsoo Kim was born on March 10, 1974 in Koje island, South Korea. He was awarded a Bachelor of Science in Aerospace Engineering and Mechanics from Inha University, South Korea in 2002. In 2004, he enrolled in the Georgia Institute of Technology to pursue a Ph.D. During his Ph.D. program, in 2005, he was awarded a Masters of Science in Aerospace Engineering from the Georgia Institute of Technology. He is a member of the Control System Society of the Institute of Electrical and Electronics (IEEE) and of the American Institute of Aeronautics and Astronautics (AIAA). His research interests include adaptive control, adaptive estimation, adaptive output feedback control, robust control, nonlinear control, optimal control, active control of flows, active control of flexible systems, flight mechanics, optimization, aeroelasticity, and finite element methods.